Zeitschrift: IABSE reports = Rapports AIPC = IVBH Berichte

Band: 67 (1993)

Rubrik: Selected papers

SELECTED PAPERS

Testing and Modelling to Assess the Capacity of Prestressed Bridges

Expérimentation et modélisation pour évaluer la capacité de ponts précontraints

Modellierung und Versuche zur Einschätzung der Kapazität vorgespannter Brücken

Charles ABDUNUR
Dr. Eng.
Lab. Central Ponts et Chaussées
Paris, France

After obtaining his civil engineering degree, Charles Abdunur worked for five years of the design and supervision of several big projects. Since receiving his doctorate, he directs a number of research projects at a civil and structural engineering laboratory.

SUMMARY

Newer assessment methods, aided with theoretical interpretation models, were developed and successfully used on a number of aging and often damaged bridges, with or without transversal cracks. No external test-loads are needed. Experimental results proved consistent and were compared with those calculated according to several models on instantaneous and time-dependent prestress losses. The more recent models better agree with experiment and enable to predict the future remaining structural capacity of a bridge.

RÉSUMÉ

De nouvelles méthodes d'auscultation, aidées par des modèles théoriques d'interprétation, ont été développées et utilisées avec succès pour évaluer la précontrainte résiduelle dans de nombreux ponts en béton, anciens et souvent endommagés, avec ou sans fissures transversales. L'auscultation n'exige aucune charge extérieure. Ces mesures se sont avérées cohérentes. Elles ont été comparées aux résultats obtenus par plusieurs modèles de calcul réglementaire définissant les pertes instantanées et différées de précontrainte. Les modèles les plus récents concordent mieux avec l'expérience, permettant de prévoir l'évolution de la capacité résiduelle future d'un ouvrage.

ZUSAMMENFASSUNG

Neue Untersuchungsmethode mit Hilfe von theoretischen Interpretationsmodellen wurden entwickelt und mit Erfolg eingesetzt, um die restliche Vorspannung bei den älteren und oft geschädigten Betonbrücken mit bzw ohne durchgehende Risse einzuschätzen. Keine Prüfbelastung ist notwendig. Die Messungen haben sich als richtig erwiesen. Sie wurden mit den Ergebnissen verglichen, die man aus mehreren regulären Rechnenmodellen erhalten hatte, und die sofortigen sowie zeitlich verschobenen Vorspannungsverluste definieren. Die neueren Modelle stimmen besser mit Versuchen überein und erlauben so die zukünftige Restkapazität der Brücke vorauszubestimmen.

1. INTRODUCTION

The initial state and evolution of the stress profile is the major parameter of structural reserves in prestressed concrete bridges. A reduced prestressing force may jeopardize their safety. In aging and often damaged structures, the remaining prestress is very difficult to compute with a sufficient accuracy, owing to uncertainties about initial frictional losses, time-dependent hydric and visco-elastic properties of concrete, bond redistribution, random steel corrosion failure and concrete cracks.

With the continuing development of this type of construction, several theoretical models were successively proposed to predict prestress losses. These models need validation or amendment in the light of experiments involving direct stress measurement. In return, modelling may guide the experiment and better interpret its results.

To evaluate the remaining capacity of structures, the present methods of field investigation do require external test loading and indirectly estimate the corresponding stress. If transversal concrete cracks already exist, their adequate intrumentation would provide a better control of test loads. On the other hand, in the absence of cracks and with no prior knowledge of the actual absolute stresses, test loading may become arbitrary and destructive, somehow beating its own purpose. Hence it was necessary to develop new parallel assessment methods that can do <u>without</u> test loading, measure <u>directly</u> the existing stress and apply in <u>both</u> the presence and absence of individual cracks.

2. ASSESSMENT METHODS REQUIRING EXTERNAL TEST LOADS.

For continuous prestressed structures with flexural cracks, experimental computer-aided methods were developed to assess the actual mechanical state and behaviour under dead and live loads.

2.1 Flexural Reserves under Dead Load

For a cracked section, under a convenient gradually increasing test load, figure 1 shows the tendon over-tension variation $\Delta\sigma_a$ with the applied moment ΔM, [1]. This curve, reflecting a reinforced concrete behaviour model, is a reliable criterion of the crack opening. Let X be the point on the curve representing the state of the crack under the dead load of the tested structure ; let I be the crack opening point. The load testing objectif will then be to locate the position of X with respect to I, and determine the bending moment reserves or deficit in the section. If the crack is completely closed under dead load, X will lie on the straight portion around A ; the applied moment experimentally necessary to open it (reaching I) gives the remaining flexural capacity. If the crack is already open, X will lie on the curved portion. In this case, a general way is first to trace, for the same test load, the theoretical strain-moment curve of the tendon $\varepsilon_a = f(M)$, similar to figure 1, using the above-mentioned reinfored concrete model. Where the experimental curve coincides with a portion of the theoretical one, the origin of the former will be the point X and its relative position with respect to I will give the flexural deficit.

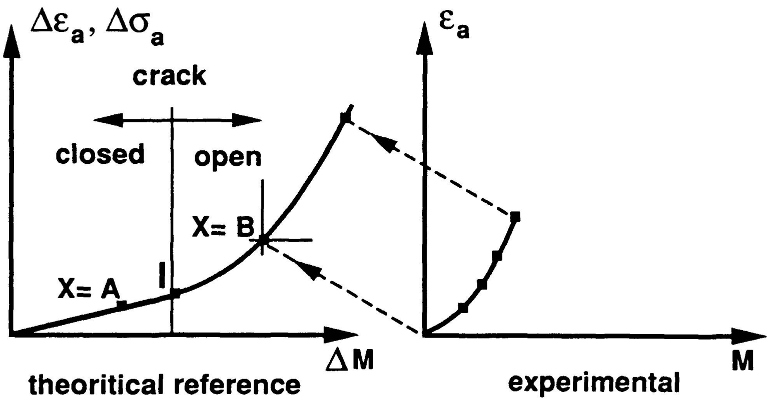

<u>Fig.1</u>
Theoretical and experimental tendon strain and stress variation with the applied bending moment.

2.2 Prediction of Flexural Stresses under Live Loads

In statically indeterminate structures, transversal cracks may be assimilated to a series of elastic or plastic hinges, alternating with sound beam segments and jointhy setting up a new system in equilibrium [2]. The hinge residual flexural stiffness is a multi-parameter function, subject to major

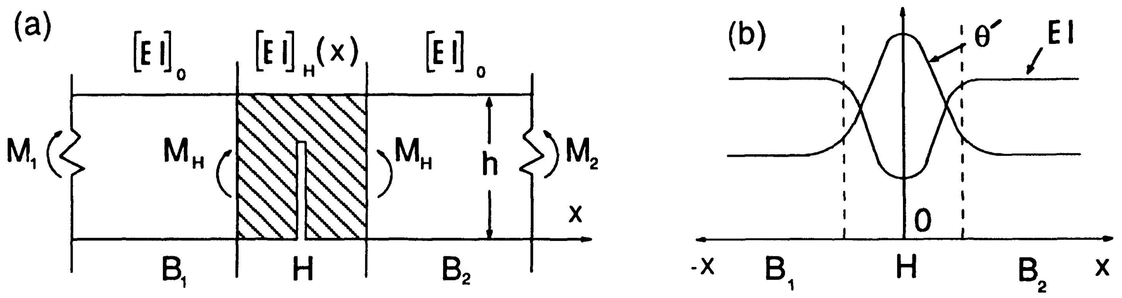

Fig.2 (a) Moments *M* and stiffnesses *EI* in cracked sections H and sound segments B
(b) Redistribution of curvature θ′ and stiffness *EI*

assumptions. An experimental evaluation was therefore adopted as follows : Under given test loads, the curvature redistribution is accurately measured throughout the spans. With the flexural stiffnesses of the sound segments usually known, a chain application of the classical beam equation leads to the bending moments and, chiefly, to the required actual stiffness functions of the hinges (Fig 2). These are introduced into a structural analysis program and the new statical system of the bridge is defined. The actual flexural stresses can thus be predicted throughout the structure, under any given live loads.

3. THE CASE HISTORY

In the 1950's, France witnessed a construction wave of prestressed simply supported concrete girder bridges, known by some as the "first generation". Confident of prior tests and careful workmanship, designers pushed the still improving materials to the verge of their performance limits.

Three decades later, hardly any concrete cracks were observed. However, the unfavourable effects of time remained almost unknown on prestress loss, but clearly materialized in severe steel corrosion with local failure of wires.

With a completely uncertaint stress profile and in the still lucky absence of concrete cracks, structural assessment through external load testing connot be recommended for the afore-mentioned reasons.

4. NEW ASSESSMENT METHODS WITHOUT EXTERNAL LOADING

In a fundamentally different approach, we developed two new parallel methods of field investigation. One can directly measure the actual stress in concrete, the other in steel. Both are now successfully applied on site. No test loads are needed.

4.1 Direct Stress Measurement in Concrete ; The Release Method

It is a local and partial release of stress, followed by a controlled pressure compensation [3]. In pratice (figure 3), a displacement reference field is first set up on the concrete surface ; a tiny slot, 4 mm wide, is then cut in a plane normal to the desired stress direction ; finally, a special very thin flat jack is introduced into the slot and used to restore the initial displacement field. The amount of cancelling pressure gives the absolute compressive stress normal to the slot. In the same way, with the same accuracy, tensile stresses are obtained by a corollary. The stress profile is traced by repeating the operation at closely successive depths of the same slot, then by treating the data numerically. The depth operating range is 80 mm. In spite of imposing a minute working scale, counter measures kept the error within 0.3 MPa. Measurement is "direct" in the sense that the same physical quantity is involved (pressure for stress) and that none of the material

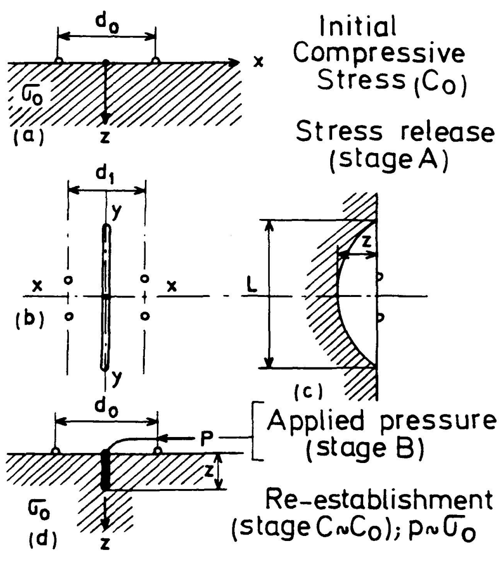

Fig. 3
Stages A, B, C of direct stress measurement in concrete by the release method

elastic properties are needed. These are even determined in the process. Material eigenstresses can now be correctly isolated and subtracted from the measured absolute stress, giving access to the mechanical normal stress acting on the section. Besides the miniaturization imperative, a post-operation specific remedial technique also restores the initial mechanical and esthetic state of the medium. The release method can thus be classified as non-destructive.

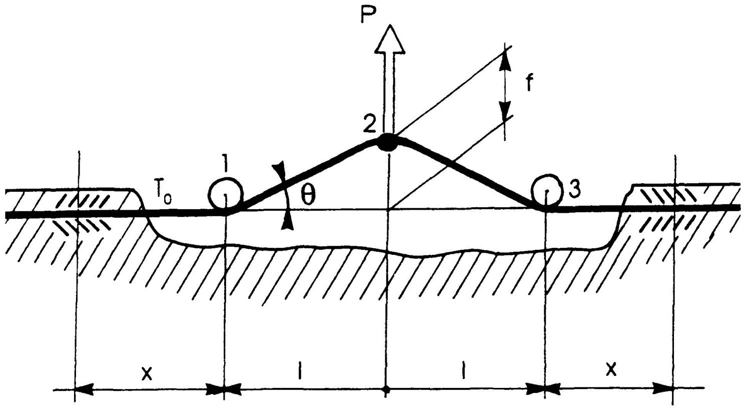

Fig. 4
Pinciple of stress measurement in steel by the crossbow method

4.2 Stress Measurement in the tendons ;
The Crossbow Method

The effort necessary to deflect a tight rope is obviously proportional to the axial tensile stress. Figure 4 outlines the application of this fact to the assessment of tendons after carefully clearing the adjacent concrete cover, duct and groute over a 60 cm length [4]. A controlled perpendicular force P, coupled with a displacement sensor, deflects successive prestressing wires throught a distance f limited to 4 mm ; the tensile force F in the steel is deduced by the formula :

$$P = 2\,(F + k)\,(f/l) + K\,(f/l)^3$$

where k and K are given constants. In practice, the parasitie effects of friction, flexural stiffness and overstretching necessitate prior calibration tests on simulating models in the laboratory.

4.3 Other remarks

The release method remains mechanically more comprehensive. Both methods, however, are complementary. They enable now to reason directly in terms of stress thus providing an immediate acces to the applied forces and moments and offering a straightforward comparison with the material strength, a main criterion of structural safety.

5.APPLICATION TO THE CONSIDERED CASE

The two new assessment methods were jointly used to evaluate the remaining prestress in a large number of the simply supported, post-tensioned concrete bridges described in chapter 3 and situated in the north eastern part of France. These structures are 22 to 38 years old, but of identical design and construction : same standard T-sections and spans, same materials and prestressing system.

5.1 Procedure

Concrete stresses at midspan were measured on the neutral axis to deduce directly the actual prestressing force. Steel stresses were evaluated near this section at convient points. Before and during the campaign, thorough inspection was carried out to detect steel corrosion. Affected bridges were left for a separate consideration. On the 12 remaining identical bridges still free from corrosion, the stress values obtained by both methods were quite consistent and fully agreed. They were selected for the following analysis on the mechanical loss of prestress.

5.2 Experimental Data Synthesis

In a homogeneous group of N bridges, solely differing in age, the N respective stresses measured at a given date may be assumed equivalent to the measurements that could have been taken on a single typical bridge at N consecutive dates of its lifetime. In our case, the 12 corresponding stress values can thus form a synthesis curve representing an experimental time-dependent loss of prestress.

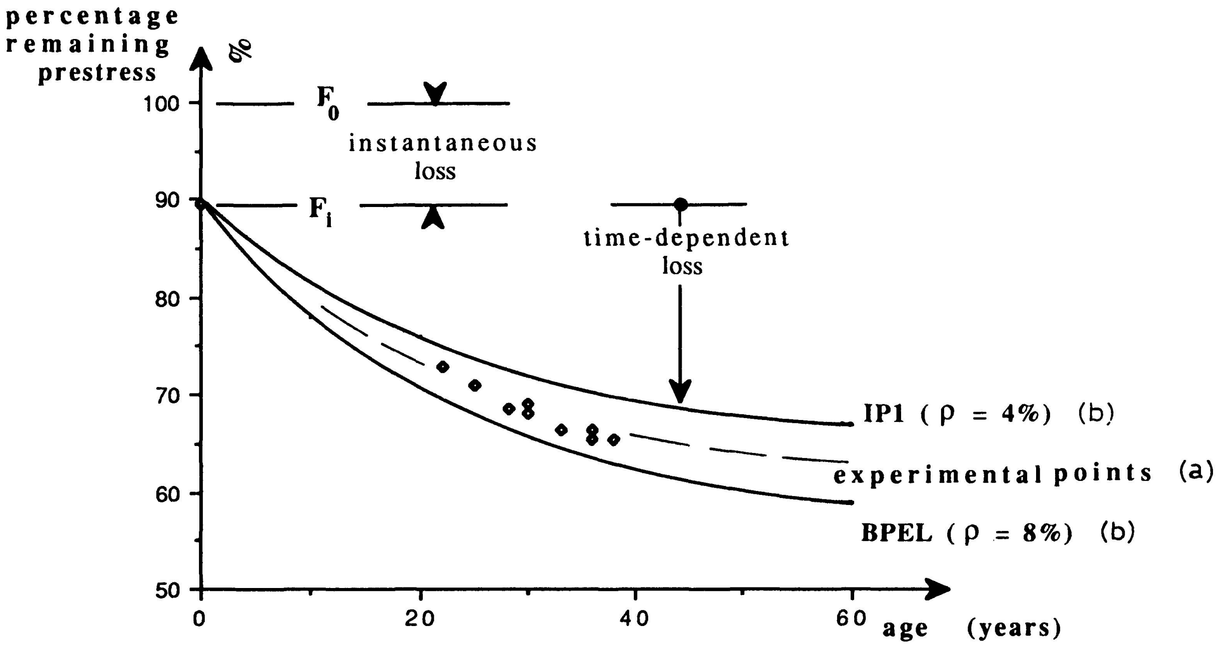

Fig. 5

a) Directly measured remaining prestress at mid-span, on 12 identical bridges of different age and with unknown steel relaxation ρ and friction coefficient μ.

b) Corresponding envelop theoretical curves obtained from two predictive models with different basic assumptions and ρ values ; they help to extrapolate the experimental results in time and determine ρ for the steel actually used ; experiment may in return improve the model assumptions.

In figure 5, these points are converted to forces over the section and expressed as a percentage of the original anchorage prestress force F_0 found in the records of each bridge. They lie between two theoretical envelop curves, stemming from constitutive models discussed below, and guiding the extrapolation of the present measurements towards the future (or the past).

6. THEORETICAL MODELS ON PRESTRESS LOSS

Three main frameworks of prestress loss estimation were proposed at sucessive periods of construction development in France : pre-code recommendations, IP1 model, BPEL code.

6.1 Instantaneous losses

The effects of friction, elastic shortening and anchorage loss are all well known. The main uncertainty concerns the values of the friction and wobble coefficients, μ and ϕ, in the exponential formula which all models use for frictional losses.

6.2 Time-dependent losses

On prestress losses due to concrete shrinkage and creep or steel relaxation, the three models diverge as follows.

* The pre-code of the1950's, construction period of the bridges now under scrutiny, gives a lump sum estimation of 12 to 15 % prestress loss in all, after the instantaneous effects [5]. It assumes proper overtensioning to reduce steel relaxation and overcome friction and anchorage losses.

* In the IP1 model of the 1960's, based on the concept of allowable stresses, a group of constitutive equations accounts for the following sources of loss [6] :

- Concrete shrinkage, depending on the mix and thickness, the atmospheric humidity and a time-dependent strain coefficient.

- Concrete creep, as a function of the initial elastic strain, atmospheric humidity, time-dependent strain coefficient and other constitutive factors.

- Steel relaxation, depending on the initial steel stress σ_i, strength R_g and percentage stress loss ρ at 1000 and 3000 hours in a standard relaxation test.

The main assumption in IP1 is the simple straightforward superposition of these three.

* The B.P.E.L., a more elaborate model of the 1980's, is based on the service and ultimate state limits [7]. Compared with the IP1, there is hardly any difference as far as concrete shrinkage. For concrete creep, in a new BPEL version : The effect of atmospheric humidity is more accurately formulated in the basic law ; an additional but different law was introduced for "creep recovery" ; a new "equivalent time" method was developed to replace the superposition principle.

Concerning steel relaxation, the same IP1 parameters were kept in a slightly different formula, less optimistic for medium relaxation steel used in the bridges under consideration.

BPEL's basic assumption is the partial interaction between concrete creep and steel relaxation.

7. MODEL-AIDED INTERPRETATION OF EXPERIMENTAL RESULTS

For both the IP1 and BPEL predictive models, detailed computer programs were elaborated [8]. Given the material properties, they calculate all the prestress loss compoments in an exact step-by-step simulation of the bridge construction phases and loading history. For the assessed bridges, the properties related to the calculation of concrete shrinkage and creep were either given or deduced from the design and construction records. However, the percentage steel relaxation at 1000 hours, ρ, did not exist as such in the early 1950's ; it was actually very high but masked by short-time tests. Another uncertainty was μ, the prestress friction coefficient. In a parametric study using both models, ρ was varied from 4 to 8% (extreme value), and μ from 0.16 to 0.23. The analysis showed that ρ had an effect several times greater than μ on the total prestress loss. Hence, we thought of fixing μ at 0.23, corresponding statistically to the type of ducts used. Left with one influential unknown material parameter ρ, it was not possible to have a clear-cut comparison between experimental and theoretical results but rather a joint contribution : the release method giving the present actual prestress force, the two models guiding its extrapolation to the future under a ρ variation range suggested by previous data synthesis and living memory. In this context, the adopted interpretation strategy is illustrated in figure 5 for the 12 assessed bridges, then explained in table 1 by an example of a typical 30-year-old bridge. In the example, interpretation proceeds as follows :

1) From the anchorage prestress force F_0 given in construction records, calculate by each model the remaining mid-span force F at infinity (∞ = 60 years), using two envelop values of ρ and the adopted constant value of μ. (M1, M2 and M4, M5 in table 1).
2) Deduce the present force F (30 years), assuming a continuons quasi-asymptotic function of time.
3) Compare the present experimental value of force F with the two theoretical ones of each model.
4) By identification or interpolation, find in each model a particular theoretical function that agrees with the present measurement (5500 KN at 30 years). The functions obtained nearly coincide and can predict the prestress losses still expected.

Thus, at 30 years, the prestress of the bridge, reflecting its structural capacity, has already actually suffered a 32 % total loss, expected to attain 38 %. Of these, 27 % are time-dependent contrasting with the 15 % estimated in the design. The two particular functions, satisfying the 30-year stress measurement and giving the same losses, correspond to ρ = 8% for IP1 and only 6.27 % for BPEL. Despite the lessening effect of its partial interaction between concrete creep and steel relaxation, BPEL seems then to grow passimistic for ρ values exceeding the 2 % of our present low relaxation steel. Finally we notice practically stable values of instantaneous losses, 10-11 %, appearing in the corresponding differences between the last two columns of table 1.

8. UP-TO-DATE ACTIONS ON THE STRUCTURE

With its remaining capacity evaluated, the structure must face external loads not necessarily équivalent to those its was designed for. The Eurocode will thus be proposing two partial load systems :

- A double-axle concentrated load model (indivisible tandem system), each axle having a weight Q_k

Means of Evaluation / modelling / Experiment	Prestress Force F (KN) 30 y	Prestress Force F (KN) ∞	Steel Stress σ_a (MPa) 30 y	Steel Stress σ_a (MPa) ∞	Concrete Stress σ_b (MPa) 30 y	Concrete Stress σ_b (MPa) ∞	Time-dept % Loss $1 - F/F_i$ 30 y	Time-dept % Loss $1 - F/F_i$ ∞	Total % loss $1 - F/F_o$ 30 y	Total % loss $1 - F/F_o$ ∞
Pre-code : M 0 approximation (design)	6430	5900	994	912	9.0	8.3	8	15	20	27
IP1 model : M 1 $\rho = 8\ \%$; $\mu = 0.23$	5500	5040	850	779	7.7	7.1	21	28	32	38
IP1 model : M 2 $\rho = 4\ \%$; $\mu = 0.23$	5800	5400	897	835	8.1	7.6	17	22	28	33
IP1 model : M 3 $\rho = 8\ \%$; $\mu = 0.16$	5600	5090	866	787	7.8	7.1	19	27	31	37
BPEL code : M 4 $\rho = 8\ \%$; $\mu = 0.23$	5340	4760	826	736	7.5	6.7	23	32	34	41
BPEL code : M 5 $\rho = 4\ \%$; $\mu = 0.23$	5710	5260	884	814	8.0	7.4	19	24	29	35
EXPERIMENT (Direct Stress measurement)	5500	—	850	—	7.7	—	21	—	32	—
Identification with M 1	5500	$\underline{5040}$	850	$\underline{779}$	7.7	$\underline{7.1}$	21	$\underline{28}$	32	$\underline{38}$
Interpolation M 4 - M 5 $\rho \rightarrow 6.27\ \%$	5500	$\underline{4980}$	850	$\underline{769}$	7.7	$\underline{7.0}$	21	$\underline{28}$	32	$\underline{38}$
Conclusion :	The bridge may still lose 10 % of its present prestress.									

Table 1 : Example of an experimental model-aided assessment of present and future prestress losses in a bridge, 30 years old at the testing date. Underlined quantities are experimental values extrapolated to infinity using these models (ρ is the steel relaxation at 1000 hours, μ the friction coefficient , ∞ assumed at 60 years. F is the present and future prestress force at mid-span ; F_i and F_o are the initial forces respectively at mid-span and the anchorage).

equal to 300, 200, 100, KN on lane 1, 2, 3, respectively.
- A uniformly distributed load (UKL system), having a weight density q_k per square metre, applied in the unfavourable areas ; q_k is assumed 9, 2.5, 2.5, 2.5 KN/m^2 on lane 1, 2, 3, elsewhere.

10. RANDOM EFFECTS OF CORROSION

On the second group of bridges, the experimental results are far less consistent. The impact of steel corrosion failure, on the remaining prestress in nearby sections, varies from negligible to considerable, depending on the ability of the broken wires to develop local friction anchorages in both senses (fig. 6). This random factor is still difficult to model. Direct stress measurement, by the release method in particular, remains the only unchallenged means of assessment for the time being.

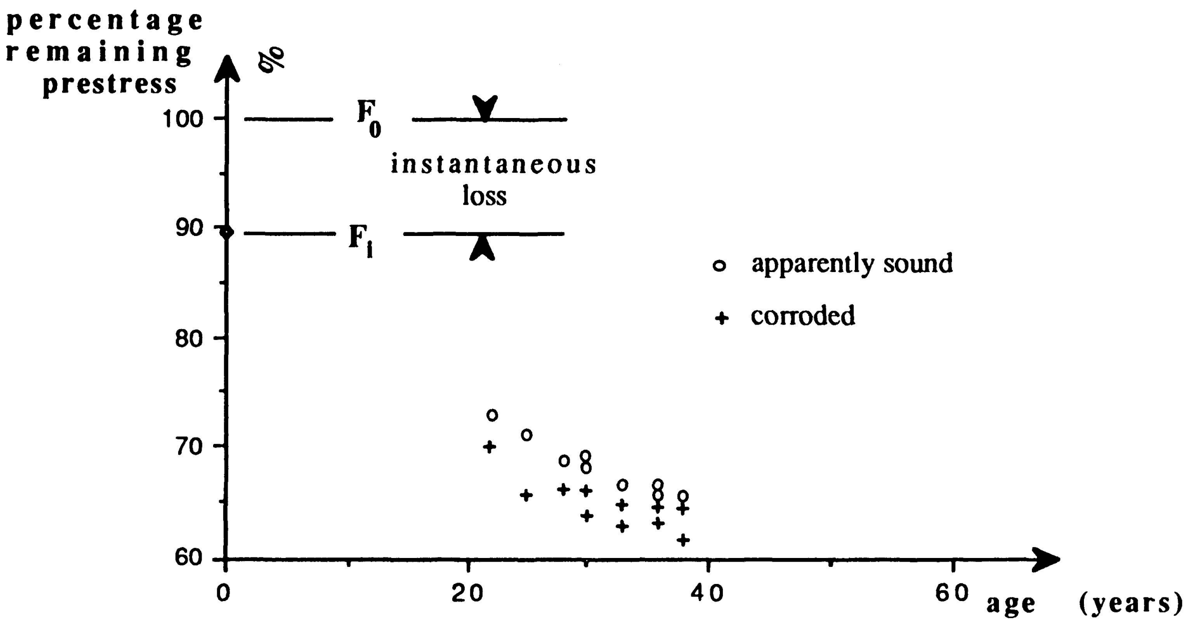

Fig. 6
Effect of steel corrosion on the remaining prestress of otherwise identical bridges. Both groups seem to have undergone similar time -dependent losses.

10. CONCLUSION

The present actual structural reserves of a prestressed concrete bridge can now be evaluated through direct stress measurements by the release method. A model-aided extrapolation of these stresses gives the time-dependent losses still expected and, hence, the future residual capacity. Proposed load models, such as "Eurocode 1", will be contributing to an up-to-date estimation of the total required capacity of a structure. The difference between the required and remaining reserves leads obviously to the needed additional external prestress. At a later stage, stress can again be measured to check the effectiveness of the operation. The release method on one hand, two predictive models on the other, can thus jointly contribute to an optimum strengthening of aging bridges, which inadequate prestressing has rendered structurally deficient or obsolete.

ACKNOWLEDGEMENT

The author expresses his thanks to Y. Jaffré and P. Paillusseau (S.E.T.R.A) for their help in the computations regarding the application of the IP1 and BPEL models.

REFERENCES

1. CHATELAIN, J. and GODART, B., "Evaluation de l'état mécanique réel de ponts en béton précontraint". IABSE Symposium, Helsinki, 1988.

2. ABDUNUR, C., "Structural assessment of a bridge with transversal cracks", First International Conference or Bridge Management, GUILDFORD, UK, 1990.

3. ABDUNUR, C., "Mesure de contraintes sur ouvrages d'art par une méthode de libération miniaturisée", Bulletin des Liaison des LPC, n° 138, Paris, 1985.

4. TONNOIR, B., "Mesure de la tension résiduelle dans les armatures de précontrainte à l'aide de l'arbalette", journée portes ouvertes au L.R.P.C de Lille, 1991.

5. DUMAS, F., "L'évolution de la précontrainte du béton armé au cours de la reconstruction des O.A. du Nord et du Pas-de-Calais", revue "Travaux", p. 588-576, octobre 1951.

6. "Instructions Provisoires sur l'emploi du béton précontraint", Paris, 1965.

7. "Règles techniques de conception et de calcul des ouvrages et constructions en béton précontraint suivant la méthode des états-limites, Paris, 1983.

8. Dossier "VIPP", S.E.T.R.A., France, 1967.

Reliability Aalysis of a Highway Bidge

Analyse de la fiabilité d'un pont-route

Zuverlässigkeitsanalyse für eine Autobahnbrücke

R. RANGANATHAN
Prof. of Civil Eng.
Indian Inst. of Technology
Bombay, India

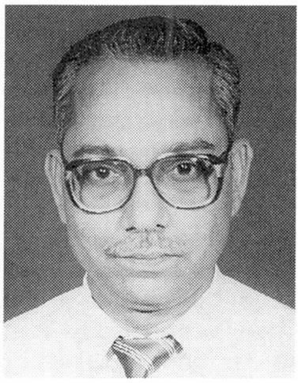

R. Ranganathan, born in 1939, received B.E. and M.Sc. (Struct. Eng.) degrees from Madras University and Ph.D. from Indian Institute of Technology, Kanpur, India. His main field of research is reliability analysis and design of structures in which he has written a text book and published number of papers.

Zubin MISTRY
Struct. Engineer
Gherzi Eastern Ltd
Bombay, India

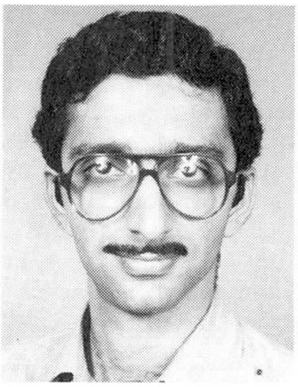

Zubin Mistry, born 1968, received his Bachelor's degree in civil engineering from the University of Bombay in 1990 and his Master degree from the Indian Institute of Technology, Bombay, India, in 1992. Since 1992 he has been involved in the design of industrial buildings and commercial complexes.

SUMMARY

The paper deals with the reliability analysis of a continuous prestressed concrete box girder bridge which is under construction across Thana Creek in Bombay, India. The bridge is considered as a system and the reliability of the same is evaluated at limit states of collapse in flexure and shear using Monte Carlo technique. Results of the statical analysis of the field data on material strength and load variables have been used in the Monte Carlo method. It is found that the probability of failure of the bridge at limit states of collabse in flexure and shear are of the order of 10^{-15} and 10^{-10} respectively.

RÉSUMÉ

Cet article traite de l'analyse de la fiabilité d'un pont-route à plusieurs travées, du type à poutre-caisson en béton précontraint, actuellement en construction pour franchir le Thana-Creek à Bombay. La méthode de Monte-Carlo est utilisée pour déterminer la fiabilité de ce système de pont à l'état limite de rupture par flexion et cisaillement. Les données statistiques en travée sur la résistance des matériaux et l'effet des charges ont été déduites pour servir de variables. Le calcul de la probabilité d'une rupture à l'état limite par flexion et cisaillement a donné une valeur variant entre 10^{-15} et 10^{-10}.

ZUSAMMENFASSUNG

Der Beitrag behandelt die Zuverlässigkeitsanalyse einer mehrfeldrigen Spannbetonkastenbrücke, die über den Thana-Creek in Bombay gebaut wird. Die Systemzuverlässigkeit der Brücke auf Biege- und Schubversagen wird mit dem Monte-Carlo-Verfahren ermittelt. Für die Variablen wurden statistische Felddaten der Werkstoffestigkeit und der Einwirkungen herangezogen. Die Wahrscheinlichkeit eines Einsturzes im Grentzzustand des Biege- oder Schubversages wurde zu 10^{-15} bzw. 10^{-10} berechnet.

1. INTRODUCTION

The development of reliability analysis and reliability based design criteria has led to the rational evaluation of structural safety. One area of reliability analysis which is receiving considerable attention from engineers is system reliability. The major source of hidden safety reserve is in the system behaviour of structures. A bridge is a system of interacting members with redundancies and load sharing. However, there is a different degree of redundancy and load sharing in different types of bridges. The difference between member and system reliabilities increases with increase in the level of redundancy. This paper uses a probability based approach, developed by Nowak and Zhou [1], considering a bridge as a system of interconnected elements. System approach has been used to evaluate the reliability of a continuous prestressed concrete bridge which is under construction across Thana Creek in Bombay, India. For the evaluation of the reliability of a bridge, different limit states of flexure, shear, fatigue, deflection, etc. are to be considered. However, only the limit states of collapse in flexure and shear are considered and the evaluation of structural reliability is presented for the same using Monte Carlo technique. Field data on the strengths of materials and traffic load have been collected and statistically analysed. Results of the same have been used in the reliability analysis.

2. DETAILS OF THE BRIDGE

The new Thana Creek Bridge is a prestressed concrete box girder bridge of total length 1.837 km. It consists of six spans viz. 205.46 m, four spans of 321 m each and 347.63 m. It is a Class AA bridge [2] with three lanes on each of the two parallel continuous girders. From the structural analysis point of view, the two girders may be considered to act independently of each other. Each span consists of a variable depth box girder - a square parabola from either support upto the midspan. The girder is supported on steel rocker/roller bearings on each pier. A longitudinal section of a typical intermediate unit and cross section are shown in Fig. 1. Details of critical sections are shown in Table 1.

Section No.	Area of section	Moment of inertia	Number of prestressing cable ducts in		Slope of duct <rads>	Area of stirrups	Centroid distance from top
	<m^2>	<m^4>	deck	soffit		<mm^2/m>	<m>
1	7.4660	13.511	2	6	0.0000	4400.83	1234.21
2	9.3258	36.725	36	6	0.1000	4997.73	2040.96
3	14.470	113.11	58	0	0.1315	6544.93	3832.94
4	9.3258	36.725	40	4	0.1000	4581.47	2040.96
5	7.2300	13.262	2	38	0.0000	4400.83	1215.74
6	9.3258	36.725	40	4	0.1000	4581.47	2040.96
7	14.470	113.11	64	0	0.1315	6544.93	3832.94

Table 1 Section properties for the Thana creek bridge

3. STATISTICS OF STRENGTH AND LOAD VARIABLES

Concrete mix M 40 (cube strength 40 N/mm^2) and 12.7 mm diameter, 1/7 ungalvanised stress relieved strands for prestressing the bridge and Torsteel (yield strength 415 N/mm^2) for vertical stirrups have been used in the bridge. Field data have been collected on cube strength of concrete, f_{cu}, ultimate tensile strength of strands, f_p, and yield strength of Torsteel, f_{sy}, and statistically analysed. It is found that f_{cu}, f_p and f_{sy} follow normal distributions with mean value and standard deviation equal to 47.28 and 4.28, 1925.8 and 24.5, and 468.9 and 34.2 N/mm^2 respectively

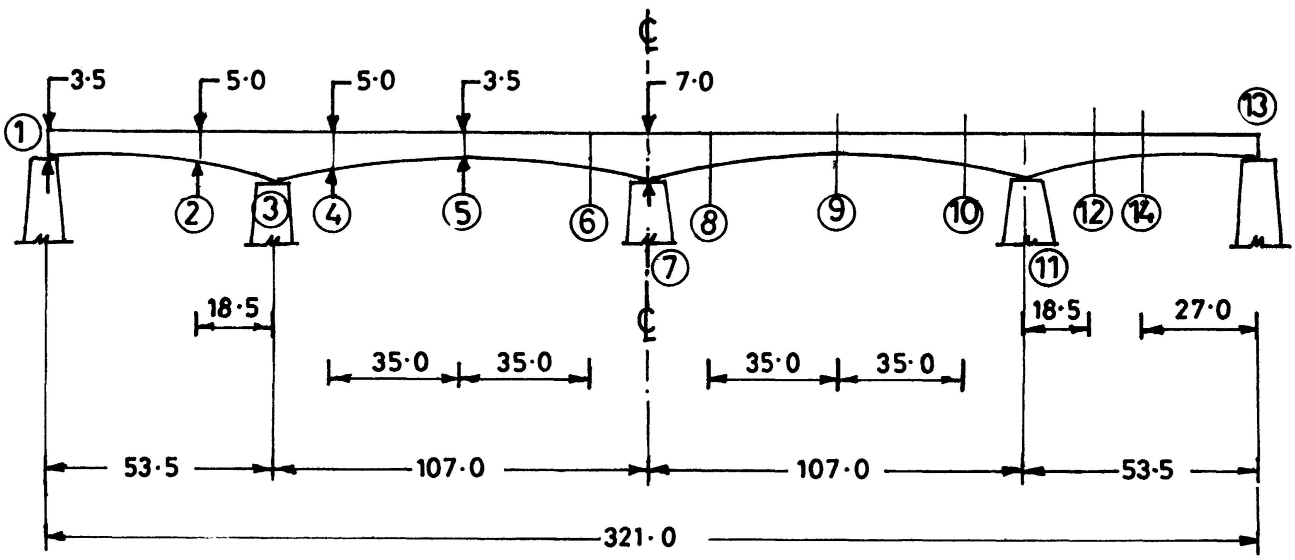

All dimensions in m

(a) Typical intermediate unit

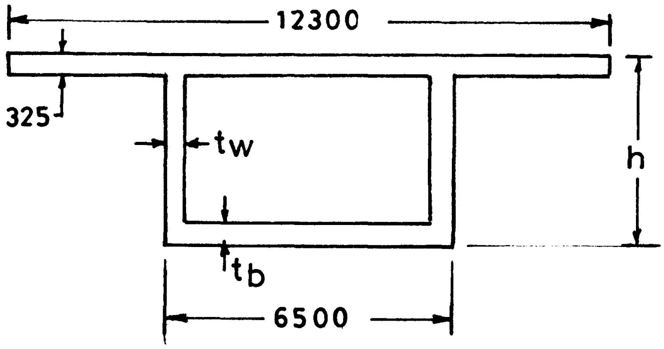

Sections	h	tw	tb
1, 5, 9, 13	3500	300	225
3, 7, 11	7000	350	1000
2, 4, 6, 8 10, 12	5000	363	335

All dimensions in mm

(b) Details of cross sections

Fig.1 Details of new Thana Creek Bridge

[3].

The live load data has been collected for the old Thana Creek Bridge as the bridge under reliability study is still under construction. The last traffic survey was conducted in 1989. The collected data has been statistically analysed. Based on the analysis of the actual loads, a new standard truck has been fixed with a mean axle load of 92 kN per axle (total load 184 kN) with a wheel base of 1.2 m. Considering the uncertainties due to several factors, the coefficient of variation of the load is found to be 30 per cent [3]. The standard truck obtained above represents the arbitrary point-in-time varying load, Q_{apt}, as obtained from the results of the traffic survey. For checking the reliability of the bridge at ultimate limit states, statistics of the lifetime maximum live load have to be used. Considering the life of the bridge as 50 years, and assuming that (i) Q_{apt} follows Type I extremal (largest) distribution [4], (ii) the live load data represents a constant traffic distribution throughout the year and (iii) all annual maximum loads are identically distributed and independent, the statistics of the lifetime maximum total load, Q_m, for the standard truck have been obtained. It is found that Q_m follows Type I extremal (largest) distribution with parameters u= 327.5 kN and α

= 0.232. The mean value of Q_m is 352.4 kN [3].

The dead load,D, is assumed to be normally distributed with mean to nominal ratio equal to 1.05 and coefficient of variation five per cent.

4. RELIABILITY ANALYSIS

Having determined the statistics of the basic random variables, both load and strength, the reliability analysis of the bridge is now considered. The criteria selected are (i) the limit state of collapse in flexure and (ii) the limit state of collapse in shear.

4.1 Limit state of collapse in flexure

The given bridge is a redundant structure. In the analysis of such structures, the failure of a section is assumed to take place when the plastic moment capacity of the section is reached. The failure is called the formation of a plastic hinge at the section. In the case of a redundant structure, a collapse mechanism forms only when a sufficient number of plastic hinges have developed.

4.1.1 Plastic rotation capacity and plastic moment

The failure of a structure through the formation of a collapse mechanism requires the plastic hinges to have a large rotational capacity. In the case of prestressed concrete structures, any critical region, hinged earlier, may fail due to insufficient rotation capacity before a collapse mechanism is formed. This failure is called a rotation failure mode. The plastic rotation capacity, θ_p, of a section is given by

$$\theta_p = d(e_u - e_{cy})/x_u \qquad \text{----(1)}$$

where d is the effective depth, e_u is the ultimate strain in concrete and e_{cy} is the strain in concrete at the extreme fibre at the start of yield in steel. The depth of the neutral axis at failure, x_u, can be determined from the equilibrium condition at failure. As per IS:456-1978 [5], the limiting values e_u= 0.0035 and e_{cy}= 0.002 are used. Thus, knowing the geometry of the section and the depth of the neutral axis at failure, the ultimate rotation capacity of the section can be found.

The ultimate resisting moment of a section is taken as the plastic moment capacity, M_p, of the section. This is given by [5]

$$M_p = B\, f_{pu}\, A_p\, (d - 0.42x_u) \qquad \text{----(2)}$$

where f_{pu} is the ultimate tensile stress in the tendons at failure and A_p is the area of prestressing tendons. Using equilibrium equations, strain compatibility conditions and the stress-strain relationships for steel and concrete, a given section can be analysed and f_{pu} and x_u can be determined. Knowing f_{pu} and x_u, M_p can be calculated.In Eq. 2, the model parameter, B, introduced to take care of uncertainty in the prediction equation, is assumed to be normally distributed with mean value 1.01 and standard deviation equal to 0.0465 [6].

4.1.2 Determination of reliability

The reliability analysis of the bridge as a system starts with the determination of critical sections in the bridge. The standard truck is placed at a critical section. Using the Monte Carlo technique, a set of values is generated for the basic random variables viz. load and strength variables (f_{cu}, f_p, Q_m, B and D). All other parameters are considered to be deterministic. Using the generated values, plastic moments and plastic rotation capacities of critical sections are calculated as explained in the previous section.

For a given position of the wheel load, the structure is analysed using the stiffness method of linear elastic and piecewise linear elastic-plastic analysis [7]. The steps involved are as follows:
i) Develop the load vector , {L}, and the stiffness matrix, [K], for the structure.
ii) Invert the stiffness matrix and obtain the displacement vector {D} as

$$\{D\} = [K]^{-1}\{L\} \qquad \text{----(3)}$$

iii) Determine the member end forces and check for excessive rotation at all locations where plastic hinges have formed.
iv) Find the load factor, λ, the ratio of the plastic moment capacity to the actual moment, at each critical location. Select λ_{min} and increase the load by multiplying the initial load by λ_{min}.
v) Introduce a plastic hinge at the node for which $\lambda = \lambda_{min}$ and modify [K]. To do this, add a row and a column to [K], the elements of which are the stiffnesses corresponding to the rotational degree of freedom at the hinge point. Add the plastic moment capacity of the section and the hinge rotation to the load and displacement vectors respectively. Check for the formation of a mechanism.
vi) Repeat steps (ii) to (v) until the check in step (iii) fails or a mechanism is formed. A mechanism is said to have formed when the determinant of the matrix, $|[K]| \le 0$.
vii) The ultimate load factor, λ_{ult} , will be the sum of the minimum values of λ in successive cycles. The above procedure results in a piecewise linear moment-curvature relationship. Hence, during the analysis, if at any stage it is found that the rotation capacity of a section is exceeded, then a direct interpolation will suffice to obtain λ and hence λ_{ult}.

The safety margin, Z, is calculated as

$$Z = \frac{resistance}{action} = \frac{ultimate\ load}{actual\ load} = \lambda_{ult} \qquad \text{----(4)}$$

Hence a value for Z is obtained. The Monte Carlo technique is repeated and a number of values are generated for Z. As the elastic-plastic analysis is to be carried out each time, the number of samples to be generated is restricted to only 200 to get estimates of mean and standard deviation of Z.

For the generated samples, mean value, $\bar{Z}$, and coefficient of variation, δ_Z, of Z are calculated. For calculating reliability, the lognormal format has been adopted. Hence for the lognormal variate Z, the parameters are calculated as follows:

$$\sigma_{\ln z} = \sqrt{\ln(\delta_z^2 + 1)} \qquad \text{----(5)}$$

$$\tilde{Z} = \bar{Z}\exp(-\tfrac{1}{2}\,\sigma_{\ln z}^2) \qquad \text{----(6)}$$

The probability of failure, p_f, and the reliability index, β, are given by

$$p_f = \Phi[\ \ln(\tfrac{1}{\tilde{Z}})/\sigma_{\ln z}\ ] \qquad \text{----(7)}$$

$$\beta = -\Phi^{-1}(p_f) \qquad \text{----(8)}$$

This gives the probability of failure of the bridge for a given load position. There are four critical load positions (Table 2). For each critical load position, the above procedure is repeated and p_f and β are calculated. The results are given in Table 2. Since the values of $p_f << 1$, the probability of failure of the system, p_{fs}, has been taken as

$$p_{fs} = \sum_{i=1}^{N} p_{fi} \qquad ----(9)$$

assuming the failure modes to be independent. p_{fi} is the value of p_f for i^{th} load position and N is the number of critical load positions. The value of p_{fs} is also given in Table 2.

Load position Section No.	$\bar{Z}$	σ_Z	p_f	β
14	4.6643	0.8716	1.018×10^{-16}	8.2191
4	4.6418	0.8581	6.159×10^{-17}	8.2827
5	4.3353	0.8174	4.538×10^{-15}	7.7548
6	4.8220	0.9152	6.537×10^{-17}	8.2691
For system			4.77×10^{-15}	7.75

Table 2 Results of analysis for limit state of collapse in flexure

4.2 Limit state of collapse in shear

4.2.1 Ultimate Shear Strength

The analysis for the limit state of collapse in shear differs from the elastic-plastic analysis for flexure in one major respect. There is no successive formation of hinges as was considered in the previous limit state (Sec. 4.1). This is because once a section fails in shear, the entire unit is considered to have failed. The ultimate shear strength of a prestressed concrete girder is considered to be the lesser of its strengths in the cracked and uncracked states. It is calculated using the Indian Roads Congress code [8]. The equations in the code are used after removing partial safety factors. While estimating the ultimate shear strength of a section, a model error parameter, B, is attached to the prediction equation and this is assumed to be normally distributed with a mean value of 1.09 and a standard deviation of 0.14 [6]. The analysis of a girder at the limit state of collapse in shear is simpler than that at the limit state of collapse in flexure.

4.2.2 Determination of reliability

The standard truck wheel load is fixed at a critical section. Using the Monte Carlo technique, a set of values is generated for the basic random variables viz. load and strength variables (f_{cu}, Q_m, B, f_{sy} and D). Using the generated values, the ultimate shear strength of each critical section is calculated. For a given load position, elastic analysis of the bridge is carried out using stiffness matrix method and values of actual shear forces at critical sections are determined. The load factor, λ, which is the ratio of ultimate shear strength to actual shear, is calculated at each critical section. The lowest value, λ_{min}, is selected and this gives the load factor for the ultimate shear capacity of the weakest section of the girder to be reached. The safety margin is calculated as

$$Z = \frac{resistance}{action} = \lambda_{min} \qquad ----(10)$$

This λ_{min} is nothing but a value for the safety margin Z. Similarly, using the Monte Carlo technique, the process is repeated and a number of values of Z are generated. Mean and standard deviation of Z are calculated. Values of p_f and β are calculated using Eqs. 7 and 8.

There are seven critical load positions (Table 3). For each critical load position, the above procedure is repeated and probability of failure calculated. The probability of failure of the system is calculated using Eq. 9. The results of the reliability analysis are given in Table 3.

Load position Section No.	$\bar{Z}$	σ_Z	p_f	β	Failure at section
1	2.9256	0.4420	7.60×10^{-11}	7.0707	1, 6 or 8
2	2.9203	0.4410	8.33×10^{-11}	7.0618	2 or 6
3	2.9257	0.4419	7.59×10^{-11}	7.0728	6 or 8
4	2.9237	0.4424	9.00×10^{-11}	7.0553	4
5	2.9296	0.4437	8.33×10^{-11}	7.0621	6 or 8
6	2.9095	0.4393	9.61×10^{-11}	7.0383	6 or 10
7	2.9256	0.4418	7.57×10^{-11}	7.0739	6 or 8
For system			5.81×10^{-10}	6.14	

Table 3 Results of analysis for limit state of collapse in shear

5. DISCUSSION AND CONCLUSION

With the available data, a fairly accurate standard truck has been developed. The mean value of the lifetime maximum live (truck) load has been found to be 352.4 kN. It is observed that this value is very close to the standard wheeled vehicle of 400 kN (200 kN per axle) specified by Indian Roads Congress [2] for Class AA bridges.

During the reliability analysis at limit state of collapse in flexure, it has been observed that the failure in each case is in the rotation failure mode. Failures take place before the last hinge is formed to cause a complete failure mechanism.

A study of the results of the reliability analysis at limit state of collapse in flexure given in Table 2, reveals a slight decrease in the reliability index when the load is over the critical section 5 (Fig. 1). This is due to the special method of analysis and design used for the bridge. The bridge is being constructed by the cantilever method. As a result, during construction, the dead load due to self-weight is carried by cantilever action. Even after the fixation of the continuity cables at midspan, only the live load and the super-imposed dead load are carried by continuous beam action. Only after a period of 10 to 12 years, due to the relaxation of steel and the creep of concrete, the dead load will be carried by continuous beam action. As a result, there is an excess of strength in flexure at the supports. When the load is over the critical section 5, the moment at midspan, the weakest section of the girder, is more than that for the other load positions. Hence the reliability index for this position is lower than that for the rest. The reliability index for the limit state of collapse in flexure, for the girder unit taken as a system, is seen to be 7.75 (corresponding to $p_f = 4.77 \times 10^{-15}$) as shown in Table 2. This is much higher than the acceptable value of 2.5 to 3, normally used abroad. Thus, as expected, there appears to be an excess reserve of strength in the girder unit.

A study of Table 3, giving values of reliability index at limit state of collapse in shear, does not reveal any sharp variations in the reliability index as was observed in the case of flexure. This is because the failure in each case is predominantly at one of the 5 m deep sections, close to the interior supports, viz. 2, 4, 6, 8 or 10 (Fig. 1). The reliability index for the limit state of collapse in shear, for the girder unit taken as a system, is found to be 6.137 (corresponding to $p_f = 5.81 \times 10^{-10}$). This is higher than the generally accepted value of 2.5 to 3.0. The reason for this is the same as that for the limit state of collapse in flexure, viz. the use of the cantilever method of construction for the bridge.

Within the limitations of the present study, it can be concluded that the bridge has high reliability (reliability index greater than 6; probability of failure less than 10^{-9}) at limit states of collapse in flexure and shear. Reliability of the bridge in fatigue is an important aspect. Currently the state of knowledge in fatigue evaluation of concrete structures is not adequate to carry out reliability studies.

7. ACKNOWLEDGEMENTS

The authors gratefully acknowledge the assistance given by CIDCO, New Bombay, India, in providing the traffic survey data for the old Thana Creek Bridge and the Maharashtra Public Works Department, Bombay, in furnishing data on the test results of concrete cubes and steel strands. Thanks are also due to STUP Consultants Limited, Bombay, for providing the structural details of the bridge.

REFERENCES

1. NOWAK, A. S. and ZHOU, J. H., Reliability Models for Bridge Analysis. Report No. FHWA/OH-85/005, Department of Civil Engineering, Michigan, March 1985.
2. IRC:6-1966-SECTION II, Standard Specifications and Code of Practice for Road Bridges - Loads and Stresses. Indian Roads Congress, New Delhi, 1967.
3. MISTRY, Z. A., Reliability Based Design of Bridges. M.Tech. Thesis, Department of Civil Engineering, Indian Institute of Technology, January 1992.
4. BENJAMIN, J. R. and CORNELL, C. A., Probability, Statistics and Decision for Civil Engineers. McGraw Hill, New York, 1970, pp. 273-274.
5. IS:1343-1980, Code of Practice for Prestressed Concrete, Bureau of Indian Standards, New Delhi, 1981.
6. ELLINGWOOD, B. R., GALOMBOS, T. V., McGREGOR, J. G. and CORNELL, C. A., Development of a Probability Based Load Criterion for American National Standard A58. NBS Special Publication 577, U.S. Department of Commerce, Washington, D.C., June 1980.
7. MAJID, K. I., Nonlinear Structures. Butterworths, London, 1972.
8. IRC:18-1985, Design Criteria for Prestressed Concrete Road Bridges (Post -tensioned Concrete). Indian Roads Congress, New Delhi, 1986.

Remaining Structural Capacities of Steel Railway Bridges

Evaluation de la capacité restante de ponts de chemin de fer

Verbleibende Tragwerksfestigkeit von Eisenbahnbrücken aus Stahl

Makoto SHIMAMURA
Chief Researcher
East Japan Railway Co.
Tokyo, Japan

Masao SUGIDATE
Constr. Supervision Sect.
East Japan Railway Co.
Tokyo, Japan

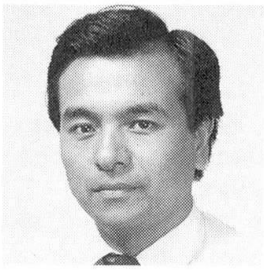

Tetsuo HORIGUCHI
Techn. Mgr.
Horigushi Consult. Corp.
Tokyo, Japan

Makoto ABE
Researcher
Railway Techn. Res. Institute
Tokyo, Japan

Akihiro KOSHIBA
Researcher
Railway Techn. Res. Institute
Tokyo, Japan

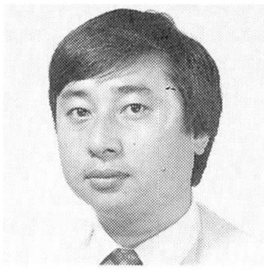

SUMMARY
The paper describes mainly the theoretical structure of the method of evaluating remaining structural strength and remaining life of steel railway bridges, as decided by committees and the fixing of reference values. This paper also describes the outlines and an embodiment of a computer-assisted system to facilitate its introduction to actual jobs.

RÉSUMÉ
Ce rapport décrit principalement la structure de la méthode d'évaluation de la capacité restante des structures de ponts de chemin de fer, ainsi que de leur longévité. Il résulte du travail d'un comité, qui a fixé des valeurs de référence. Ce rapport traite aussi de la création d'un système d'assistance par ordinateur, afin de faciliter l'introduction de cette méthode.

ZUSAMMENFASSUNG
Diese Abhandlung beschreibt hauptsächlich den theoretischen Aufbau eines Verfahrens zur Beurteilung der verbleibenden Tragwerksfestigkeit von Eisenbahnbrücken aus Stahl, das von verantwortlichen Ausschüssen auf der Grundlage von Bezugswerten festgelegt wurde. Die Abhandlung gibt ausserdem eine Übersicht über ein computerunterstüztes System zur Erleichterung seiner Einführung in die Praxis.

1. INTRODUCTION

Maintenance and management of steel railway bridges in Japan is faced with two problems. One is a fatigue problem as exemplified in Tokaido Shinkansen. The other is that the average age of steel railways is higher than 60 years-the design age. Both problems are based on fatigue. Evaluating remaining life is necessary. This remaining life evaluation was not generalized sufficiently. Recently, however, remaining life evaluation procedures and standards also have been developed. In addition, development of systems to process such evaluation has been made. This report is an outline of a fatigue damage evaluation system developed by Railway Technical Institute and BMC Corp.

2. DEFINITION OF SERVICE LIFE

Remaining life evaluation is made in relation to the following two points.
(1)"Structural life" when a main member reaches the end of its service life as a result of repetition of nominal stress.
(2)"The time of occurrence of fatigue crack" when members suffer fatigue damage due to local stress.
There are several definitions of "service life" which determines a period of time when a steel railway bridge can survive. According to one theory, service life expires when a bridge has suffered a fatal damage, economically and physically to such an extent that justifies the judgment that its structural strength and functions have been lost. Under this theory, service life means a physical service life considering the economic aspects of a bridge. Remaining service life is estimated by this method.
The "time of occurrence of fatigue crack" due to local stress is when fatigue damage has impaired the function of a particular member.

3. CALCULATING REMAINING LIFE

The Fig.1 illustrates an idea about formulation.

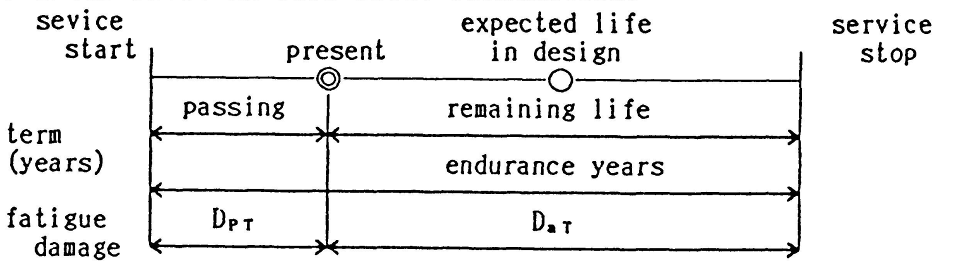

D_{aT} : (annual cumulative fatigue damage anticipated thereafter)×Tr
D_{PT} : up to a given time and cumulative fatigue damage

Fig.1 Life vs. passing years of a steel railway bridge

This analysis needs following data.
(1) History of live load
(2) Relation of live load with active stress
(3) Fatigue strength of joints in the precise target position.
These will generally require large data and practically made the work

troublesome. Therefore, the following items were taken into consideration for generalization.
(1) Regarding live load, axle load distributions were investigated for all railroad line territories and statistically processed to obtain a central value.
(2) For the relation of live load with a stress, an actual stress ratio (measured stress divided by design stress) was examined and rearranged. Fig.2 shows stress ratios (α) used for railway bridges at present.
(3) A fatigue test was conducted for long-life areas by service stress to determine evaluation strength.
This is a specimen. Live load was determined from the result of long-term (from about three months to one year here) measurement of real bridges.
The remaining life evaluation formula is as Fig.3.

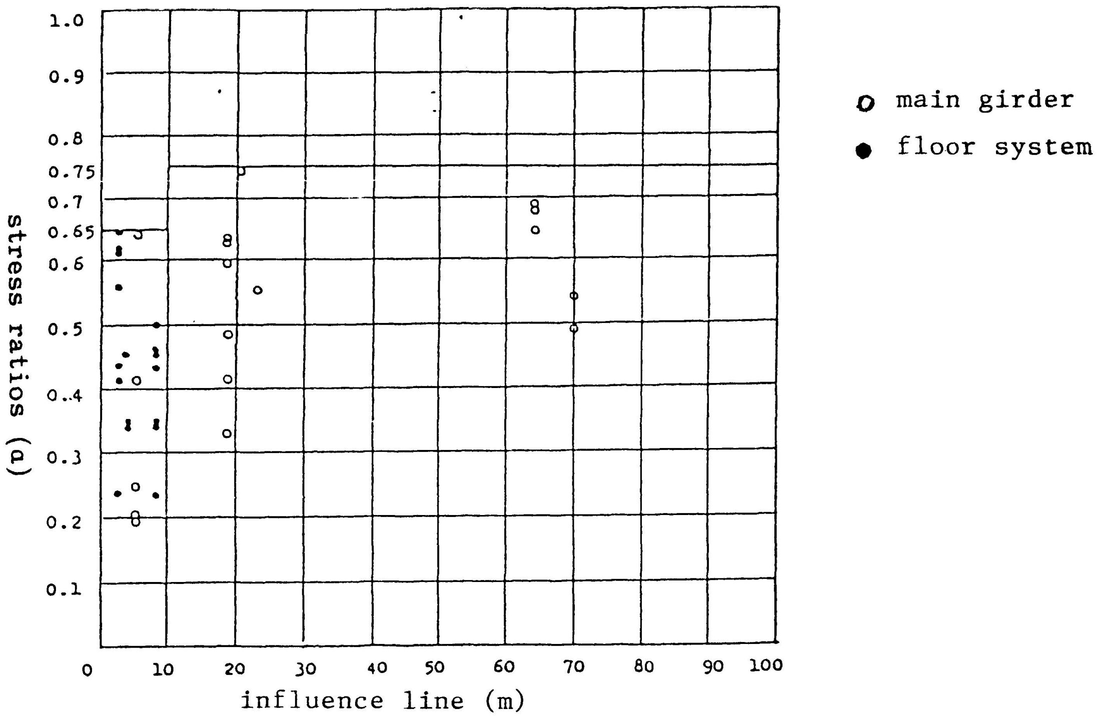

Fig.2 Research result of stress ratio

$$Tr = N_0(\ 1-D_{PT}\ )/\ \sum_{i=1}^{ka} \{n_{aeq(i)} \left(\frac{\Delta\sigma_{amax(i)}\ \alpha}{\Delta\sigma_{f0}} \right)^m \}$$

$\Delta\sigma_{amax(i)}$: maximum stress range exerted by trains operated in future.
$n_{aeq(i)}$: one year-equivalent number of cycles of maximum stress ranges exerted by passing trains.
$\Delta\sigma_{(i)}$, $n_{(i)}$: respectively stress range and its cycle, as obtaind by analizing the frequencies of variable stresses exercised by trains.
nn : level of stress range for frequency analysis of one passing train
Ny : number of trains passed in a year; if this is not a variable, $N=365\times n_{ad}$
n_{ad} : number of trains passed in a day.

Fig.3 Remaining life evaluation formula

4. BMC (Bridge Maintenance Consulting) SYSTEM

The results as mentioned above were programmed and rearranged into a fatigue diagnosis system capable of automatic processing. We call it FATIDAC system. This FATIDAC system is a part of the bridge maintenance and management system called BMC system. BMC system consists of :
(1) Bridge database
(2) Bridge diagnosis system
(3) Supporting system (expert system)
FATIDAC system forms a part of the bridge diagnosis system. The system has functions as a measuring instrument and executes measurement, evaluation analysis and outputting of a diagnosis report on the spot in a series of process. Data is registered on the database of the system and outputted in the form of a tabulation when necessary. This system is used for bridge diagnosis of decaying bridges abroad. BMC system performs also the following.
(1) Live load calculation
(2) Bearing capacity calculation
(3) Calculating vibration in relation to running performance
(4) Bridge stability calculation

5. EXAMPLE

Items for processing are as shown in the fig.4. The first example relates to prediction of occurrence of a local fatigue damage.
(1) Stress in the precise target position in measured. Concerning fatigue to be measured, a position to which a gage is fitted is shown in the standardized manual.
(2) Sampling is made several times, which is necessary for stress frequency analysis. (generally for statistical purpose)
(3) Live load history is inputted on the basis of the result.
(4) The cumulative fatigue damage ratio calculated.
(5) D value as a result of this calculation is judged in accordance with the category of judgment. A requires some measure and B will be confirmed on a priority basis by inspection in the future.(Fig.5)
(6) Finally an examination report is outputted. In this

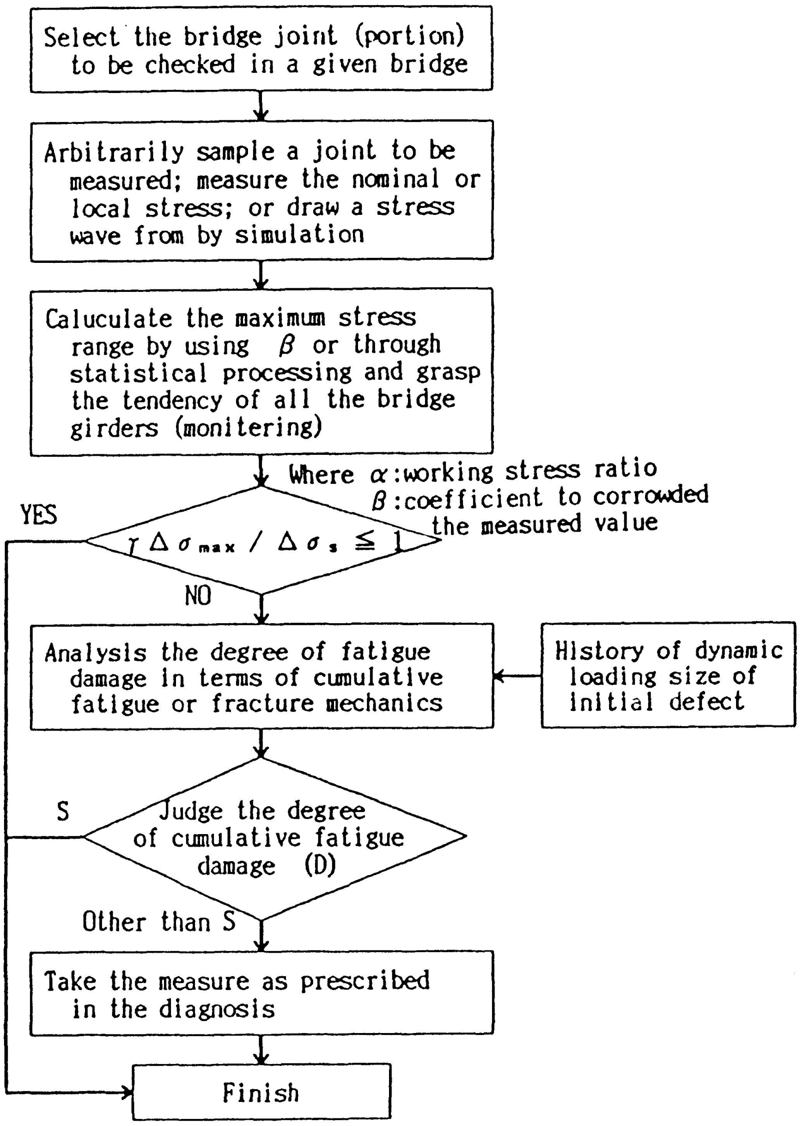

Fig.4 Flow chart of fatigue damage cheking

case, in accordance with the results of judgement early, a specific remedy is suggested. A suggests that a measure should be taken immediately in accordance with S-13 in the manual. B indicates that it should be inputted as a priority inspection item in the next general inspection. (Fig.6) This system is being employed widely for diagnosis of steel railway bridges by all Japanese Railway Companies, including Tokaido Shinkansen and private railway companies. Timely diagnosis ensures quantitative and objective bridge diagnosis.

累積疲労損傷度による健全度判定区分

累積疲労損傷度（D）		判定区分	検査への反映
D ≧ 1.0		A1	個別検査の実施
1.0 ＞ D ≧ 0.8		A2	
0.8 ＞ D ≧ 0.5		B	重点検査項目へ
0.5 ＞ D ≧ 0.2	D ≧ 経年 / 設計想定寿命		
	D ＜ 経年 / 設計想定寿命	C	検査の着目箇所へ
D ＜ 0.2		S	通常通りの検査

注）1．Dの値は、個別に着目した箇所か、もしくは桁全体に適用する場合は、サンプリングした調査箇所）の平均値で判断してよい。
2．設計想定寿命：普通鉄道は６０年、新幹線は７０年を想定している。
（本四架橋は１００年）

Fig.5 Category of cummulative fatigue damage ratio

疲労損傷に対する診断書（累積疲労損傷度）

（1） 一 般 BMC Fatidac SySTEM

橋梁名	日本橋梁		桁番号	13	図面番号	WDG610－101
部材名	主桁	部位	上下フランジ		グループ名	BMC－1
適用する評価基準	JR保守標準（仮）				処理日	1992. 6. 4

（2） 各着目箇所に対する評価結果

解析内容		評価の基準値			累積疲労損傷度	累積疲労損傷度に対する判定区分
No	着目継手箇所	200万回強度 (MPa)	m	打切限界 (MPa)		
1	主桁下フランジガセット	65	3	21	2.72	A₁
2	主桁下フランジ	100	3	39	0.75	B
3	主桁上フランジガセット	65	3	21	0.61	B
4						
5						

（3） 判定結果と措置

解析No	判定区分	記事
1	A₁	「鋼構造物補修・補強・改造の手引き」のS－13を参考に対策を検討して下さい。
2	B	次回の「全般検査」では、重点検査項目として追加し、必ず確認して下さい。
3	B	次回の「全般検査」では、重点検査項目として追加し、必ず確認しこ下さい。

Fig.6 Example of examination report

REFERENCES

1. ABE,M. et al., Development of a System for Estimating the Remaining Life of a Steel Railway Bridge. The Second Japan-Korea Joint Seminar on Steel Bridges, Tokyo, Japan, July 1992.

2. HORIGUCHI,T. et al.,Development of Fatigue-Damage Rating System for Steel Bridges.
Proc. of the 4th Inst. Conf. on Fatigue and Fatigue Thresholds, July 1990 in Honolulu.

Remaining Service Life of a Riveted Railway Bridge
Durée de vie restante d'un pont-rail riveté
Restnutzungsdauer einer genieteten Eisenbahnbrücke

Eugene BRÜHWILER
Dr. Eng.
Swiss Federal Railways
Zurich, Switzerland

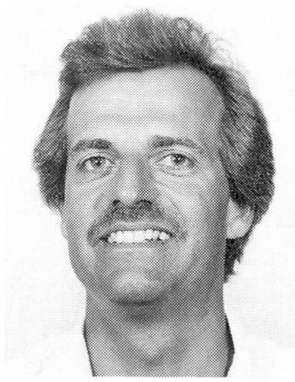

Eugene Brühwiler, born 1958, received his civil engineering and doctoral degree from the Federal Institute of Technology in Zurich and Lausanne. Since 1990, after a post-doctorate at the University of Colorado, Boulder (USA), he is involved in the evaluation of the remaining service life of bridges for the Swiss Federal Railways.

Peter KUNZ
Research Associate
Swiss Fed. Inst. of Technology
Lausanne, Switzerland

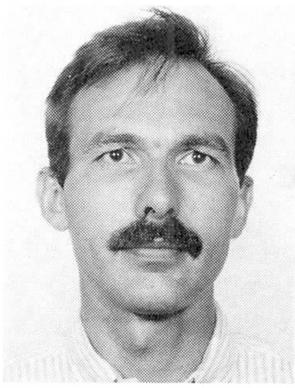

Peter Kunz, born 1959, graduated from the Federal Institute of Technology in Zurich and obtained his doctoral degree at the Federal Institute of Technology in Lausanne. He works in the fields of fatigue and evaluation of existing bridges at ICOM (Steel Structures).

SUMMARY
The remaining service life of a riveted wrought-iron bridge from the last century is assessed. The case study concentrates on the application of probabilistic concepts for evaluating fatigue safety. The theoretical studies are complemented by strain measurements on the most fatigue critical members and by a thorough visual bridge inspection. Based on the results of this study, allowable rail traffic load and optimum inspection intervals are established.

RÉSUMÉ
La durée de vie restante d'un pont-rail riveté en fer-puddlé du siècle passé est évaluée. L'étude se concentre sur l'application de méthodes probabilistes pour vérifier la sécurité à la fatigue. Ces études théoriques sont complétées par des mesures d'élongation sur des éléments de pont les plus critiques concernant la fatigue et par une inspection visuelle du pont. Sur la base des résultats de cette étude, la charge de trafic admissible et les intervalles d'inspection sont établis.

ZUSAMMENFASSUNG
Die Restnutzungsdauer einer genieteten, schweisseisernen Eisenbahnbrücke aus dem letzten Jahrhundert wird untersucht. Die Fallstudie konzentriert sich auf die Anwendung probabilistischer Methoden für die Ermittlung der Ermüdungssicherheit. Die theoretischen Studien werden ergänzt mit Dehnungsmessungen an ermüdungskritischen Bauteilen und einer visuellen Inspektion. Basierend auf den Ergebnissen dieser Studie werden zulässige Bahnlasten und optimale Inspektionsintervalle festgelegt.

1 INTRODUCTION

Riveted bridges were built until the 1950s. There are thousands of riveted bridges around the world which are still in service. Most old bridges have been restricted to reduced permissible loads or repaired; critical elements have been reinforced or even replaced. Some bridges are subjected to more severe loading than was envisaged during their design due to increased traffic and higher axle loads. Economically, it is not possible nor justified to replace all bridges when they reach their "design lives". Often there is a considerable reserve and a remaining service life may be justified provided that inspection guidelines are followed.

This paper deals with the investigation of the reliability and remaining service life of a 118 year-old bridge on a branch railway line. Standard engineering methods revealed various bridge members to be fatigue critical. Since fracture of a chord member could result in collapse of the bridge, a severe load restriction was imposed on the bridge. This load restriction hampered the freight service on the line resulting in substantial financial loss. As a consequence, a thorough investigation of the structural reliability was conducted applying, the method for evaluating the fatigue safety as developed in [1] and summarized in a companion paper [2].

2 DESCRIPTION OF THE BRIDGE

The investigated bridge crosses the Rhine river in Northern Switzerland near Lake Constance. It was built in 1875 and comprises riveted wrought iron members. The straight through truss bridge is a continuous girder bridge over four spans with a total length of 254 m (Fig. 1). The two main girders are of a truss-type construction with parallel chords and cross-wise diagonals. The single track is not ballasted; the timber sleepers are fixed directly to the stringers.

The bridge structure has been strengthened several times to allow for higher traffic loads. At the end of the last century, all major elements of the bridge were reinforced. In 1936, the stringers were strengthened for a second time, and in 1964 several truss nodes of the main girders were reinforced using high-strength bolts. Apart from some local corrosion, the present state of the bridge structure is satisfactory.

From 1875 until 1968, a mixed freight and passenger traffic of about 25 trains per day was crossing the bridge. Since 1969, this branch line has been exclusively in service for a daily traffic of 15 freight trains. To date, a total of 850'000 trains have crossed the bridge which is a moderate traffic compared to main lines with a daily traffic of about 120 trains.

3 LOAD CARRYING CAPACITY

A structural analysis is performed first to determine the load carrying capacity of the bridge. The action effect S is calculated using actions and load factors according to the Code SIA 160 [3] with the load model corresponding to UIC 702 [4]. The resistance R for wrought iron is chosen based on [5, 6, 7] which include test results for wrought iron specimens from bridges built in Switzerland in the last century. The load carrying capacity is expressed by

$$\mu = \frac{R/\gamma_R}{S} \tag{1}$$

μ : load carrying capacity ratio
R : resistance
γ_R : resistance factor (=1.20)
S : action effect

For $\mu > 1$, the investigated element fulfills the structural safety required by SIA Code. For $\mu < 1$, the load carrying capacity in terms of admissible rail traffic load is established. The structural analysis reveals that the main girders are the governing elements regarding load carrying capacity of the bridge. The minimum value for μ, equal to 0.80, is obtained for the top chord members over the piers.

4 FATIGUE SAFETY

4.1 Proceeding in stages

The fatigue safety is verified using a method described in [1], proceeding in stages with increasing level of sophistication:

1. Simplified deterministic method (chap. 4.2)
2. Simplified probabilistic method (chap. 4.3)
3. Inspection intervals (chap. 4.4)
4. Detailed probabilistic method (chap. 4.5)

The aim of the first stage is to identify the fatigue critical members of the structure. The probability of failure p_f due to fatigue is calculated in stages 2 and 4. The probability of crack detection $\bar{p}(cd)$ during inspection is evaluated in stage 3, and subsequently linked to p_f to obtain the probability of rupture p_{rupt} :

$$p_{rupt} = p_f \cdot \left[1 - \bar{p}(cd)\right] \tag{2}$$

p_{rupt} : probability of rupture
p_f : probability of failure
$\bar{p}(cd)$: probability of crack detection in a construction detail

The probability of rupture can also be expressed by means of the reliability index β_{rupt} according to the standard normal distribution. Finally the reliability of a structural element is compared to the target value β_t :

$$\beta_{rupt} > \beta_t \tag{3}$$

β_{rupt} : reliability index with respect to rupture
β_t : target reliability index

The target value β_t for fatigue safety is adopted based on proved values assumed in the design of structures where a reliability index of 4.7 is often used; this corresponds to a probability of rupture of about 10^{-6} per year. Assuming a design life of 100 years, p_t drops to 10^{-4} or β_t = 3.7 over the entire service life of the structure. The probability of rupture due to fatigue should not be larger than structural safety. Consequently, a target value β_t = 3.7 is considered in this study for the total collapse of the structure resulting from fatigue failure of the detail being assessed.

4.2 Simplified deterministic method

The fatigue safety of all bridge members is checked by the following ratio:

$$v_{fat} = \frac{\Delta\sigma_C/\gamma_{fat}}{\Delta\sigma_e} \tag{4}$$

with

$$\Delta\sigma_e = \alpha_{SIA} \cdot \alpha_N \cdot \Delta\sigma(\Phi \cdot Q_{fat}) \tag{5}$$

v_{fat}	:	fatigue safety ratio
$\Delta\sigma_C$	:	fatigue resistance to $2 \cdot 10^6$ cycles (= 67 N/mm^2) [5, 7, 8]
$\Delta\sigma_e$	:	fatigue load effect refered at $2 \cdot 10^6$ cycles
γ_{fat}	:	fatigue resistance factor
α_{SIA}	:	correction factor from the SIA Code 161
α_N	:	correction factor taking into account the number of trains in the past [1]
$\Delta\sigma(\Phi \cdot Q_{fat})$	:	stress difference due to the fatigue load defined by UIC (International Union of Railways) multiplied by the dynamic factor

The resistance factor γ_{fat} is adopted to obtain a reliability index β_t of 3.7 [1]. For redundant details causing local failure, γ_{fat} = 1.20 is chosen, and for elements leading to total collapse of the structure, γ_{fat} = 1.34 is considered.

Based on this deterministic method, the bridge members are compared, and a ranked list identifying fatigue critical bridge details is established. Details with v_{fat} < 1 require further investigation and inspection. Fatigue safety is verified if v_{fat} > 1.

The lowest v_{fat}-values are calculated for truss elements of the main girders. This is an uncommon result because frequently the stringers are the most fatigue critical elements of old bridges with non-ballasted track. This result is explained by the various strengthening measures; stringers and cross girders were reinforced more than the main girders.

Due to the continuity of the bridge over four spans, the influence line for the chord members (Fig. 4) shows both high compressive and tensile stresses at the zero-moment locations. The fatigue action is thus greater than the action effect that was considered for structural safety during design and strengthening. Consequently, the simplified deterministic method identifies the chord members at zero-moment locations between the nodes 7 and 8, 12 and 13 as well as 19 and 20 as the most fatigue critical members of the main girders (Fig. 1).

The minimum value for v_{fat} (= 0.69) considering 850'000 trains is calculated for chord member 18/19. This is considerably smaller than 1, and a more thorough investigation based on probabilistic concepts is therefore performed.

4.3 Simplified probabilistic method

The reliability index for fatigue failure of a bridge member is evaluated as follows:

$$\beta_t = \frac{m_R - m_S(N_{fut})}{\sqrt{s_R^2 + s_S^2}} \tag{6}$$

m_R : mean of the fatigue strength (= $\log\Delta\sigma_C + 2 \cdot s_R$)
$m_S(N_{fut})$: mean of the fatigue load effect as a function of the number of future trains N_{fut}
s_R : standard deviation of the fatigue strength (= 0.11)
s_S : standard deviation of the fatigue load effect (= 0.04)

The background and the assumptions as well as the results and the correction factors needed to calculate m_S are presented and discussed in [1, 2].

The reliability index β_f as a function of the number of future trains N_{fut} is calculated. The probability of crack detection due to inspections is not considered, thus $\bar{p}(cd) = 0$; and from equation (2) follows: $\beta_{rupt} = \beta_f$. The result is shown in Figure 2 with N_{fut} represented on a log-scale.

The reliability index is now compared to the target value $\beta_t = 3.7$. The calculated β-value of chord members 18/19 is smaller than β_t; a more detailed analysis is necessary. There are two ways to influence the calculated reliability index:

(1) to optimise the **inspection intervals**, considering the probability of crack detection, and
(2) to refine the assumptions and calculate p_f using a **detailed probabilistic method**.

4.4 Inspection intervals

By a fracture mechanics analysis, the critical crack length of the most likely crack in chord member 18/19 is calculated using the R6-method [9]. Assuming fracture toughness values K_{IC} of 1500 N/mm$^{3/2}$ and 2000 N/mm$^{3/2}$, critical crack sizes a_c of 70 and 100 mm respectively are calculated. Subsequently, the probability of detecting a crack shorter than the critical crack is assessed. For this, the relation between the probability of crack detection and visible crack length must be known for steel bridges. Due to the lack of relevant information, an estimate based on literature regarding offshore structures is adopted [1].

Figure 3 shows the probability of crack detection $\bar{p}(cd)$ as a function of the number of trains between two inspections $N_{p,insp}$. Inspection intervals can be fixed; for example for

$\bar{p}(cd) = 0.95$, the chord member must be inspected after every 17'000 trains. Putting $\bar{p}(cd)$ equal to 0.95 in equation (2) a value of 3.3 is obtained for β_{rupt} for the present state, which is still smaller than the target value (Fig. 2).

4.5 Detailed probabilistic method

For the detailed probabilistic analysis, refined rail traffic models for the past and future are needed. The rail traffic model in the past is based on statistical data provided by the Swiss Federal Railways regarding the number of trains and towed load. The rail traffic model for the future considers the expected freight traffic on this line.

The calculated reliability index as a function of the number of future trains is shown in Figure 2. β is equal to 3.4 for $N_{fut} = 150'000$. Fixing the inspection intervals so as to give a 95 % probability of crack detection, a reliability index β_{rupt} of 4.15 is obtained using equation (2), which is greater than the target value β_t of 3.7. Fatigue safety could also be verified for even more trains; yet the bridge owner is primarily interested in the reliability of the bridge for the next 25 years.

Figure 2 shows a striking increase in β from the simplified to the detailed probabilistic method. This is explained by the significantly smaller towed load and length of the trains on this branch line when compared to the traffic load models used in the simplified method. For main lines with usually higher loads and longer trains, there is a better agreement between service and traffic model loads, and consequently, the difference in β between the simplified and the detailed probabilistic method is smaller.

5 FIELD TESTING

The main objective of the field testing is to verify the structural models. Top and bottom chord members between the nodes 18 and 19 (Fig. 1) have been equipped with strain gauges, and the strain history due to an engine of six axle loads equal to 177 kN has been recorded. There is a small difference between the measured and calculated influence lines for the bottom chord member 18/19 (Fig. 4); such good agreement is frequently observed for truss girders.

6 BRIDGE INSPECTION

The field investigation included a thorough visual bridge inspection. Cracks have been detected at details with sharp corners located at the reinforced parts of the stringers. These cracks may not affect the structural integrity because crack propagation is likely to stop. Such "undangerous" cracks are usually not revealed by analysis, which emphasizes the importance of bridge inspection and study of construction details.

"Dangerous" fatigue cracks affecting the structural integrity (such as those investigated in the foregoing sections) could not be detected. This is in agreement with the theoretical investigation predicting that - at present - any fatigue crack is likely to be shorter than the crack that could be detected by visual inspection.

7 CONCLUSIONS

1. Comprehensive assessment of the remaining service life of railway bridges includes theoretical studies of the structural reliability, bridge inspection and field testing.
2. A method for the evaluation of fatigue safety which proceeds by stages of deterministic and probabilistic calculations of increasing sophistication has been demonstrated. Probabilistic methods enable the consideration of the scatter of the parameters that influence both the fatigue strength and damage accumulation.
3. Based on fracture mechanics and probabilistic concepts, inspection intervals are assessed and considered in the evaluation of structural reliability.
4. By means of strain measurements on fatigue critical members, the load carrying behaviour of the structure is evaluated and a more accurate (and usually lower) value for the stress range is determined, which is the most dominant parameter influencing the fatigue safety.

As a consequence of this study, the severe load restriction imposed on the bridge was removed for the next 170'000 trains. In addition to the main inspection every 5 years, a supplementary inspection of the fatigue critical chord members of the main girders is now conducted at yearly intervals. This thorough evaluation is cost effective because it now allows for practically unrestricted rail traffic for the next 25 years.

ACKNOWLEDGEMENTS
The Measurements and Instrumentation group of the Swiss Federal Railways is thanked for the carefully prepared and conducted bridge measurements.

REFERENCES

[1] KUNZ P., Probabilistic method for the evaluation of fatigue safety of existing steel bridges. Doctoral Thesis Nr. 1023, ICOM - Steel Structures, Swiss Federal Institute of Technology Lausanne, Switzerland, 1992. (in German)
[2] KUNZ P. and HIRT M.A., Remaining fatigue life of steel railway bridges. Proceedings, IABSE - Colloquium "Remaining Structural Capacity", Copenhagen, Denmark, March 17-19, 1993.
[3] SIA Code 160: Actions on structures. Swiss Society of Engineers and Architects. 1989.
[4] UIC 702 V. Load model for the analysis of structures of international lines. International Union of Railways, 1974.
[5] UIC 779-1 E. Recommendation for the evaluation of the load carrying capacity of existing steel bridges. International Union of Railways, 1986.
[6] KULAK G., FISHER J.W., STRUIK J.H., A Guide to Design Criteria for Bolted and Riveted Joints. Second Edition. New York: John Wiley & Sons, 1987.
[7] BRÜHWILER E., SMITH I.F., HIRT M.A., Fatigue and fracture of riveted bridge elements. Journal of Structural Division, ASCE, Vol. 116, No. 1, January 1990, pp. 198-214.
[8] ECCS Publication Nr. 43. Recommendations for the Fatigue Design of Steel Structures. European Convention for Constructural Steelwork, Brussels, 1985.
[9] HENSEN W., Concepts for the evaluation of the remaining service life of old steel bridges. Doctoral Thesis, Technical University RWTH Aachen, 1992. (in German)

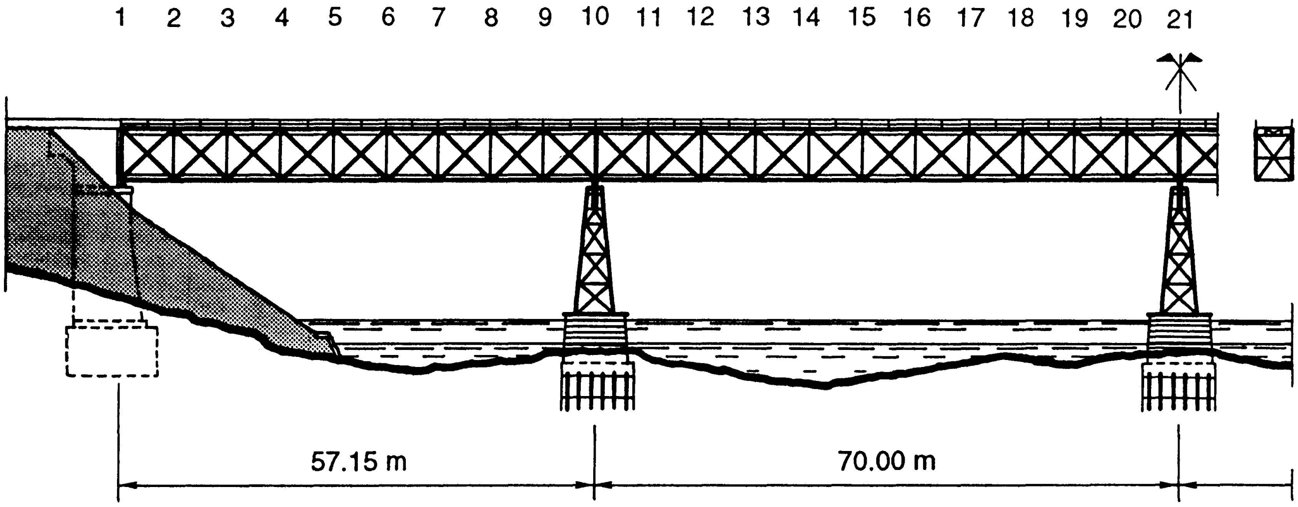

Figure 1 View of the investigated truss bridge (one half)

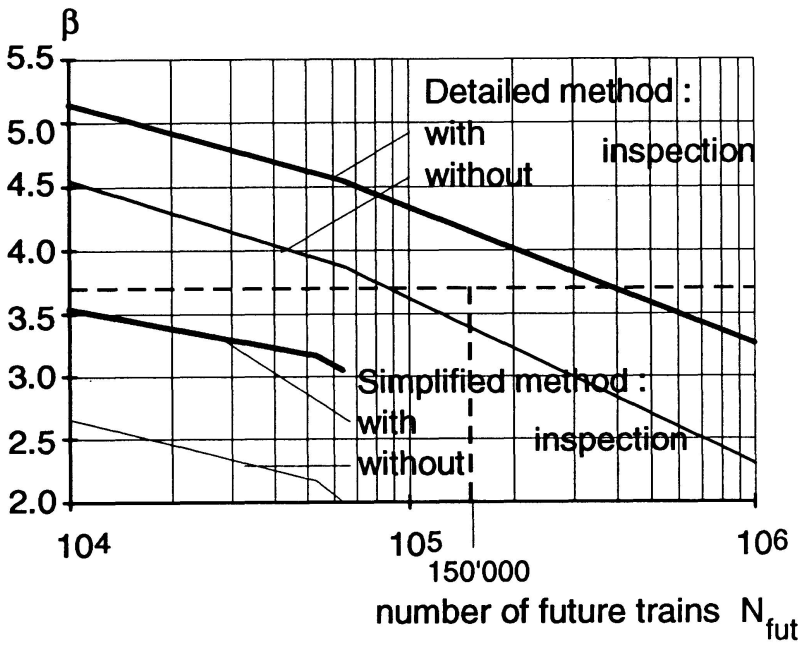

Figure 2 Reliability index for chord member 18/19 as a function of the number of future trains for simplified and detailed probabilistic approach

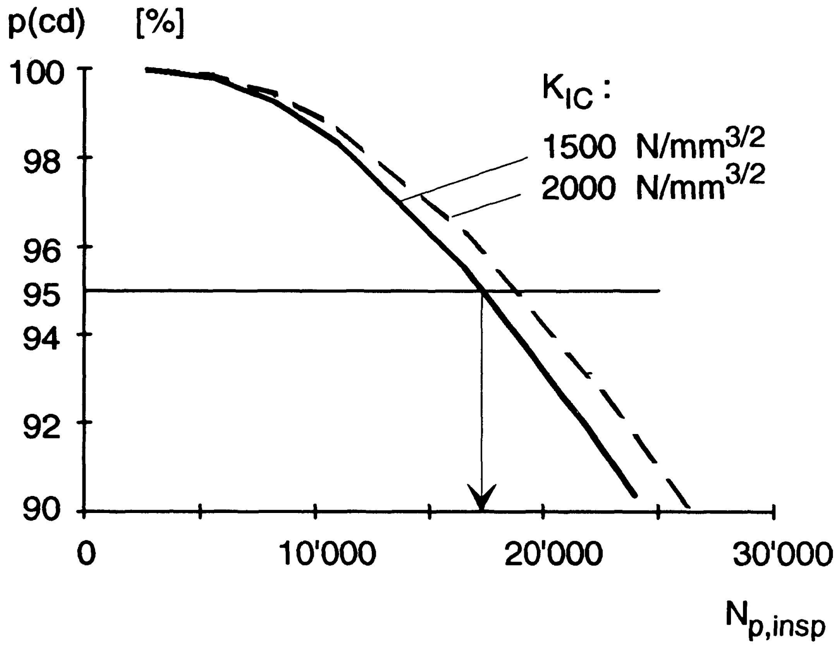

Figure 3 Probability of crack detection in chord member 18/19 as a function of inspection intervals

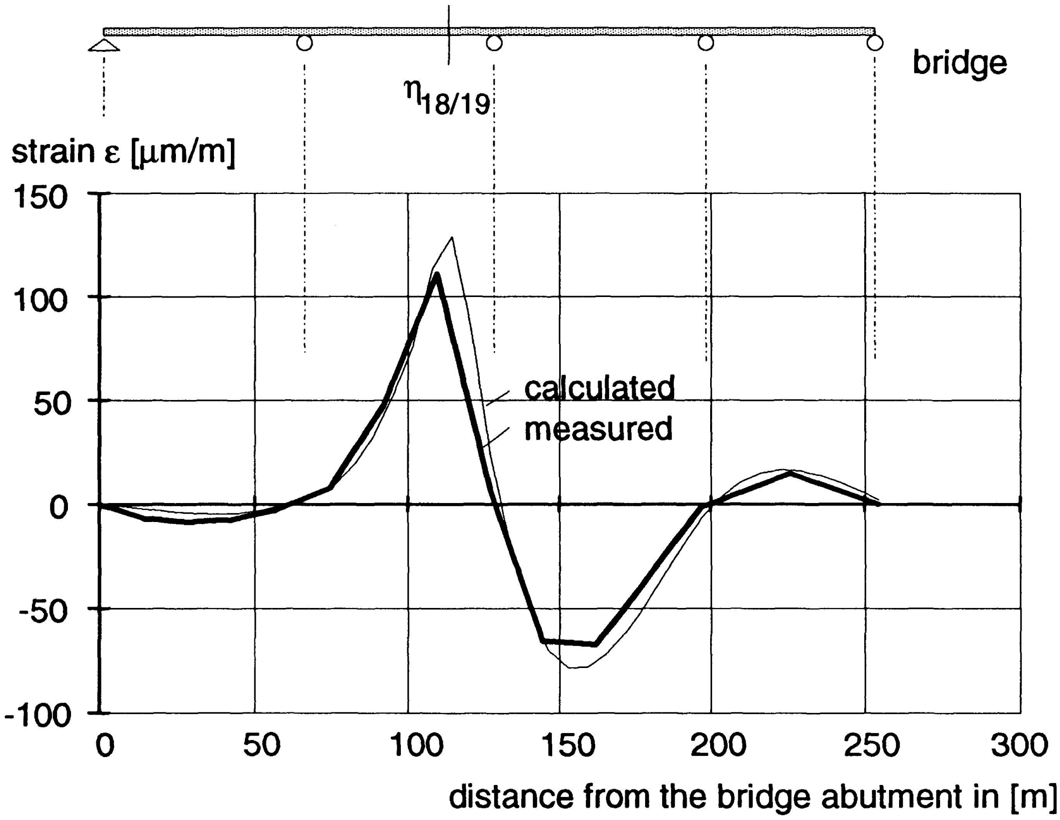

Figure 4 Comparison between calculated and measured influence lines for bottom chord member 18/19 due to the passage of the engine. (The stress values are evaluated from the strain readingsusing an elastic modulus of 200'000 MPa.)

Test Results from Suspension Cables Preloaded in Practice
Résultats d'essais sur des câbles de suspension préchargés en pratique
Erkenntnisse aus der Prüfung baupraktisch vorbelasteter Brückenseile

Wolfgang HARRE
Dr. Eng.
Otto-Graf-Institut
Stuttgart, Germany

Wolfgang Harre, born 1938, got his civil engineering degree at the University of Karlsruhe, Germany. In 1966, he moved to the University of Stuttgart, Germany, where he got his doctor degree in 1972. Since 1980, Wolfgang Harre is responsible for materialtesting and research on metal structures at the Otto-Graf Institute.

SUMMARY
The report deals with test results of suspension cables, which were dismantled from existing bridges after more than 25 years in service and then tested under static and dynamic loadings. The results show a remarkably high remaining fatigue strength. Furthermore the tests clearly showed that fretting corrosion has a dominating influence on the extension of damages. The introduced stress range is the most effective load parameter governing the fatigue strength.

RÉSUMÉ
Un rapport est donné des études réalisées sur des câbles de suspension qui, après 25 années de service dans des ponts existants, ont été démontés et soumis à des essais sous charges statiques et dynamiques. Les résultats révèlent une résistance à la fatigue restante remarquable ainsi qu'une influence dominante de la corrosion par frottement sur l'extension des dégâts. La variation de contrainte introduite s'avère comme le paramètre le plus effectif qui domine la résistance à la fatigue.

ZUSAMMENFASSUNG
Es wird über Untersuchungen an Brückenseilen berichtet, die nach über 25jähriger Betriebsbeanspruchung und Brückenbauwerken ausgebaut und anschliessend statischen und dynamischen Beslastungsversuchen unterworfen wurden. Die Ergebnisse lassen u.a. eine bemerkenswert hohe Resttragfähigkeit sowie einen dominierenden Einfluss der Reibkorrosion beim Schädigungsverlauf erkennen. Die einwirkende Schwingbreite der mechanischen Beanspruchung erweist sich als vorherrschender ermüdungswirksamer Belastungsparameter.

1. INTRODUCTION

Despite the spread use of cables as tension members in bridge structures since many decades, the knowledge concerning the fatigue behavior of these cables is still very poor. Neither a sufficiently supported Δσ-N-curve (Wöhler-diagram) is known, nor the substantial proof of a fatigue strength limit for such cables really exists. Completely unknown is the effect of variable amplitude loading, i.e. the increase of fatigue strength respectively fatigue life when the fatigue loading changes from constant amplitudes to variable amplitudes, the more realistic loading. Testing with variable amplitudes related to the practice will shift the WÖHLER-diagramm (Δσ-N-curve for constant amplitude loading) towards a higher fatigue strength equivalent a longer fatigue life. The amount of increase in fatigue life depends on the amplitude spectrum.

In consequence of the lack of comprehensive basic knowledges concerning their fatigue behavior, the cables for every cable-stayed bridge going under construction have to pass a standard test program according to formerly DIN 1073 respectively now DIN 18809, which has no relationship at all to practice and which represents a very unsatisfactory proceeding since many decades! There are mainly two reasons for the lack of basic knowledges: a) in the earlier past no suitable testing equipment was available to run tests under random load conditions as well as with comparatively high forces (~1 to 10 MN), and b) to create a complete WÖHLER-diagram or Δσ-N-curve requires a great number of specimens, i.e. the enormous financial expense even only for the specimens has prevented until now the realization of any proposed test program.

Nowadays the situation has somewhat changed: Suitable testing equipments are developped and available. However the fabrication costs of the specimens remain still extraordinarily high, so that extensive and systematical investigations on new fabricated test specimens of cables will be quasi out of reach now and in the near future. On the other hand, there are meanwhile several cable-stayed bridges in service, which will be or should be overhauled partly or completely soon. In the course of such bridge "renovations" the cables will often be replaced. Instead of scrapping them, the dismantled cables could be used on for experimental investigations as practically preloaded test specimens almost free of charge!

First aim of such investigations would be to set up a sufficiently covered WÖHLER-diagram of preloaded cables in the sense of a lowerbound-curve for the classification of the fatigue behavior of cables in general, as well as to obtain founded informations regarding the damage progress and the remaining fatigue life of preloaded cables.

The recently accomplished investigation program, carried out at the Otto-Graf-Institut, on dismantled cables of the NORDERELBE-bridge near Hamburg and of the FEHMARNSUND-bridge to Denmark can be considered as a first step in the above described direction.

The gained results-partly contradictory-reveal the considerable deficit in knowledge at present and the actual inability to evaluate the fatigue strength, the influence of damaging factors and the remaining fatigue life of cables. In this report, the most important results of the conducted investigations up to now are presented in a compact form and conclusions are pointed out.

2. FEHMARNSUNDBRIDGE

2.1 Statement of the problem

In 1980 the Otto-Graf-Institut was commissioned to investigate a cable dismantled of the Fehmarnsundbridge. During an inspection and examination of the bridge it was found out that some of the 80 suspension cables had a badly corroded surface. The protection against corrosion came partly off, the gaps between the wires in the outer layer were opened and there were intense corrosion induced pittings. As a decision base for the neccessary sanitation, the dismantled cable should be subjected to detailed material testing and technological investigations. In this report, only the most important mechanical-technological results will be presented. More detailed informations can be found in [1].

2.2 Testing program

The following testing program was arranged and carried out.

2.2.1 Cable specimen A

Constant amplitude fatigue test with $\Delta\sigma$ = 125 N/mm², N_G = $3{,}3\cdot10^6$ cycles; afterwards a constant amplitude fatigue test with $\Delta\sigma$ = 200 N/mm² until N = $0{,}20\cdot10^6$ cycles; afterwards a statical rupture tension test.

2.2.2 Cables specimen B

Constant amplitude fatigue test with $\Delta\sigma$ = 125 N/mm², N_G = $2{,}0\cdot10^6$ cycles; afterwards a constant amplitude test with $\Delta\sigma$ = 200 N/mm² until N = $0{,}50\cdot10^6$ cycles.

The tests were conducted in a hydraulic 5-MN testing machine, see figure 1.

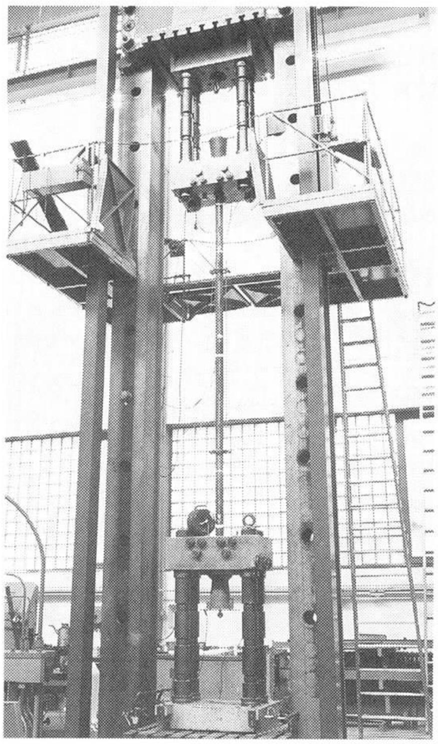

Fig. 1 Test set-up

2.3 Fabrication of the cable specimens A and B.

Figure 2 shows where the cable selected for testing (D9') was taken from the bridge.

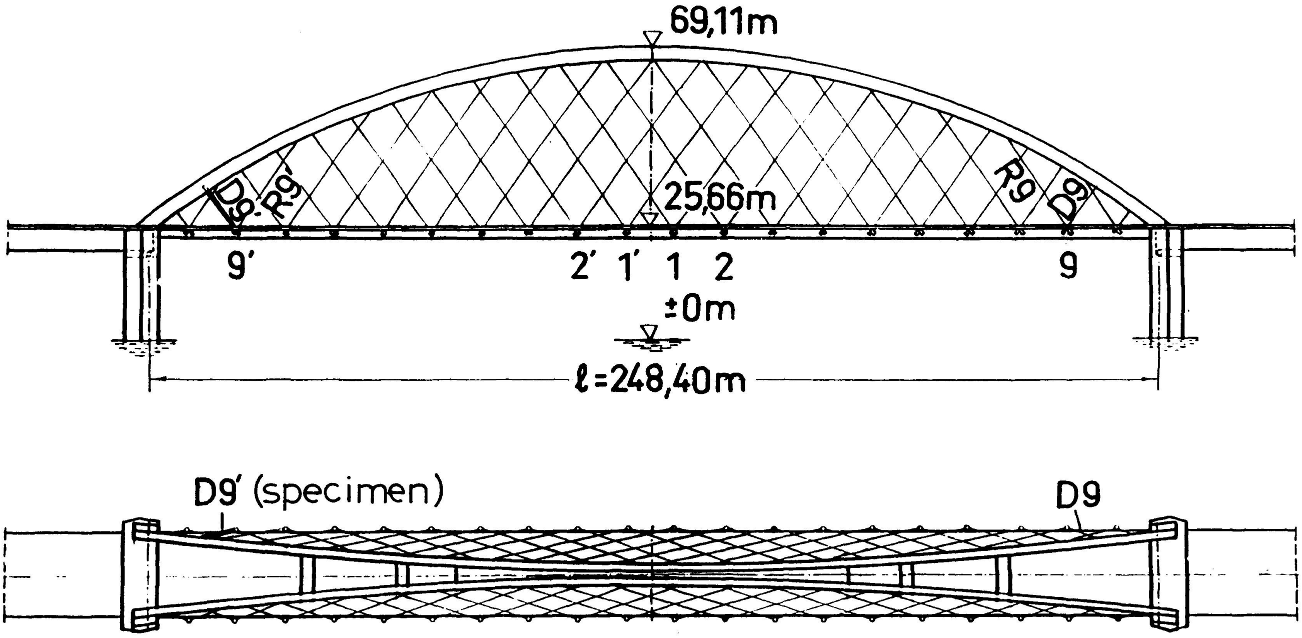

Fig. 2 Fehmarnsundbridge-survey

The cable, about 14,20 m long, ϕ 81 mm, was substantially divided into 3 different segments.

The upper part of the dismantled cable with a length of about 3,60 m was used for material- and corrosion tests. After cutting off the upper anchorage and extrusion of the anchor socket, the latter one was applied as anchorage to the upper end of cable specimen B.

Cable specimen A was made of the middle part (length = 5,40 m) of the dismantled cable by attaching special test anchor sockets on both ends.

From the lower part of the dismantled cable (length = 5,20 m) with the remaining original anchorage at the lower end, cable specimen B was made by attaching as mentioned above the anchor socket of the initially upper cable part to the upper end of the test specimen.

The casting of the sockets was done by Thyssen Draht AG, Gelsenkirchen. Casting metal was ZnAl6Cu1 (Zamak 610). Test specimens A and B had a free cable length of 4,50 m each.

3. NORDERELBEBRIDGE

3.1 Statement of the problem

When the highwaybridge over the river Norderelbe near Hamburg (built in 1962) was subjected to a comprehensive sanitation in 1985, the Otto-Graf-Institut was commissioned to investigate the dismantled cables ϕ 72 mm. On the base of the test results obtained from Fehmarnsundbridge [1], the intention was to achieve further contributions and clarifying informations in the field of longtime fatigue behavior and remaining fatigue life of cables and cable-stayed bridges. Detailed descriptions are given in [2].

3.2 Testing program

The following testing program was planned and conducted.

3.2.1 Cable specimen C

The specimen was taken from the free length of the dismantled cable. Constant amplitude fatigue test with $\Delta\sigma$ = 150 N/mm² and with simultaneously applied transverse pressure of 19 kN/cm. The same test was made in 1962 with a specimen of the new cables when the bridge was under construction. It was expected from this test repetition to find out, whether the fatigue strength of the cables is reduced by the service over a period of more than 25 years and if yes, how much it is reduced.

3.2.2 Cable specimen D

The specimen was taken from the end area of the cable with an original anchorage kept on; constant amplitude fatigue test with $\Delta\sigma$ = 150 N/mm², no transverse pressure.

3.2.3 Cable specimen E

Constant amplitude test with an original cable-saddle, containing two cables turned around, one upon the other, $\Delta\sigma$ = 150 N/mm². The aim of this test was to study the behavior of the cables under realistic transverse pressure conditions existing in such saddle-or turn around structures with several layers of cables.

All the tests were designed to run until the provided limit number of cycles N_G = $2{,}0 \cdot 10^6$ is reached respectively until the recorded wire cracks increase progressively. At the end of the tests, a

controlled opening of the cables and anchorages was planned in order to register the wire cracks and analyse the damage.

In the following report, only the most essential mechanical-technological results are presented. Further details and informations can be taken from [2].

The tests with the specimens C and D were carried out in the 5-MN testing machine in the same way like the tests with the specimens A and B of Fehmarnsundbridge [1]. As to speciment E a special testing equipment had to be developped (see figures 3 and 4), a detailed description of it is given in [2].

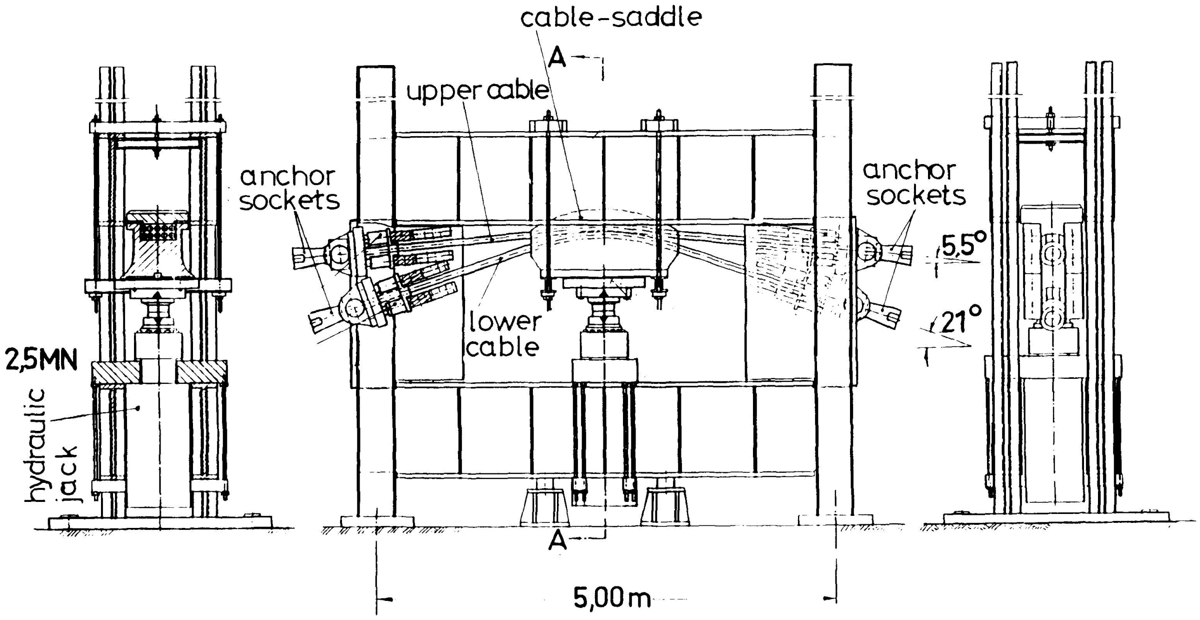

Fig. 3 Schematic diagram of test set-up

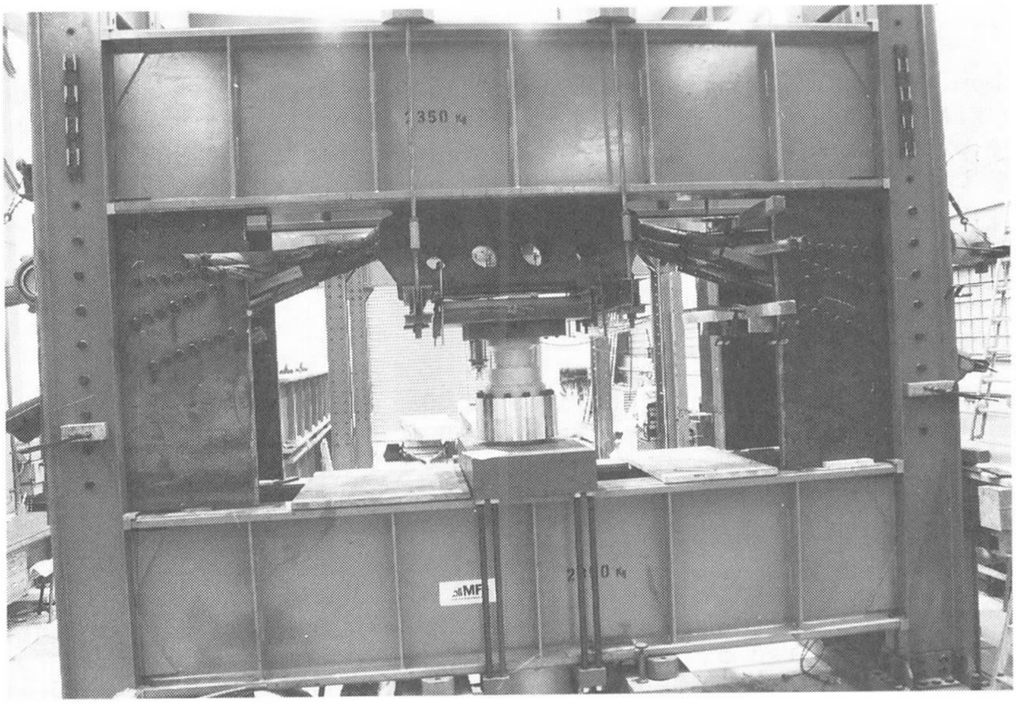

Fig. 4 Test set-up

3.3 Fabrication of the cable specimens C, D and E.

Fig. 6 shows the different points of the Norderelbebridge, where the parts for the specimens were drawn from. The cable bundles consisted of ten spiral wire ropes, ϕ 72 mm, arranged in two layers of five cables respectively.

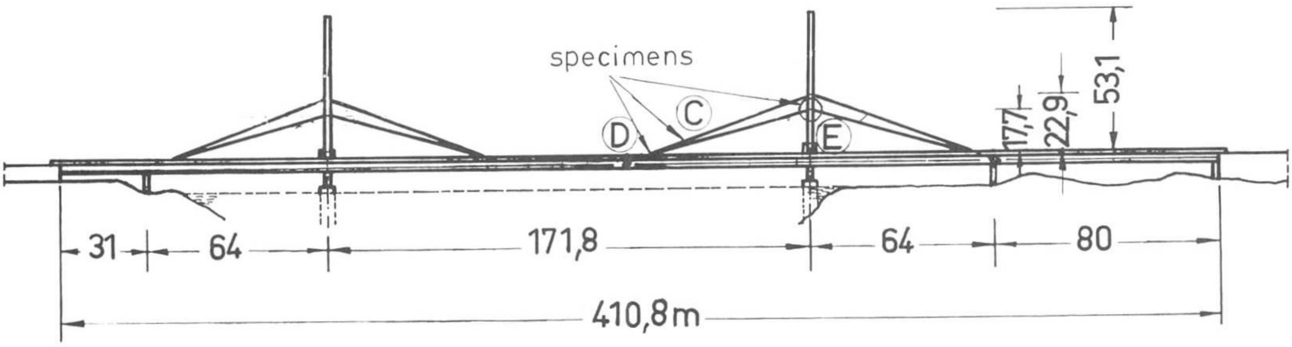

Fig. 5 Schematic diagram of the Norderelbebridge with the points where the specimens were drawn from

On both ends of the cable cutted to length for specimen C, anchor sockets taken from the bridge were attached. Casting material was again ZnAl6Cn1 (Zamak 610). In order to compare the test results of specimen C with those obtained in 1960 during the construction of the bridge, a transverse pressure equipment was installed in the same way like it was done at that time (details are given in [2]).

Specimen D was similar to C, however without transverse pressure equipment. One end of specimen C had the remained original anchorage whereas at the other end an anchorage taken from the bridge was attached by Thyssen Draht AG, using again Zamak 610.

Specimen E consisted of the so called cable-saddle and two fixed cables one upon the other of about 6 m length respectively. From the initial ten cables (two layers by five) going over the saddle in the bridge, only the middle one of each layer was used for the fatigue test. At the four ends of the two cables anchorages taken from the bridge were attached.

4. RESULTS AND CONCLUSIONS

The investigations performed on cables dismantled after more than 25 years in service from the Fehmarnsundbridge and the Norderelbebridge have yielded the following results and findings:

a) After more than 25 years in service, the cables itself showed a remaining fatigue life of more than $2{,}0 \cdot 10^6$ cycles. This can be stated for the cables "in relatively good condition" of the Norderelbebridge as well as for the cables "considerably damaged by corrosion" of the Fehmarnsundbridge. Consequently the tests have proved a still sufficient fatigue strength according to the relevant DIN specifications. Even after fatigue loading of more than 25 years, no significant loss of carrying capacity of the cables could be found, i.e. an increased risk of damage or failure did not yet exist for both bridges as far as the cables are concerned.

b) Analysing the wire cracks observed during the investigations showed numerous proofs and confirmations for a dominating influence of fretting corrosion among all the known corrosive damaging phenomenas like tension crack corrosion, pitting corrosion etc.

   Beside of the pure mechanical induced fatigue damaging process, the mechanical-chemical combined damaging by fretting corrosion exerts the most decisive influence on the reduction of lifetime of cable structures. The remarkable difference between the fatigue strength limit of the single wires ($\Delta\sigma$ = 400 N/mm²) and the fatigue strength limit of the complete cables ($\Delta\sigma$ 150 - 200 N/mm²) is mainly referred to the influence of fretting corrosion.

c) Points of turn around the multi layered cable bundles (cable-saddles, turn around anchorages etc) which are usually characterized by high local transverse pressures, had always been considered therefore as very problematical details of cable structures related to the fatigue strength. On the base of the presented test results [1, 2], it can be pointed out that these details are less critical as formerly assumed. They can be classified as at least not more "delicate" than the anchorages of the cables.

d) The acting stress rate $\Delta\sigma$ (stress amplitude $\sigma_o - \sigma_u$) has an essential influence on fatigue life of the cables. $\Delta\sigma$ is the dominating parameter governing the fatigue life, whereas the level of the maximum stress σ_o is of subordinated influence as long as it is kept under the yield stress level.

On of the urgent aims of the investigations on preloaded cables is to improve the understanding and fundamental knowledge of the fatigue behavior of cables by means of the elaboration of a sufficiently supported $\Delta\sigma$-N-curve (WÖHLER-diagram). The set up of such a diagram however implies the derivation and the definition of a damage - and failing criterion corresponding to the actual cable behavior.

The failing of cables submitted to fatigue loading is fundamentally different from that of the usual steel structures: Depending upon structural boundary conditions and the grade of notch effect, damaging and destruction in usual steel structures proceeds more or less steadily after a first crack occurred and almost the whole fatigue life of the structure is related to the period before the first crack happened, i.e. the crack initiation phase representes usually a life period multiple of the period of crack propagation.

In contrast to this, observations and results of fatigue tests with cables have shown, that the first wire crack may occur comparatively soon without having any connection with or relation to the much later total failing of the cable. The first wire crack is therefore unsuitable to be used as a failing criterion. Moreover the cables consist of up to 300 single wires nowadays, i.e. the first crack of one wire in a cable has quasi only the dimension of a micro crack for instance in a welded steel structure. In the course of the continual fatigue loading a considerable number of wire cracks and breaks may occur succeeding one another in realtively short time (so called infection breaks) withount causing immediately a total failure of the cable. The respective net sections are able to carry on the acting forces with corresponding increased stresses. Only after a further number of cycles, when finally about 25 to 30 % of the wires are broken, a progressive ascent of the registered wire break accumulation curve can be observed, which clearly announces the approaching total collapse of the cable. The fatigue failure of cables can be characterized as a real tough rupture with a kind of previous notice.

The described phenomenas and findings underline the idea discussed at times by experts, to introduce as Δσ-N-curve (WÖHLER-diagram) for cables a 25 %-damage curve, i.e. a 25 %- wire crack line as a realistic base for the design of safe and economical cable-stayed structures. With the results obtained in the presented investigations [1, 2], a first sketch of a 25 %-damage curve - of course still sparsely supported - was developped, see figure 6.

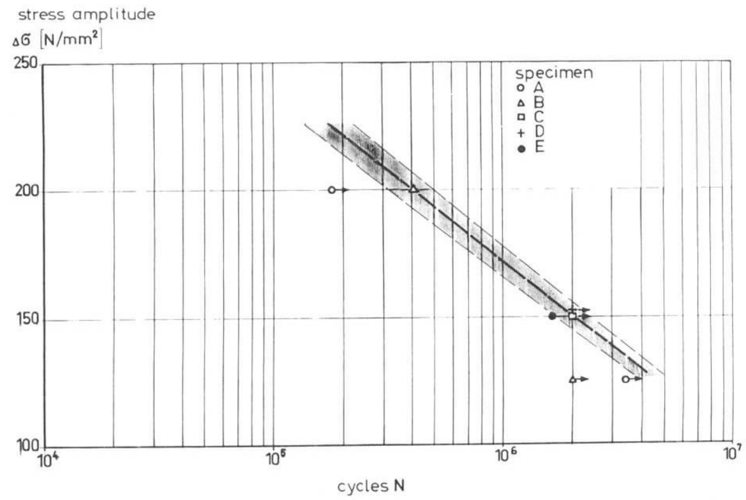

Fig. 6 Δσ-N-curve (WÖHLER-diagram) for preloaded cables on the base of 25 % wire crackes

The graph shows that the exponent of inclination of the curve comes out to K ≃ 5,5. It is self-evident, that this first sketch has to be completed and extended by further investigations in order to reach a reliable and safe design base for cables submitted to fatigue loading. Only by means of initiatives like taken in the two projects of Fehmarnsundbridge and Norderelbebridge, the presently still very poor knowledge regarding the fatigue behavior of cables can be improved and brought to an adequate level in an economic way.

REFERENCES

[1] HARRE, W. : Test results of preloaded cables dismantled from the Fehmarnsund-bridge. Bauingenieur 66 (1991) H. 7, S. 301 - 309.

[2] HARRE, W. : Test results of preloaded cables dismantled from the Norderelbe-bridge. Bauingenieur 67 (1992) H. 2, S. 91-99.

Safe Capacity of Suspension Bridge Cables
Sécurité de la capacité portante des câbles de ponts suspendus
Sichere Traglast von Hängebrückenseilen

Peter SLUSZKA
Senior Vice President
Steinman
New York, NY, USA

Peter Sluszka received his engineering degree from Hofstra University, Uniondale, NY. He has supervised design and construction of new bridges and inspection and rehabilitation of existing bridges throughout the United States. He is currently in charge of Steinman's firm-wide operations and is responsible for technical direction of the firm's suspension bridge evaluation projects.

Martin KENDALL
Project Manager
Steinman
New York, NY, USA

Martin Kendall graduated from Birmingham University, England. Starting on London Bridge reconstruction, his career has included design and construction of bridge-works and long span structures on four continents. He is now responsible for the firm's operations on the cable rehabilitation projects for the Williamsburg and Bear Mountain Bridges.

SUMMARY

A common type of deterioration and resultant defects in the main cable wires has been observed in recent in-depth inspections of some older suspension bridges. The deterioration and defects are highlighted in the description of a typical case history of a suspension bridge inspection undertaken on the Bear Mountain Bridge. A description of the bridge, its inspection and relevant testing of wires is described. The deterioration of the wires and resultant defects are discussed and compared with similar defects observed on three other comparable suspension bridges also inspected recently. An estimation of remaining cable capacity is described, together with a discussion of the effects of the reduction of safety factors on the design loads.

RÉSUMÉ

Des types communs d'usure et de dommages consécutifs ont été tout dernièrement découverts au cours d'inspections minutieuses effectuées sur un certain nombre d'anciens ponts suspendus. L'auteur en fait la description à l'aide des résultats fournis par le cas d'une inspection typique et des essais de fils de câbles opérés sur le pont Bear-Mountain. Il donne également l'estimation de la capacité portante résiduelle des câbles et cite les effets de la réduction des coefficients de sécurité sur les charges de calcul.

ZUSAMMENFASSUNG

Bei kürzlich durchgeführten gründlichen Inspektionen einiger älterer Hängebrücken, wurde eine ihnen gemeinsame Art der Abnützung und entsprechende Folgeschäden gefunden. Sie werden anhand eines typisches Inspektionsergebnisses der Bear-Mountain-Brücke und zugehörigen Drahttests beschrieben. Die Abnützungs- und Schadensmerkmale der Drähte werden mit denen vergleichen, die kürlich an drei ähnlichen Hängebrücken entdeckt wurden. Die Abschätzung der Resttragfähigkeit der Seile und die Folgen der verminderten Sicherheitsbeiwerte auf die Bemessungseinwirkungen werden erörtert.

1. INTRODUCTION

1.1 In-depth inspections have been undertaken recently on a number of older suspension bridges with the primary purpose of inspecting the condition of the wires of the main suspension cables. This was in order to determine if any deterioration has occurred, if so how much, and to compute the remaining structural capacity of the overall cable.

1.2 Steinman has undertaken such in-depth inspections on the Bear Mountain Bridge across the Hudson River approximately 40 miles north of New York City, the suspension span of the Triboro Bridge across Hell's Gate in New York City, and the Golden Gate Bridge in San Francisco. In addition, Steinman has been involved in a consulting capacity for the in-depth inspection of the Mid-Hudson Bridge across the Hudson River at Poughkeepsie.

1.3 All four of these bridges were completed more than 55 years ago. The Bear Mountain Bridge was completed in 1924, the Triboro Bridge was completed in 1936, the Golden Gate Bridge was opened to traffic in 1937, and the Mid-Hudson Bridge was completed in 1936. As such, they represent a good sample of the type of medium to long span bridges being constructed in the United States between the two World Wars.

1.4 In-depth inspection techniques for viewing and establishing the condition of suspension bridge main cable wires were developed by Steinman in the early 1980's initially for inspecting the main cables of the Brooklyn Bridge, in New York City. These techniques were successfully utilized on the special investigation of the Williamsburg Bridge, also in New York City in 1988/89 when it was demonstrated that the condition and capacity of the cables was fully adequate for the design loads imposed.

1.5 The four bridges which are the subject of this paper represent a more commercial and standardized practice of the construction of suspension bridges than either the Brooklyn Bridge or the Williamsburg Bridge. All four bridges have main cables that were constructed using the aerial spinning techniques for cable wire developed by the John A. Roebling Sons Company. All four bridges have galvanized bridge wire of approximately 4.95mm in diameter with a minimum ultimate tensile strength varying from 1500 N/mm^2 to 1600 N/mm^2. The wire for the Bear Mountain Bridge and the Golden Gate Bridge came from John A. Roebling Sons Company, and the wire for the Triboro Bridge and the Mid-Hudson Bridge was supplied by American Steel & Wire Company.

1.6 The size of the spans and cables, with the exception of the Golden Gate Bridge are all roughly comparable. The make-up, size of cable, and spans are listed in Table 1 and the bridges are illustrated in Figure 1.

2. IN-DEPTH INSPECTION - A CASE STUDY

2.1 A description of the inspection of the Bear Mountain Bridge is provided to illustrate the means of inspecting the cables.

2.2 The Bear Mountain Bridge was constructed in 1923/4 as the first fixed crossing of the Hudson River south of Albany, which is approximately 100 miles north of the bridge. At the time of construction it had the longest clear span in the world, 497.2m.

	Bear Mountain	Mid-Hudson	Triborough	Golden
Year Completed	1924	1936	1936	1937
Main Span (m)	497.4	457.2	420.6	1280.2
Cable Diameter	464	425	527	924
Number of Wires per Cable	7292	6080	9176	27572
Minimum Ultimate Tensile Strength (N/mm^2)	1500	1500	1600	1550
Residual Diameter of Wire Curvature	1680	1830	1470	1830

TABLE 1
SUMMARY OF CABLE DATA
(all dimensions in millimeters unless noted)

2.3 The two towers of the bridge are 106.7m high. The clearance from mean high water level to the underside of the stiffening truss at the towers is 42.1m, rising to 46.6m at mid-span. The designed span to sag ratio is 8.16 under dead load. The bridge has straight backstays with truss supported end spans. The main stiffening truss is 9.14m deep, supported by two part 57mm diameter wire rope suspenders connected to cantilever extensions of beams supporting the bottom chord. The cables are at 18.70m centers, outside the face of the stiffening truss, and dip down at mid span below the top chord of the stiffening truss.

2.4 The construction of the bridge incorporated certain advances in technology which have subsequently permitted the adoption of unlimited size of cables on other bridges. Previous to the construction of the Bear Mountain Bridge it had been the practice to spin the strands and serve them with round wire to hold together the parallel wire. When the first seven strands had been completed, they were formed into a circle, the serving wires to the strands removed, the whole formed into a homogeneous group and re-served with round wire. The next set of strands were then spun, and formed to a layer around the central core. Again the serving wire to each strand and the core was removed, and the whole re-served. The process continued until the full cable was completed, and then the whole was compacted. This was an extremely lengthy and time-consuming process.

2.5 With the Bear Mountain Bridge, the use of flat steel wire serving bands was adopted for the strands. This permitted the spinning of each strand and its placement in the overall preliminary hexagon shape, without the tedious forming procedure. When all strands were completed, the flat bands were all cut, the bands to all external strands were removed and the compaction undertaken.

2.6 In-depth inspection of the cable was undertaken at four points along the cable. These were the backstay just outside the anchorage, the tower top at one panel point into the main span from the saddle, at mid span, and at the one-third point of the main span. The backstay and mid span location were selected as those locations most likely to reveal any water that may have entered the cable. The tower top location is that point of maximum cable load, and the one-third point is that location subject to the most flexure under live load. All locations selected were on the north cable except for the one third point location.

2.7 Inspection of the cable is undertaken by removing the protective wrapping wire and driving wedges into the cable in order to provide a visual check of

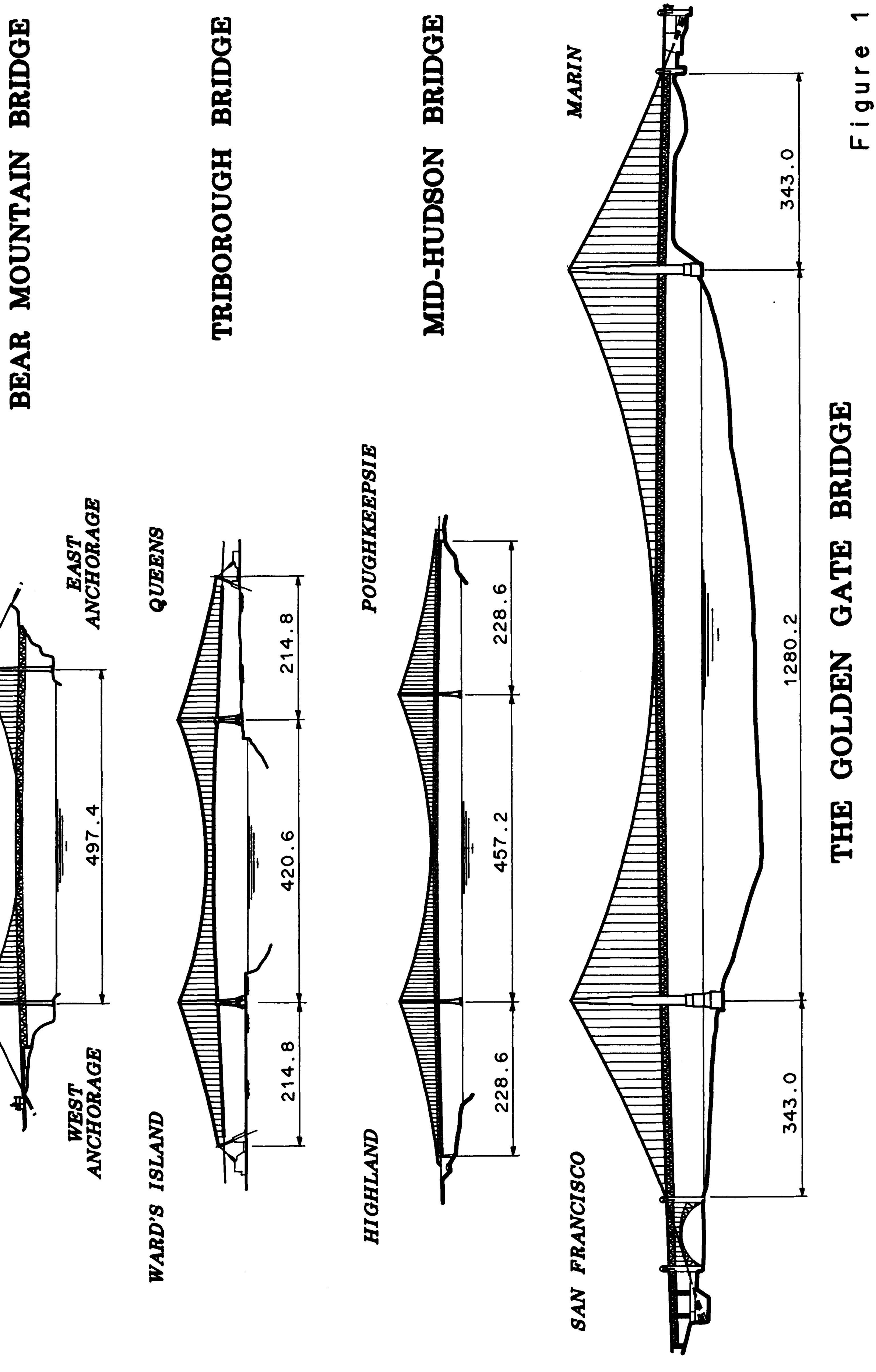
BEAR MOUNTAIN BRIDGE
WEST ANCHORAGE
EAST ANCHORAGE
497.4
TRIBOROUGH BRIDGE
WARD'S ISLAND
QUEENS
214.8
420.6
214.8
MID-HUDSON BRIDGE
HIGHLAND
POUGHKEEPSIE
228.6
457.2
228.6
SAN FRANCISCO
MARIN
343.0
1280.2
343.0
THE GOLDEN GATE BRIDGE

Figure 1

interior wire conditions. Wedges were driven into the cable at four radial positions around the cable, except at the mid span location where four additional grooves were opened.

2.8 At the three main span locations, suspender ropes and associated cables were removed in order to provide observation of conditions under the cable bands. Purpose made jacking equipment was designed and supplied in order to free the suspender rope, and subsequently re-tension the new ropes after installation.

2.9 After full inspection of the cable surfaces and wedged grooves, the wedges were withdrawn and the cable recompacted using a specially designed and supplied compactor. After completion of compaction, the cable bands were replaced on a new layer of red lead paste applied over the cable wires, and the new suspender ropes installed and tensioned.

2.10 The cable was then wrapped with soft galvanized wire by means of a purpose built two ply wrapping machine, also laid over a fresh layer of red lead paste applied to the main cable. A minimum tension in the wire of 665N was specified.

2.11 Full visual inspection of the exposed wires was undertaken using photographs and a standardized form of recording corrosion levels. All broken wires were located on position charts showing both the cross section, and longitudinal locations. Broken wires were labelled and sampled and the samples sent to Carleton Laboratory at Columbia University for detailed visual and microscopic inspection, and physical testing.

2.12 Wherever possible broken wires were respliced using a technique developed for Brooklyn Bridge, incorporating the use of repair wires joined to bridge wire with hydraulically crimped ferrules and the repair wires themselves joined and tensioned with threaded ferrules.

3. TESTING OF SAMPLES

3.1 Visual inspection of all wire samples was undertaken, with special effort being given to the broken ends of the wires. Microscopic examination of all broken ends was undertaken and two specimens were viewed under the Scanning Electron Microscope. Five wires were tested for hydrogen embrittlement with two samples showing elevated hydrogen levels.

3.2 Longitudinal sections of two wire samples were prepared and viewed under the microscope in order to provide further information on the failure patterns.

3.3 Standard tensile tests were made on a number of wire samples, with specimens approximately 450mm long. Additional tensile tests were performed on long sections of wire up to 5.2m in length in order to compare the possible effect of the straightening of the wire from the coil set. Four fatigue tests were undertaken on short wire samples and finally additional tensile tests were performed on the broken ends of certain of the long samples which had failed at low ultimate tensile stresses.

4. DISCUSSION OF RESULTS FROM BEAR MOUNTAIN BRIDGE

4.1 The primary cause of the observed wire breakages appears to be stress corrosion, with all fracture surfaces observed exhibiting the characteristic fracture profiles. Representative longitudinal sections of wires also revealed the typical secondary cracks running into the wire.

4.2 A significant number (approximately 40%) of the wire breaks were observed to be immediately adjacent to the strand straps that had been left inside the cable. In addition, the large majority (approximately 90%) of all wire breaks are located in the 300 mm diameter central zone of the cable, thus being topographically situated in the zone where the flat wire serving bands were cut but not removed.

4.3 These banding straps have almost certainly initiated zinc depletion of the galvanized wires as the straps were made of low carbon steel, with no protection. The indication of a possibility of hydrogen embrittlement of the wire breaks tends to support the above-described zinc-depletion effect, and in addition would render the wire itself susceptible to corrosion.

4.4 The definitive reasons for the occurrence of the stress corrosion cannot be readily defined. However, the initial crack planes on all fracture surfaces were located on the inside of the residual curvature of the wire. This seems to indicate that initial occurrence, and subsequent propagation of the crack could be related to the initial manufacture of the wire and its subsequent decoiling.

4.5 The strength testing of the wires showed that the wire generally had the same capacity as when it was originally manufactured, except where stress corrosion has commenced. All tensile tests undertaken showed an average ultimate tensile stress of $1400N/mm^2$ except where stress corrosion crack planes were located. Retests of four (4) wires taken from the broken ends of two (2) tensile tests where the failure stresses were low, exhibited revised failure stresses averaging $1375N/mm^2$ indicating that the balance of the wire did not have pre-existing cracks comparable to those at which the initial breaks occurred.

4.6 It was noted that in all cases the in-place wire breaks showed corrosion across the entire faces of the fractures. This indicated that the majority if not all of the breaks occurred a significant time past, and that the stress corrosion attack has been retarded in the recent past. This is in agreement with reported maintenance operations where an increased attention to maintenance and painting of the cables has been in effect for approximately the last 10 years.

5. SUMMARY OF RESULTS FROM OTHER BRIDGES

5.1 The inspection of the Golden Gate Bridge showed that the wires generally were in excellent condition. One location was unwrapped and wedged open at six (6) radial positions for inspection, and other than the exterior wires at the low points of the cable where some medium surface corrosion was observed, the interior wires of the cable only exhibit light zinc oxidation with spots of minor ferrous corrosion. Observation of the samples removed for testing showed that these minor corrosion locations were generally on the inside of the residual curvature of the wire. It is to be noted that the wire wrapping system of the cables was very well applied during original construction, and has been maintained during the life of the bridge. The cable was dry when inspected, but this may have been related to the lengthy drought that California has just experienced.

5.2 The inspection of the Triborough Bridge showed that the wires are suffering from some significant corrosion to the surface layers of wires. Four (4) locations were unwrapped for inspection, with one location being wedged open to a depth of 250mm and the other three only to a depth of 50mm. Fractures have occurred in wires at the surface layers, apparently due to hydrogen assisted stress corrosion cracking. These wires were invariably heavily corroded with visible section loss. Interior wires observed exhibit corrosion of the zinc coating with localized areas of ferric corrosion similar to those observed at

Bear Mountain. Observation of the samples removed for testing showed that these corrosion locations, again, were generally located on the inside of the residual curvature of the wire. The wire wrapping system of these cables was not well applied with gaps between the wires evident, and red lead paint was used as a seal layer between the wrapping and main cable wires, instead of red lead paste used on Bear Mountain and Golden Gate. The combination of these two last factors has permitted water to enter the cable and initiate corrosion of the wires.

5.3 The inspection of the Mid Hudson Bridge showed that the wires are suffering from active stress corrosion attack. Forty eight (48) locations have been unwrapped and wedged open full depth for inspection, and a large number of fractured wires have been discovered. In addition there is a wide distribution of local corrosion locations showing pitting and craters, with severe local loss of zinc and local corrosion attack of the steel wire. All fracture surfaces observed were typical of stress corrosion, and all fractures had the initial normal fracture surface on the inside of the residual curvature of the wire. In addition, in a number of samples, when the zinc had been removed from the wire, transverse cracks were observed on the surface of the steel wire at approximately 3mm intervals, and all were located on the inside of the residual wire curvature. Cracking occurred at local areas exhibiting a hard, black corrosion product, even where little loss of section had occurred.

6. <u>DEFECTS EVIDENT IN BRIDGE WIRE</u>

6.1 Three of these bridges are exhibiting common defects and deterioration of the bridge wire making up their main cables. These defects originate with the failure of the overall protective wrapping wire system to the outside of the main cable wires, resulting from a combination of failure of the external paint system, inadequately installed or maintained wrapping wire, and incorrect material specification of the protective paste system to the outside of the main cable wires.

6.2 After water has entered the main cable system, depletion of the zinc galvanizing to the main bridge wires can occur, with the water acting as the electrolyte. In the case of the Bear Mountain Bridge this has been aggravated by the flat wire serving bands remaining in the cable.

6.3 The bridge wire appears to be susceptible to stress corrosion of the main steel wire itself. This can only occur after depletion of the zinc, but after the zinc is lost, local corrosion of the steel wire seems to occur in concentrated local positions, with resultant pitting and cratering.

6.4 The stress corrosion cracking appears to be induced to initiate its action on the inside of the residual curvature of the wire. All three of the Bear Mountain, Triborough and Mid Hudson Bridges have the initial crack planes of the wire fractures originating on the inside of this curve. The wire from the Golden Gate Bridge, exhibited relatively little ferrous corrosion, moderate zinc oxidation, but no cracking.

6.5 It is considered possible that the stress corrosion may be directly related to the initial curvature of the wire. The approximate measured diameters of the curvature are recorded in Table 1. The simple calculation of the equivalent decoiling stress from the minimum radius of 1830mm on the Mid- Hudson Bridge gives an indicative extreme fiber stress of 345N/mm^2. Early research into stress corrosion cracking indicated that the threshold for crack initiation is around 270N/mm^2. Typically, dead load cable stress is somewhat below this on these older bridges. However, the secondary "decoiling stress" appears to be sufficient to exceed this threshold.

7. PROTECTION OF CABLES AND REMAINING CAPACITY

7.1 It is evident from the condition of the wires in the four bridges inspected that the corrosion pattern is only initiated after failure of the protective wrapping system to the main cables and the entrance of water into the cables. It is also evident that even if the corrosion attack has commenced, it is possible to slow, or even halt the attack by increased maintenance of the protective wrapping system, thereby stopping the entry of water into the cable.

7.2 The primary recommendation therefore, is to undertake some means of wrapping to the cables which will totally seal the cables from any entry of water. This can be achieved by means of wrapping the cables with a neoprene sheet wrap, comprising 150mm wide uncured neoprene tape wrapped around the cable with a 50% overlap. The curing of the tape is effected by its exposure to air, and the ends are sealed to the cable bands. The whole is coated with a three-coat liquid chlorosulfonated polyethylene paint system. Overall, this results in a totally impervious flexible sheath to the cable.

7.3 This system can be applied either directly to the surface of the main bridge wires or over the original wire wrapping system. It is considered preferable to leave the original wire wrapping system in place if possible, as this will maintain the compaction of the cable wires. Removal of the wrapping wire can result in loss of compaction up to 5% on the diameter of the cable, thus providing an increased voids ratio of the whole cable. The cable should therefore be at least strapped at sufficient intervals to maintain sufficient compaction. Under no circumstance is it recommended to use neoprene wrap alone, without a positive compacting provision.

7.4 Calculation of remaining cable capacity can be considered as a reduction in the Factor of Safety to failure under load. Such reduced factors of safety have been calculated for the Bear Mountain Bridge and Mid Hudson Bridge. Insufficient data was available for this to be undertaken for the Triborough Bridge, but the Factor of Safety is not considered to be at or near any level to cause concern. It was not considered necessary to make any estimate of reduction of Factor of Safety for the Golden Gate Bridge, due to the good condition of the wires.

7.5 Conservative assumptions were made in projecting the available figures into calculations for remaining cable capacity for both the Bear Mountain and Mid Hudson Bridges. These were:

7.5.1 The percentage of broken wires as a proportion of all wires actually observed at any location is considered to extend through the complete cable cross section.

7.5.2 The strength of unbroken wires is taken as an average strength of the laboratory test values for that location. It is to be noted that all such test values were measured on previously fractured wire samples.

7.5.3 All breaks observed at any one location are effective in conjunction, ignoring any transfer of load by friction and clamping.

7.6 The Factor of Safety on the Bear Mountain Bridge was calculated as having been reduced from 3.74 to 3.25, and on Mid Hudson Bridge from 3.90 to 3.20. In both cases, this still represents an ample reserve of capacity, and presents no cause for alarm. However, the recommended measures referred to above for sealing the cables have been put into effect and the cable wires will continue to be monitored on a regular basis to ensure that the corrosion attack is halted.

Nonlinear Analysis of an Existing Prestressed Shell

Analyse non linéaire d'une coque précontrainte existante

Nichtlineare Berechnung einer bestehenden vorgespannten Schale

Pere ROCA
Assoc. Prof.
Univ. Politècn. de Catalunya
Barcelona, Spain

Alex. C. SCORDELIS
Prof. Em.
University of California
Berkeley, CA, USA

Climent MOLINS
Civil Engineer
Univ. Politècn. de Catalunya
Barcelona, Spain

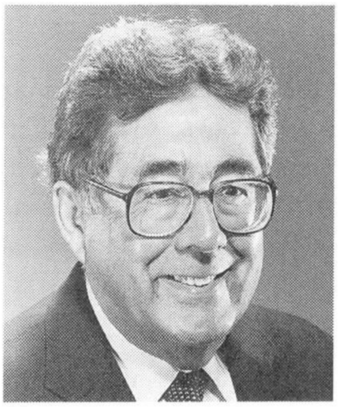

SUMMARY

In this paper, a model developed for the nonlinear analysis of prestressed concrete shell structures is briefly described together with its application to the study of an existing shell constructed in Puerto Rico in 1971. Different types of analysis have been carried out in order to determine the influence of the material and geometric nonlinear effects on the structural behaviour until failure. This simulated behaviour is discussed and related to original design aspects.

RÉSUMÉ

Un modèle développé pour l'analyse non linéaire de structures de coques précontraintes est brièvement décrit ainsi que son application à une coque réalisée en 1971 à Puerto Rico. Différents types d'analyses ont été effectuées pour visualiser l'influence du matériau et des effets géométriques non linéaires sur le comportement de la structure jusqu'à rupture. Ce comportement simulé est décrit et relié aux aspects du projet original.

ZUSAMMENFASSUNG

Der Artikel beschreibt ein entwickeltes Berechnungsmodel zur nichtlinearen Analyse von Schalenstrukturen aus Spannbeton und seine Anwendung bei der Berechnung eines existierenden Tragwerks in Puerto Rico. Verschiedene Berechnungen wurden ausgeführt, um den Einfluss von Material- und nichtlinearen Geometrieeffekten auf die Struktur bis zum Versagen aufzuzeigen. Das simulierte Tragwerksverhalten wird diskutiert und mit den ursprünglichen Entwurfsaspekten in Verbindung gebracht.

1.- INTRODUCTION

Although powerful numerical tools for structural analysis have been developed during the past twenty years to simulate the nonlinear behavior of concrete structures, very few estudies have been effectivelly carried out on their use for the nonlinear analysis of large span shell existing structures. However, a knowledge of the complete structural response of shell concrete structures through their elastic, cracking, inelastic and ultimate ranges, is usually difficult to achieve by means other than a nonlinear analysis which takes into account both the geometric second order effects and the nonlinear aspects of the true behavior of the materials, including concrete cracking and crushing, yielding of steel, and the time-dependent effects of concrete creep and shrinkage.

The present paper describes the nonlinear finite element analysis of an existing prestressed concrete shell structure: the Ponce Coliseum roof, constructed in Puerto Rico in 1971. Through this analysis, the different causes of nonlinear behavior are characterized and their partial influence on the service and ultimate behavior is measured. The simulated behavior as obtained by the analysis is discussed in relation to the resulting reliability of the structure under instantaneous vertical loading.

The original structural design of the Project was carried out during the period 1968 to 1970 by a Joint Venture of T.Y. Lin International, San Francisco, California, and R. Watson, Engineer, and Sanchez, Davila and Suarez, Engineers of San Juan, Puerto Rico.

2.- DESCRIPTION OF THE SHELL

Ponce Coliseum consists of a 82.6 m span prestressed HP shell roof built in Ponce, Puerto Rico, in 1971 for the 1974 Pan American basketball chanpionship games. The complete roof is made up of four similar 10 cm thick saddle type shells connected to interior and cantilever edge beams to form a structure supported by four piers at the low points located at the centers of the four exterior panels. The high points of the shell, which rise 12.2 m above the low points, are at the four corner tips and at the center of the shell. The clear spans between opposite support piers in the two directions are 82.6 m and 69.2 m (Fig. 1). The cantilever edge beams are supported only at the piers and have a constant width of 76 cm throughout their entire length. These depth decreases gradually from the abutment to the corner tips, as may be seen in Fig. 2.

Reinforcing for the shell consists of reinforcing bars in the top and bottom surfaces throughout the shell with additional bar reinforcement added in the zones adjacent to the beams and near the tips. Prestressing is provided as well by a two-way set of tendons parallel to the straight line generators. The cantilever edge beams contain both normal reinforcing steel and prestressing steel, while the interior beams contain only normal reinforcing steel and are not prestressed.

The final original design used for the structure in 1970 was based on a detailed computer analysis using a linear elastic finite element model which coupled a system of one dimensional beam type elements with another system of two dimensional triangular plane stress finite elements. This analysis showed the high degree of interaction that occurs between the shell and the beams when subjected to their dead load, so that the resulting stress states can not be completely understood using membrane theory, and coupled states of axial force and bending moments appear both in the beams and the shell.

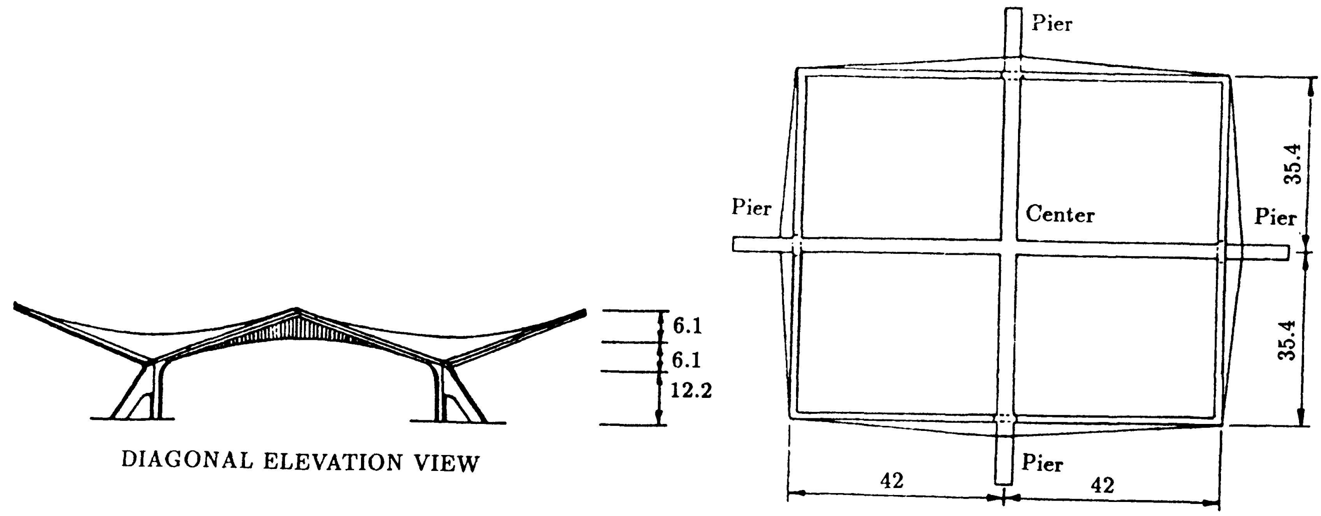

Fig. 1. General dimensions of the structure

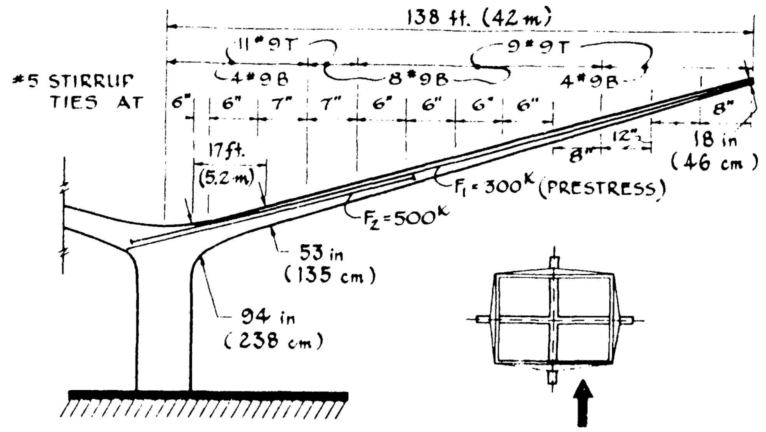

Fig. 2. 42 m cantilever edge beam

Prestressing in the edge beam was used to partially balance its dead load bending moments and deflections while increasing its axial forces, thus resulting a set of stresses found acceptable for design. In the shell, the remaining tensile forces after the introduction of the prestressing were resisted by providing normal steel reinforcement. Also, to minimize cracks, prestressing shell tendons were used in combination with reinforcement. For bending moments in the shell adjacent to the edge beam and the tips, additional reinforcement was used.

Additional detailed information regarding concrete dimensions, reinforcement and prestressing, as well as the original desing and construction of the Ponce Coliseum may be found in [1-4].

3.- NUMERICAL MODEL USED IN ANALYSIS

Chan's [5-7] previous numerical model for the nonlinear analysis of reinforced concrete shells, extended by Roca [7-8] to include both beam and shell internal prestressing tendons, has been adopted for the present study. This model includes both shell and beam elements to account for shell systems with edge beams, internal ribs or supports. The nine node Lagrangian isoparametric element shown in Fig. 3 was adopted to model two dimensional curved shells, while beams are simulated by adding two straight one dimensional beam elements to the side of a curved shell element. Beam elements are prismatic but may have an arbitrary cross-section made up of discrete numbers of concrete and reinforcing steel filaments.

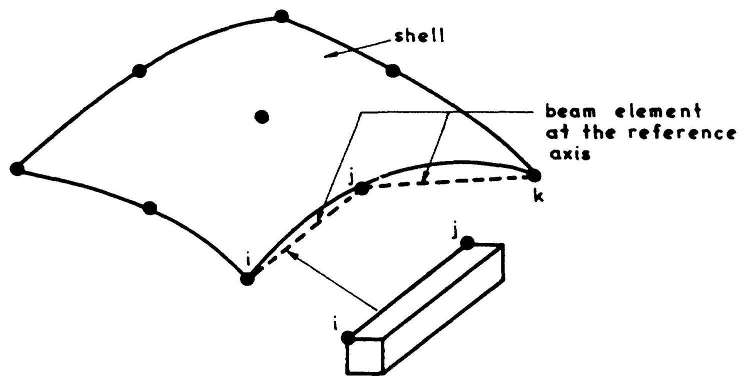

Fig. 3. Adopted L7 shell and straight beam elements

The shell element is regarded as a multilayered system where each layer is assumed to be under a biaxial state of stresses. The stresses and the state of the materials vary independently at each layer to account for the mechanical changes of the materials throughout the loading process. An hypoelastic biaxial concrete model is adopted together with a biaxial strength envelope [5] to reproduce the compressive behavior of concrete and crushing. In tension, concrete is assumed to behave as a linear elastic- perfect brittle material, accounting for tension stiffening in the reinforcement. Smeared cracking is initiated once the tensile stregth is reached. A second crack is permitted to appear normal to the first. Reinforcement strength is included as a set of additional layers of uniaxial behavior characterized by an equivalent thickness. A bilinear diagram is used to model the elasto-plastic behavior of reinforcing steel.

Shell prestressing tendons are individually defined as arbitrary spatial curves contained in the shell thickness. The geometric treatment of tendons is based upon a method where analytical parametric expressions are used for the definition of the mid surface of the shell as well as the tendon curves. Thus, an authomatic calculation of their geometric properties, as well as the further updating of their whole geometry and forces in the nonlinear geometric analysis, are possible. Prestressing in beams is treated consistently with the adopted beam straight finite element, by dividing the tendon into a number of straight segments, each of which spans a single beam element and is assumed to have a constant force. A multilinear stress-strain curve is adopted to model the stress-strain relationship for prestressing steel. In addition, the usual empirical formulae are used for stress relaxation and friction properties.

Nonlinear geometric effects are caused by the consideration of finite movements and finite rotations. First, the compatibility equations are used with their quadratic terms to obtain the strains from the displacement field. Furthermore, the geometry of the structure is continuosly updated by adding the displacement increments to the current nodal coordinates, according to the Updated Lagrangian Description. This requires an interactive procedure until convergence is obtained meaning that the equilibrium condition has been finally satisfied on the deformed geometry of the structure.

4.- DISCRETIZATION OF THE STRUCTURE

Advantage is taken of the structural symmetry, so that only one of the four connected HP quadrants is numerically modelled. Two meshes with a different degree of refinement were defined: Firts, a coarse mesh having 15 shell elements and 24 beam elements, and, second, a fine mesh with 55 shell elements and 52 beam elements. Although satisfactory results were obtained using the coarse mesh for linear elastic analyses, it was necessary to use the fine mesh to accurately reproduce the strongly local effects and local type of failure finally observed in the ultimate behavior. The results that are presented below were thus obtained using the fine mesh (Fig. 4).

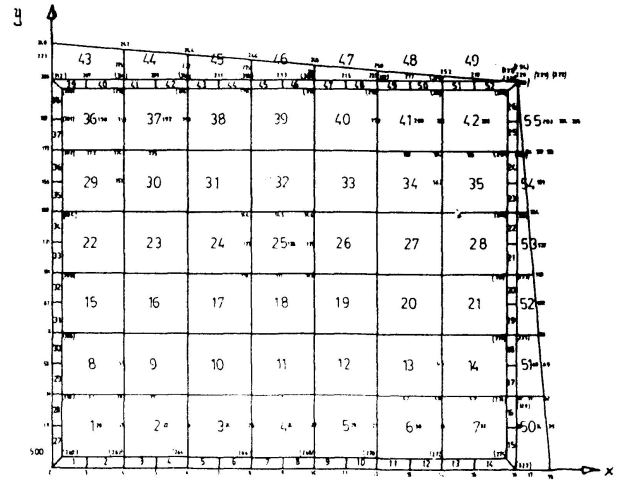

Fig. 4. Fine mesh including 50 shell and 52 beam elements

An automatic procedure for the generation of the shell finite element mesh and the courses of the tendons has been used which needs as input data the parametric description of the geometry of the choosen HP quadrant and the axial curves of the tendons included in it.

All mesh reinforcement keeps the direction of the HP generatrices parallel to the X,Y global axes. Untensioned reinforcement in the shell is defined by a set of layers of equivalent thickness and provided at each integration point in the mesh.

All shell tendons are defined with a cross steel area of $A_{pi} = 3.13\ cm^2$, and stressed to $1158 N/mm^2$. Their distribution is designed to fit the expected average compression throughout the shell membrane.

Each straight beam element was defined with its cross sectional dimensions, flexural reinforcement and torsional reinforcement, which are assumed to be constant throughout the element. Each flexural reinforcement pattern consists of a set of discrete reinforcing bars defined by their position in the cross section and their individual amount of steel. Torsional patterns are determined by the core dimensions in x' and z' local directions, the area and spacing of hoop reinforcing bars, and the top and bottom longitudinal perimeter steel.

The four beam tendons included in the discretized quadrant of the structure produce a total prestressing force of 3550 kN and 2440 kN respectively for the 42.10 m and the 35.35 m edge beams. In both cases, the minimum cover between tendon axis and beam top surface is about 11.5 cm. Based on the available design data, the following mechanical properties were considered in the analysis: Concrete: $E_0 = 26320\ N/mm^2$, $f_c' = 28\ N/mm^2$, $f_t' = 3.0\ N/mm^2$, $\varepsilon_c = 0.002$, $\nu = 0.15$, and $\gamma_c = 24\ kN/m^3$. Reinforcing steel: $E_s = 210000\ N/mm^2$, $E_{sh} = 0\ N/mm^2$, $f_{sy} = 270\ N/mm^2$, and $\varepsilon_{su} = 0.10$. A prestressing steel with $f_{pu} = 1680\ N/mm^2$ and $f_{py} = 0.7 f_{pu}$. is considered. A penta-linear stress-strain diagram has been generated based on standard shape fitting these properties.

5.- PERFORMED ANALYSES AND RESULTS

5.1- Linear Elastic Analysis

The study in [9] (1991) by Molins of several loading cases in a linear elastic analysis showed a very good agreement with the similar results first obtained by Lo and Scordelis [1] (1969), thus illustrating the suitability of the geometric modelling adopted for the present study. The discussion of the linear elastic analysis, together with more details relative to the nonlinear analyses which are presented below, may be found in [9].

5.2.- Nonlinear Geometric Analysis (NLG) with Prestressing

In this case, the design live load Q_0 ($1.437\ kN/m^2$) is increased indefinitely until a maximum load is obtained for the structure. The materials are considered to be linear elastic, so that no limiting tensile or compressive strengths are defined for the concrete or the steel, while the nonlinear effects caused by finite displacements are considered.

A failure was obtained for a vertical load of $1.0DL + 32.3Q_0$, followed by a descending post-failure branch (Fig. 5). The maximum deflection at failure is reached in the external X—edge beam at a distance of 11.0 m from the top (Fig. 6). The obtained geometric instabilty seems related to an excessive deflection of the X—edge beam, which tends to work like a simply supported beam rather than a cantilever, having a support at the tip of the Y—edge beam. Thus, the geometric failure is partly related to the geometric asymmetry of the structure.

5.3.- Nonlinear Geometric Analysis (NGL) with no Prestressing

A similar type of analysis was performed without any prestressing to study this effect. No significant change was observed during the loading process for live load, as illustrated by Fig. 5. As known, prestressing should not affect the global nonlinear geometric behavior of the structure since the set of equivalent forces caused by prestressing consitute a self-balanced system.

5.4.- Nonlinear Material Analysis (NLM) with Prestressing

In this case, the limiting material strengths defined in Sec. 4 are considered, together with the nonlinear constitutive equations included in the numerical method of analysis. Displacements and rotations are assumed to be small.

An ultimate load of $1.0DL + 4.23Q_0$ is obtained (Fig. 7). The maximum vertical deflection at failure appears at the tip of the HP quadrant and reaches 22.1 cm. Almost no post-failure branch is obtained, so that a rather brittle behavior is detected. An inspection of the analytically obtained state of the materials shows that the failure is mainly due to exceeding the tensile strength at certain membrane zones near the HP tip which are under-reinforced while submitted to a state close to pure tension.

5.5.- Nonlinear Geometric and Material Analysis (NLGM) with Prestressing

The coupling of both types of nonlinearity, material and geometric, caused a reduction in the

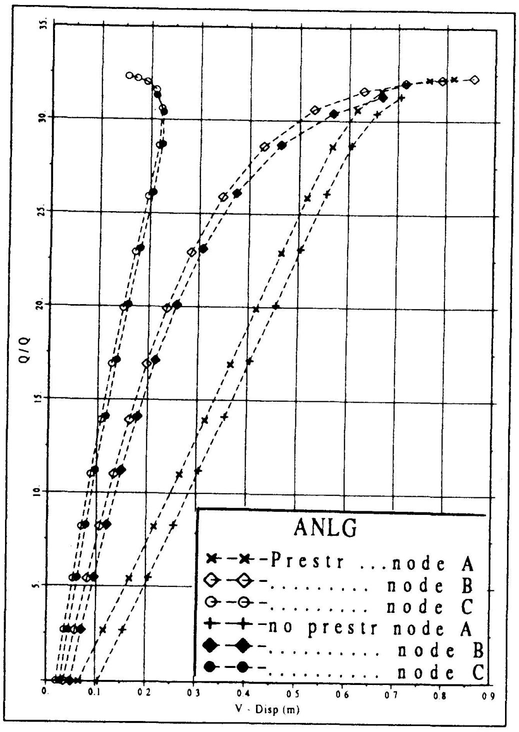

Fig. 5 Load vs. vertical deflection for NLG analysis, (a) with prestressing (b) without any prestressing.

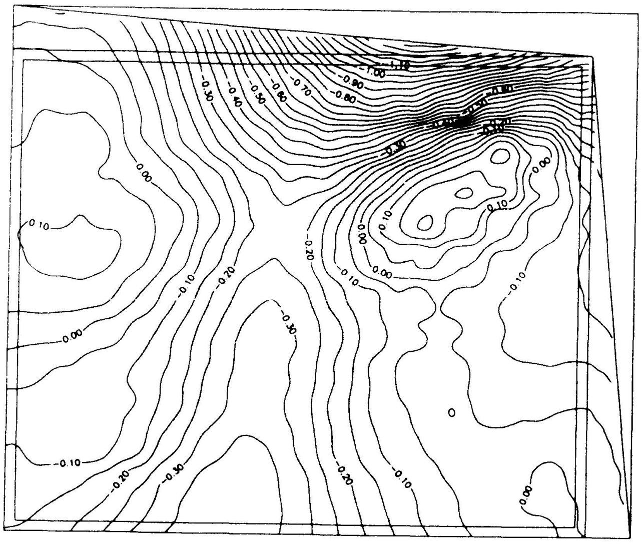

Fig. 6 Vertical deflection in shell at ultimate load for NLG analysis with prestressing.

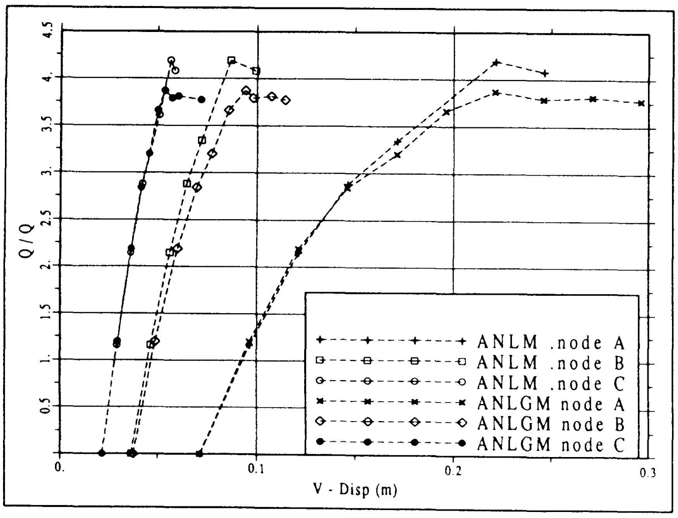

Fig. 7 Load vs. vertical deflection for NLM and NLGM analyses

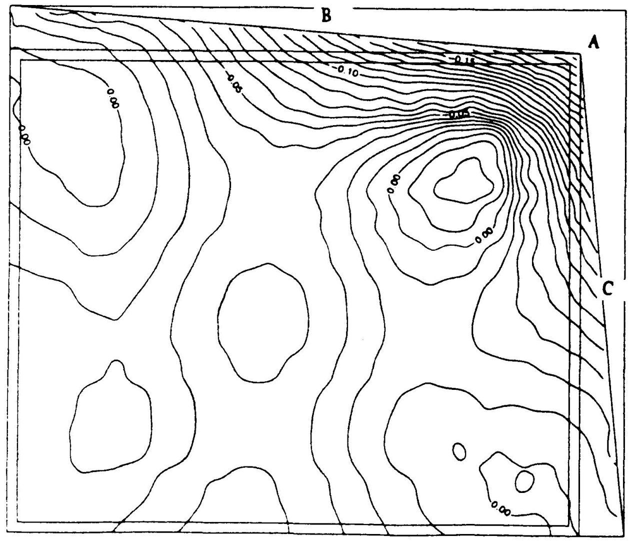

Fig. 8 Vertical deflection at ultimate load for NLGM analysis.

ultimate load of the structure with respect to the analysis in which only material nonlinearities were considered. The obtained ultimate load is now $1.0DL + 3.87Q_0$, showing a drop in the maximum live load Q of 8.5% from that for the nonlinear material alone analysis (Fig. 7). A maximum deflection of 22.1 cm for the ultimate load, appears at the tip of HP quadrant. As Fig. 8 shows, the deformed shape of the roof is qualitatively similar to that one obtained by the nonlinear material analysis. The influence of the nonlinear geometric effects may be seen in the slight reduction of the ultimate load and in the ductility acquired in the post-failure behavior. However, failure is still due to excesive cracking of concrete near the tip of the shell. Considering the live load capacity of $3.87Q_0$ found in this nonlinear analysis, in which Q_0 was the design live load of $1.437kN/m^2$, it can be said that a design level of safety for the structure exists, and the adequacy of the original design process is shown for the structure subjected to instantaneous vertical loading. Shell and edge beam prestressing affect in a strong way the performance of the structure not only during service conditions, but also at the ultimate range.

6.- CONCLUSIONS

A numerical model for the nonlinear geometric and material analysis of prestressed concrete shells has been used to study an existing long span prestresed concrete shell structure: the Ponce Coliseum, in Puerto Rico. Using an accurate discretization which included both shell and beam finite elements, several different analyses were carried out under vertical loads to study the service and ultimate behavior of the structure, together with its failure mechanism. In an analysis considering both the geometric and the material nonlinear effects, the designed safety of the structure under short-term vertical loading was demonstrated.

Some aspects not yet included in the analysis, such as the influence of the actual construction sequence, as well as the time dependent effects of creep and shrinkage of the concrete and the long-term losses in the prestress are planned for future studies.

REFERENCES

1 Lo, k.S., Scordelis A.C., Design of a 271 ft. Span Prestressed HP Shell, Proceedings of the IASS Congress, held at Madrid, October 1969.

2 Scordelis, A.C., Lin, T.Y., Ponce Coliseum Shell Roof in Puerto Rico, Proceedings of the IASS Congress, held at Calgary, July 1972.

3 Yang, Y. C., Record Concrete Shell Roof Featured in Coliseum, Civil Engineering Magazine— ASCE, June 1972.

4 Lin, T. Y., Kulka F., Lo, K., Giant Prestressed HP Shell for Ponce Coliseum, Journal of the Prestressed Concrete Institute, Vol. 18, No. 5, September-October 1973.

5 Chan, E.C., Nonlinear Geometric, Material and Time Dependent Analysis of Reinforced Concrete Shells with Edge Beams, Division of Structural Engineering and Structural Mechanics, University of California, Berkeley, UC-SESM Report 82-2, December 1982.

6 Scordelis, A.C., Chan, E.C., Nonlinear Analysis of Reinforced Concrete Shells, Proceeding of Symposium on Computer Applications in Concrete Technology held at American Concrete Institute Convention in San Francisco, March 1986, ACI Special Publications, SP-98 1987.

7 Scordelis, A. C., Nonlinear Material, Geometric and Time Dependent Analysis of Reinforced and Prestressed Concrete Shells, Bulletin of the International Association for Shell and Spatial Structures, Vol. 31-1,1,2, Nos. 102,103, April-August 1990.

8 Roca, P., Un modelo de análisis no lineal para el estudio del comportamiento de estructuras laminares de hormigón pretensado, Departament d'Enginyería de la Construcció, Universitat Politècnica de Catalunya, Barcelona ,September 1988.

9 Molins, C., Estudi del comportament en servei i fins a ruptura d'una lamina pretensada real: el Coliseo de Ponce, Universitat Politècnica de Catalunya, Barcelona ,1991.

Remaining Strength of Bridges in Rotterdam
Capacité restante des ponts à Rotterdam
Resttragfähigkeit von Brücken in Rotterdam

Kors NOORLANDER
Civil Engineer
Public Works Rotterdam
Rotterdam, The Netherlands

Kors Noorlander, born in 1941, got his civil engineering degree at the Technical University of Delft in 1963. After military service he joined the Public Works in 1965. Since then he was involved in the design of bridges and special steel structures as well as in the evaluation of existing bridges.

SUMMARY
In the City of Rotterdam there are over 600 bridges. Decisions concerning maintenance are only possible on a responsible basis if the remaining strength of the structures is taken into account. This is illustrated by some case studies.

RÉSUMÉ
La Ville de Rotterdam compte plus de 600 ponts. Pour prendre des décisions relatives à leur entretien, il est nécessaire de prendre en compte la capacité restante des constructions. Quelques exemples illustrent cette situation.

ZUSAMMENFASSUNG
In der Stadt Rotterdam stehen über 600 Brücken. Um Entscheidungen über ihre Unterhaltung zu treffen ist es notwendig, mit der Resttragfähigkeit der Konstruktionen zu rechnen. An einigen Beispielen wird dies weiter erläutert.

1. INTRODUCTION

The Public Works Service of the City of Rotterdam is responsible for the maintenance of more than 700 bridges with a total value far exceeding 10^9 Ecu. Lifetime varies from new to over a century. The spans vary from some meters to over 270 m. Nearly every type of construction is present.
It is quite clear that, with such a diversity of structures, it can be expected that a considerable number is not confirming to present day design standards. Remaining strength of these structures is of vital importance in decisions concerning maintenance or replacement.
In this paper selection criteria, remaining strength assessment and some selected cases will be dealt with.

2 SELECTION OF STRUCTURES

2.1 Selection criteria

Selection of structures can not be done on the base of an elaborate structural analysis. The intention of the selection is to decide which structures have a high priority. Because it is out of question to base the selection on a thorough analysis good engineering judgement is the only tool available. But of course there are some criteria which can be helpful in this respect: age of the structure, damage reports, maintenance reports, absence of drawings and/ or calculations, changed loading conditions, settlements, problems with similar structures.
Age is, of course, the most important criterium, but damage and maintenance-reports are also quite useful in this respect.

3 ASSESSMENT PROCEDURE

3.1 Introduction

The procedure for the assessment and, as pointed out in the introduction, the loading and finally the risk involved is in nearly all cases the same.

3.2 Procedure

After the decision to evaluate a certain structure the following procedure is applied:

a Retrieval of archival material
This involves the material in the technical and administrative archives, historical archives of the municipality, old engineering handbooks, historical descriptions of the City, whatever may be useful.
In a number of cases drawings as well as design calculation are absent, because the original ones were destroyed during the war.

b Review of drawings and design calculations
In this stage the reliability of drawings and calculations is established. Drawings are compared with the real structure; calculations are checked, especially with respect to modelling and loading.

c Drawings

Depending on the situation drawings should be updated, or, if necessary, completely renewed. This should be based on a recent survey. Under no circumstances it is allowed that any serious work is done before this step is completed.

d Updating design calculations
If the reliability of the existing calculation is not enough it should be updated, or even completely renewed. This can be a quite laborious operation. After this phase it is possible to make conclusions on the static strength of the structure and to perform the fatigue analysis.

e Fatigue life assessment.
Based on the updated calculations and combined with loading spectra derived from recent traffic counts, and, in the case of movable bridges, bridge operation records, the life of the structure is determined.

f Test loading
In a lot of cases the structural system leaves a lot of questions with respect to the reliability of the modelling. In these cases test loads can be conducted.

g Inspection
After static and fatigue analysis detailed directions for the inspection of the structure are given. These can involve searching for cracks in members or welds, corrosion, loose bolts or rivets, specific locations and so on.

h Final conclusions
Based on the finding of the foregoing steps the real state of the structure is determined . In this conclusion static strength and fatigue life are the main items.

i Recommendations.
Depending on the findings actions are recommended; these can be:

- Strengthening of the structure
- Intensive periodical inspection of critical parts
- Partly or complete renewal

4 CRITERIA

Relating remaining strength of a structure to a fixed value in a standard is, to my opinion, not giving any answer to the question how safe or dangerous it is, because strength as well as loading are both stochastic in nature. Risk is the only criterium which has any value for taking decisions. The level of risk that is acceptable depends on a lot of circumstances.
Most important point is the question how serious the collapse really is. Is it a complete collapse of the structure or is it merely regarded by the public as a minor nuisance comparable to a pothole in a road-surface.
So minor damage is accepted by us in a lot of cases provided it is detected within a reasonable time.
Another important point in the possibility of inspection. If it is possible to detect damage just in time we can accept a greater risk.

It is quite clear that in the case of a total collapse of the structure higher levels of safety are

required.
In all these cases a lot of commonsense should be in our judgement. After all if we are predicting problems there is a chance of a near miss. And the smaller safety-margin the greater the chance.
That is the reason that we use recent observations and measured intensity of the actual traffic on the bridge. BS 5400:prt 10 is extremely useful because, in this respect, the level of safety can be varied.

5 CASES

5.1 Bridge with hot-rolled beams and oversized cut-outs.

This fixed bridge which is of a very simple structural concept of parallel INP380 , 0.79 m' c.t.c, with a span of 5.83 m' covered with wooden shelfs.

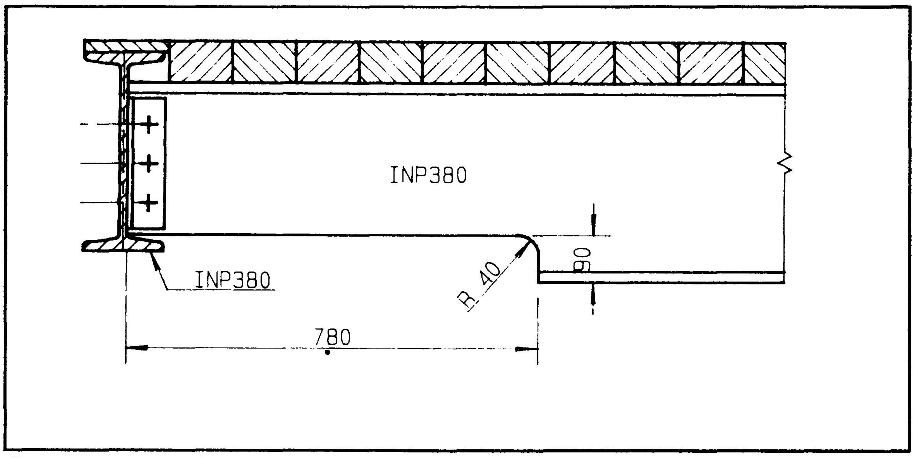

figure 1 Oversized cut-out near support

5.1.1 Selection
The structure was selected because the drawing gave rise to questions with respect to details.

5.1.2 Existing documents

Historical research revealed that the bridge, originally, was a movable bridge. Between 1940 and 1945 it was converted to a fixed structure using the original beams. On the only available drawing a cut-out near one of the abutments showed up. No dimensions were available. In the stress-calculations no reference was made to this detail.

5.1.3 Strength assessment
The analysis of the bridge was preceded by a measurement of the cut out. At the same time the corner of the cut-out was inspected by dye-penetrant; no cracks were found.
On behalf of the existing design calculation it could be concluded that the bridge could be rated as Class 45 which is regarded as quite sufficient in the occurring situation.
A detailed analysis revealed that the cut-out gave a reduction of the classification to 22; if the stress-concentration around the corner was taken into account the classification was further reduced to 15; equivalent to a wheel-load of 12.5 kN. The collapse load, with plasticising crossection occurred at a wheel-load of 69 kN (without impact) that explained why there was no collapse.

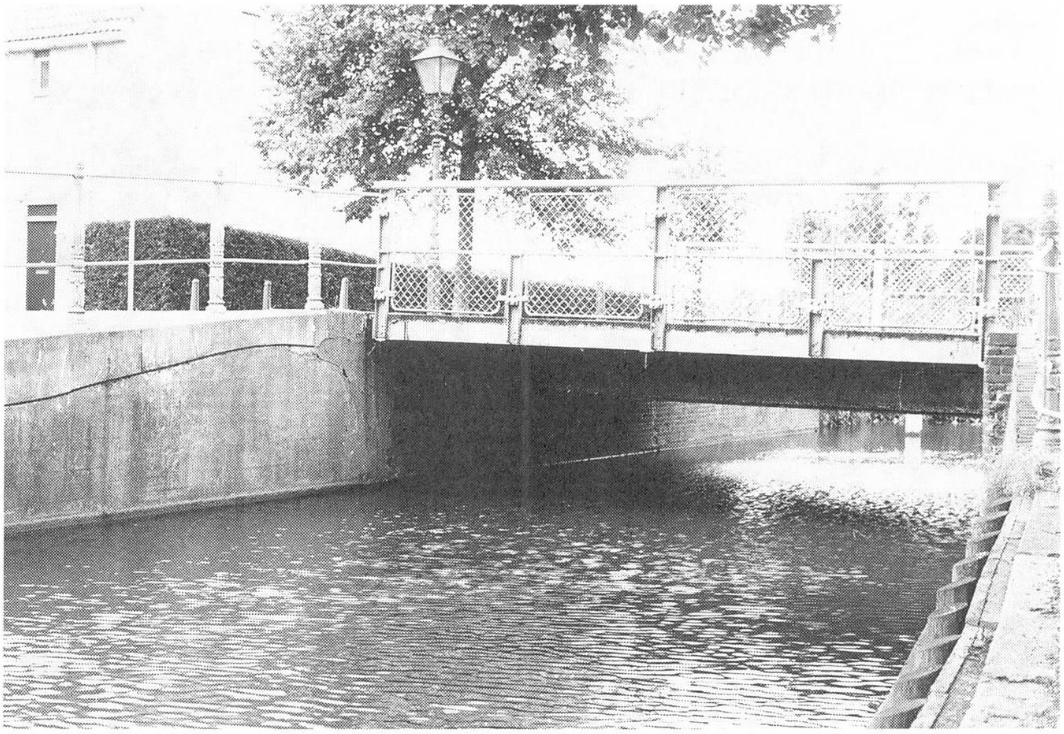

Photo 1 bridge

Recently we analyzed the detail by finite elements. The results didn't differ much from the former calculations by hand.

5.1.4 Recommendations

On account of the result of the analysis a strengthening of the detail was proposed.

5.2 Modelling faults

Modelling faults of the structural system of bridges have been quite numerous in the past. The calculations on their own are quite accurate, but the underlying structural system or loadings are apt to a number of anomalies.
In movable bridges this is quite notable. Especially the modelling of loads is apt to a lot of mistakes; often the fact that opening of the bridge completely changes the loading conditions was completely ignored.
The bridge, of the type pictured in photo 3 and 4 is a specific example of this fact. In closed situation the beam coupling the axles of the balance is a double plate-girder. But after opening this beam is a Vierendeel-truss with high shear-force resulting a high variation of bending-stresses (140 N/mm^2) which was confirmed by means of strain measurements.

5.3 Load testing of cantilevers

In most of the bridges in our city cantilevers are supporting the sidewalks, so loading is only by pedestrians and cyclists.

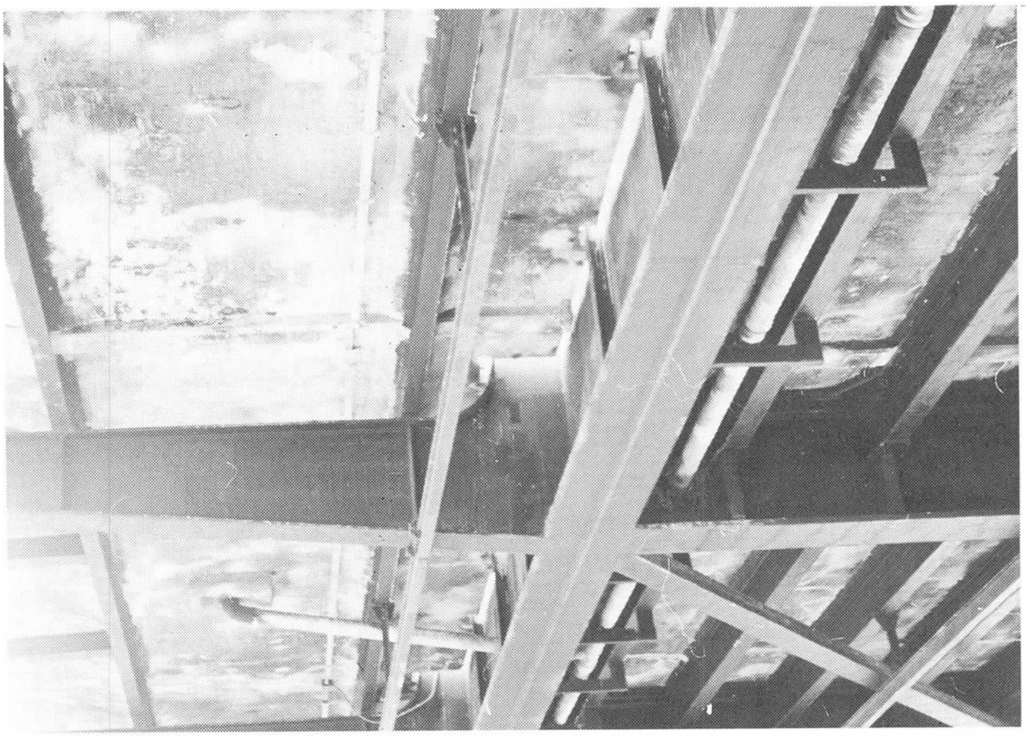

Photo 2 construction of cantilevers

Compared to the loadings specified in the standards real loadings are much lower.
In this case the probability of a high loading on the sidewalks is much higher because the bridge is in the route to the most important football stadium of the city.

The bridge has two spans and serves as an overpass of a railway. The structural system is a double stiffened arch connected by crossbeams with a reinforced concrete deck.
Build in the late thirties, this was the first all welded larger bridge in the Netherlands.
Details were strongly related to riveted construction. In this respect the strength of the cantilever was doubted.

Theoretical analysis revealed that the strength was less than the standards required.
But the reliability of this analysis was questionable. So we decided to test the loading capacity by test loading. During the test deformations as well as strains were recorded.
The testload was applied by means of a loaded truck.
The results were that the safe load was over 50 % higher than the theoretical calculated load.
Plastic deformations were not observed.

5.4 Strain measurements

Strain measurement in stead of analysis

One of the main problems with the analytical stress analysis is that the modelling must confirm to the real structure. In a lot of cases the modelling of more or less loose bolts and rivets, eccentricities, stress-concentrations are quite unreliable or extremely labour consuming.
In these cases the structure itself is the best model we have.

Photo 3 movable bridge

Strain-measurements are quite a good answer to this problem, provided that the restrictions of the method (existing stresses can not be measured by applied strain gages) are not a problem.
In this case the structure is a movable bridge. the problem was the stress-variation resulting from the opening and closing of the bridge. The structure is of a type which is completely balanced; balancing is accomplished by a counterweight supported on a beam above the bridge deck. Eccentricities, stress-concentr-ations, protruding axles, and so on play an important role in the distribution of the stresses. This is an ideal case for strain gages. The only equipment used were straingages, measuring equipment, electrical wire, a mobile scaffolding an some small hand tools.

The strain measured indicated that the structure was nearly at the end of its life . Subsequent inspection did not reveal any cracks but some doubts existed in this respect because not all parts were good visible.
So it was recommended to strengthen the structure.
To my opinion strain measurements are a neglected tool in the field. In a lot of causes it can be much more economical than extensive analytical approaches. In this case it took only 2 days; the cost that was about 15 % of an analytical approach.

5.5 Ship collisions

Collision of ships to a structure are always a potential danger to most bridge-structures.
Questions of remaining strength may deal with danger of immediate collapse,
the allowance of traffic, the urgency of repairs and so on.

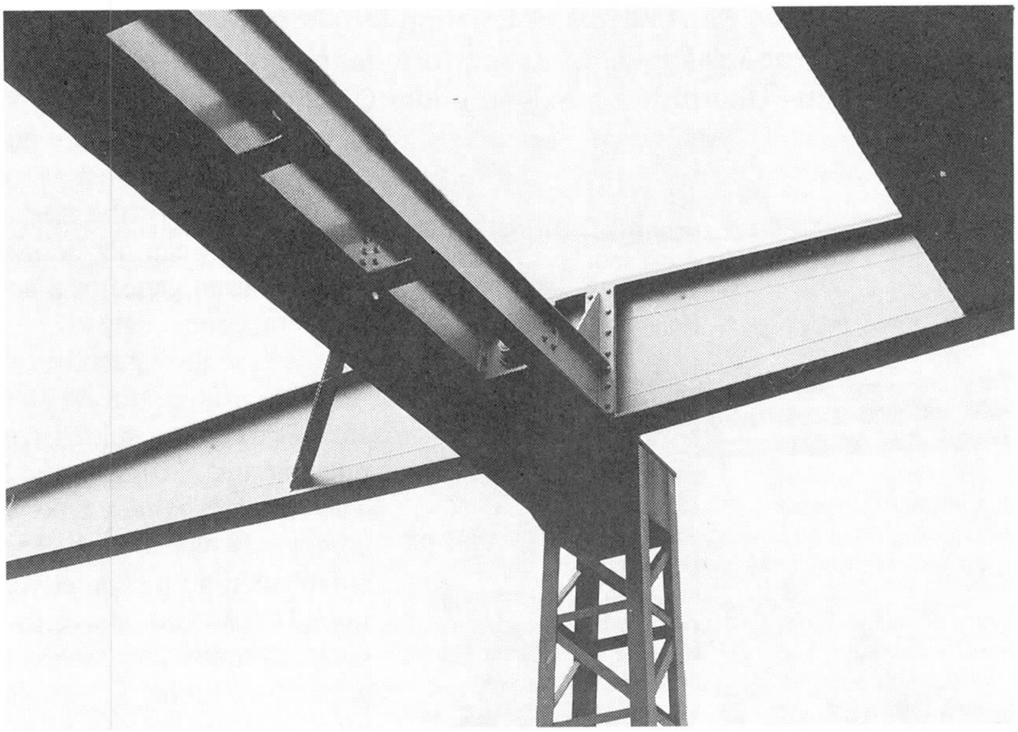

Photo 4 detail of movable bridge

6. CONCLUSIONS

Experience in the past 25 years has learned us that it is possible to make decisions with regard to maintenance or replacement of structures. Remaining strength is of vital importance in this process. It should be based on the risk which is involved in the decision we are making. The risk, but also the cost must be acceptable to the community.
In all our decisions we must seek for the balance between economic and human factors. There is always an opportunity, but a small one, that we are to optimistic. The chance that we are to pessimistic is much greater. It is our responsibility, as engineers, to find the right equilibrium. If there is never any near miss, than the authorities and the public will regard our advices as theoretical, and unpractical.

Probabilistic Re-Analysis of Existing Offshore Structures
Contrôle probabilistique de plates-formes marines existantes
Probabilistische Überprüfung existierender Offshore-Konstruktionen

Marcello BERANGER
Nuclear Engineer
Snamprogetti S.p.A.
Milan, Italy

Dimitris DIAMANTIDIS
Professor
Fachhochschule Regensburg
Regensburg, Germany

Gian Maria MANFREDINI
Director of Operations
D'Appolonia S.p.A.
Genoa, Italy

Marcello Beranger, born 1962 in Italy, got his Laurea in Nuclear Engineering at the Polytechnic of Milan, Italy. After joining Snamprogetti in 1988, he has been involved in several studies on structural reliability analysis of components for the Offshore, Petroleum and Chemical Industries. Presently he is a Project Safety Leader of the Safety and Reliability department of Snamprogetti S.p.A.

Dimitris Diamantidis, born 1957 in Athens, Greece, got his Diploma and Doctor degrees in Civil Engineering at the Technical University of Munich, Germany. Since then he has been senior research engineer with Det Norske Veritas in Oslo, Norway, and Project Manager with D'Appolonia S.p.A. in Genoa, Italy. From September 1992 he is Professor of Structural Engineering at the Fachhochschule Regensburg.

Gian Maria Manfredini, born 1943 in Italy, holds a Laurea in Mechanical Engineering from Polytechnic of Milan, Italy, and a M.S. in Civil Engineering from Michigan State University. He has been involved in research, analysis and design related to steel and concrete structures for the Nuclear, Offshore and Transportation Industries. He is currently Director of Operations at D'Appolonia S.p.A.

SUMMARY
When the necessity for re-qualification of an offshore structure arises, the basic problem encountered is that decisions may not be supported by code criteria. Current code criteria are not flexible in terms of additional information aquired after the design stage. One has to turn to methods based on reliability analysis supported by the information gained from field experience, maintenance and monitoring. These methods are briefly discussed here and three case studies are presented to illustrate their applicability to various situations.

RÉSUMÉ
Lorsque se présente la nécessité de reclassement d'une plate-forme marine, le problème principal est que les décisions ne peuvent s'appuyer sur les critères de projet existants. Les critères de projet courants ne se prêtent guère à l'assimilation des informations supplémentaires acquises après la phase d'étude d'un projet. Il faut par conséquent adopter des méthodes basées sur des analyses de fiabilité en exploitant les données obtenues directement sur le terrain, dans le domaine de la maintenance et du contrôle. Ces méthodes sont brièvement expliquées et trois cas sont présentés pour illustrer leur faculté d'application à différentes situations.

ZUSAMMENFASSUNG
Das Hauptproblem beim nachträglichen Nachweis existierender Offshore-Konstruktionen besteht darin, dass Entscheidungen nicht von Normenkriterien getragen werden können. Aktuelle Normenkriterien sind nicht flexibel genug, um zusätzliche Erkenntnisse nach der Bemessungsphase zu berücksichtigen. Mann muss zu Methoden der Sicherheitstheorie zurückgreifen, unterstützt von Informationen, die während der Betriebs- und Überwachungsphase der Konstruktion gewonnen wurden. Diese Methoden werden hier kurz diskutiert und drei Fälle werden beschrieben, um ihre Anwendung in verschiedenen Situationen dazustellen.

1. INTRODUCTION

Offshore exploitation is nowadays a mature field. Several platforms have been in operation for over twenty years, often exceeding their original design lifetime and experiencing extreme environmental actions, damages and possible reduced maintenance and repair due to periods of depressed international offshore market. Re- qualification of these structures for extended lifetime is a major issue in the offshore industry. Offshore operators must balance their decisions between required levels of safety and available budgets.

This has resulted in the rationalization of the decision process and of the re-analysis procedures necessary to re-qualify existing offshore structures. Efficient and sophisticated techniques have been developed in the last decade for that purpose which incorporate modern structural and reliability analysis methods.

This contribution discusses experience gained from the implementation of reliability methods and appropriate criteria for the re-qualification of existing offshore structures. The difference between prior uncertainty modeling and reliability updating on the basis of available information is emphasized. The methodological approaches are illustrated in case studies dealing with re-qualification of platforms in various offshore locations.

2. OVERALL RISK DECISION APPROACH TO OFFSHORE REQUALIFICATION

Various aspects have to be taken into account in the decision process for offshore platform re-evaluation, and consequently several parties might be involved, each of them contributing with, or requiring, different types of information. The final decision is gradually reached by pooling all these contributions into one. These contributions are coming from:

- Design.
- Field experience.
- Re-qualification analysis.
- Economical analysis.

The above listed contributions lead to the collection of information that are of very diverse nature, e.g. in terms of type of data and category of persons/deciders who provide them. In particular, both numerical and non numerical information have to be used.

The general practice in re-evaluating offshore structures is that of relying on a "rational approach". The safety and economy implied by certain decisions are evaluated by means of both statistical/probabilistic considerations (risk analysis), and economical analysis (cost/benefit analysis).

3. USE OF RELIABILITY METHODS

3.1 Prior uncertainty analysis (design stage)

The largest uncertainties exist at the design stage. Not only is the loading environment partially known but also the specific quality of manufacture and construction is under control to a limited extent. Furthermore the actual load-effect relationships involve some systematic but also random variability. All these uncertainties can be modeled by random variables. In order to provide safety criteria appropriate limit states "g" have to be defined; failure occurs when $g < 0$.

Safety is assured by requiring that the limit state will be reached with a small probability, which is dependent from the joint probability density function of the stochastic variables defined in the problem.

Numerical methods for reliability calculation have been developed during the past decade and the first order reliability methods FORM have been recognized as very accurate and efficient [1-3]. The probability of failure by using FORM is estimated by:

$$P_f \approx \Phi(-\beta) \qquad (1)$$

where $\Phi(.)$ is the standard normal distribution function and β is the reliability index.

3.2 Updating through additional informations (re-design stage)

Additional informations gained during lifetime of the structure can be quantified and implemented in order to update original or codified safety levels. Two basic cases are briefly described next, updating of limit states and updating of random variables.

In many cases, inspection results can be interpreted as artificial limit states and can be applied directly in the updating procedure of the originally estimated failure probabilities. The updated failure probabilities P'_f are then evaluated as conditional probabilities. The following two fundamental cases are classified:

$$P'_f = P[g_0(X) \leq 0 \mid g_1(X) = 0] \qquad (2a)$$

$$P'_f = P[g_0(X) \leq 0 \mid g_1(X) > 0] \qquad (2b)$$

where $g_0(X)$ is the original limit state function and $g_1(X)$ the artificial limit state function formulated from the inspection results. The vector (X) includes all basic variables in g_1 and g_0. Examples of equation (2a) are measurements carried out under proof - loading, observations of crack lengths, and of deformations (or settlements). A typical example for equation (2b) is the survival of the structure (or of the structure components) under high loads. Updated failure probabilities are derived within a first-order reliability method framework [3]. The influence of a possible lifetime extension can be taken into account by modifying the distribution function of the time dependent basic variables in the original limit state function $g_0(X)$.

In some cases only specific influencing parameters such as material strength or geometrical dimensions are inspected. After the inspection, updated distributions are given to the influencing random variables resulting to a decrease or an increase of the reliability index.

3.3 Compatibility of safety requirements with reliability analysis techniques

Safety requirements for structural design and re-design cannot be established on the basis of pure science. A rational approach for the requirements must be a synthesis of:

1. basic understanding of structural behavior;
2. basic knowledge of current practice concerning workmanship, equipment, and construction methods etc.;
3. experience gained from the behavior of existing structures;
4. economical, social, political and legal considerations;
5. reliability theory;

The classical codified safety requirements, for example the partial safety factor format, cannot be applied in the evaluation of the reliability of existing structures since they are not flexible in terms of additional information. The probabilistic reliability theory constitutes a rational tool for updating additional information and comparing the actual reliability level with the assumed reliability level (inherent in present codes).

4. CASE STUDIES

4.1 Mechanical impact re-assessment of North Sea platform

Re-qualification of an existing platform located in the British sector of the North Sea was required both for production systems reliability and structural integrity. The platform is a "K"- bracing steel jacket type, located at a water depth of about 142 m. The aim of the study was to extend the platform lifetime and to update the overall safety level.

Structural safety assessment was performed taking into account:

- updated environmental load;
- re-analysis of ship traffic in the vicinity of the platform;
- structural re-analysis of the jacket;
- jacket inspection.

Due to over-stressed members found after the jacket structural re-analysis, the main emphasis was paid to assess the platform damage resistance after a ship collision. The scope was also to verify the British authority requirements which state that the structure should be capable of withstanding an impact from a 2500 tons vessel with a velocity of 0.5 m/s. Assuming that all the kinetic energy is absorbed by the installation and that an added mass factor of 0.4 must be applied an impact energy of 0.44 MJ is obtained. Norwegian authorities requirements were also considered, which specify a design impact from a supply vessel of 5000 tons at a velocity of 2.0 m/s and an added mass factor of 0.4 for broad side collisions and 0.1 for bow collisions. This results in impact energies of 14 MJ and 11 MJ respectively.

The probability of failure is evaluated as follows:

$$P_f = P_c \bullet P_m$$

where P_c is the probability of platform-ship collision and P_m is the member probability of failure conditioned to ship impact.

The failure probability analysis associated to passing vessels was simplified by the fact that P_m was considered equal to unity. A ship traffic analysis in shipping lanes near the platform location was performed, considering also updating for future ship traffic development.

In case of a visiting vessel (supply vessel) platform collision, the limit state can be defined as:

$$g = E_m - E_s$$

where E_m is the energy absorption capability of the impacted member and E_s is the ship impact energy. The probability of failure has been calculated using FORM by introducing the following random parameters:

- ship mass and impact velocity;

- strength and geometric characteristics of the impacted member.

The results have shown that the Norwegian authorities requirements are not fulfilled; the British authorities requirements are fulfilled and the annual probability of failure considering revised data on distributions of impact masses and impact velocities found in the literature is in the order of 10^{-3}.

The reliability analysis has indicated that the structure cannot sustain an impact from a vessel since stress redistribution is not possible. This is due to the high number of members over-stressed and to the type of joints.

In these platforms the ability of a "K"-bracings panel to transmit shear is lost if the compression brace buckles. From the study it was concluded that appropriate provisions to avoid vessel impact or to increase the impact load absorption capability must be considered.

4.2 Fatigue re-analysis of steel gravity platforms in the Gulf of Guinea

For offshore structures the fatigue limit state is governing the structural dimensions of several member and particularly of joint connections. Therefore, efforts of inspection campaigns for re-qualification purposes are aimed to assess the structural integrity of such joints, and to detect possible cracks and corrosion damage. However, due to the considerable costs, only a limited number of joints can be inspected.

The inspection results together with the design data representative of the platform have been first implemented in a software system that integrates the data base with procedures of analysis required in a re-qualification process [8]. Procedures include statistical analysis, damage accumulation analysis, crack growth analysis.

The statistical analysis package was required to correlate damage joint characteristics in order to define probability distributions of representative deterioration parameters for not inspected joints. Where applicable, such an approach has been integrated in three steps:

- creation of the sample population and definition of explanatory variable such as water depth, element type, joint geometry, material, design fatigue life, etc.;
- definition of statistical model for the deterioration parameters (i.e. pitting depth, probability of crack presence, crack depth, actual thickness) by using analytical methods of variance;
- computation of response for not inspected joints.

The damage accumulation package has allowed to compute, for each joint, the probability of failure due to fatigue in the hypothesis of linear damage accumulation (Miner's rule).

A crack growth analysis was performed, to determine failure probabilities by means of a fracture mechanics approach. The model based on the Paris and Erdogan [10] law was established for a semi-elliptical crack in an infinite plate according to current practice [9,11]. The stochastic model applied to fatigue crack growth accounts for uncertainties in loading, initial defects, material parameters and in computation of stress intensity factors. The crack growth model has been combined with FORM to compute failure probabilities.

Figure 1 shows the decrease of the reliability index with time for a critical joint. The three curves represent:

- prior reliability index without considering inspection results;
- posterior reliability index "conditioned" by inspection results, i.e.:
  - joint itself has been inspected and no crack, or a crack of given depth has been found,
  - other joints of similar characteristics have been inspected and found without crack, or with a crack of given depth, thus resulting in an updating of the considered not inspected joint.

Figure 2 illustrates results obtained for another critical joint of the same platform and emphasizes the time dependency of the following parameters:

- prior reliability index without information through inspection;

- posterior reliability index corresponding to conditional failure probability index "given" that no crack has been observed;

- range of acceptable safety level (based on the considerations mentioned before);

- inspection effort to achieve acceptable safety level for a desired additional lifetime.

The results have been generally used to judge the Inspection Repair Maintenance (IRM) program versus extended life of service. The benefits associated with the use of the illustrated procedure include:

- improved safety related to the knowledge of the risk associated to the extension of the platform life;

- sound evaluation of the relative importance of detected defects on the structural safety;

- optimization of future survey by screening out not critical joints.

4.3 Re-assessment of seismic loading for a platform in the Adriatic Sea

This example deals with the re-assessment of seismic loading for a platform offshore Ancona in the Adriatic Sea. This platform has been designed in the late 70's according to the following criteria:

- design lifetime of 20 years;

- probabilistic evaluation of ground acceleration based on the attenuation law of McGuire [12] which is based on strong motion recordings from Western United States;

- definition of two different peak ground acceleration (PGA) levels [13]; Strength Level Earthquake (SLE) associated to a return period of 100 years, corresponding to an acceleration of 0.11 g; Rare Intense Earthquake (RIE) associated to a return period of 1000 years, corresponding to an acceleration of 0.2 g.

Figure 3 illustrates peak ground accelerations versus return periods for design and re-design.

After 10 years the safety of the platform has been addressed together with the consideration of a total lifetime of 30 years. Therefore, the criteria used in the design stage have been reviewed, evidencing in particular that recent developments allowed to account for:

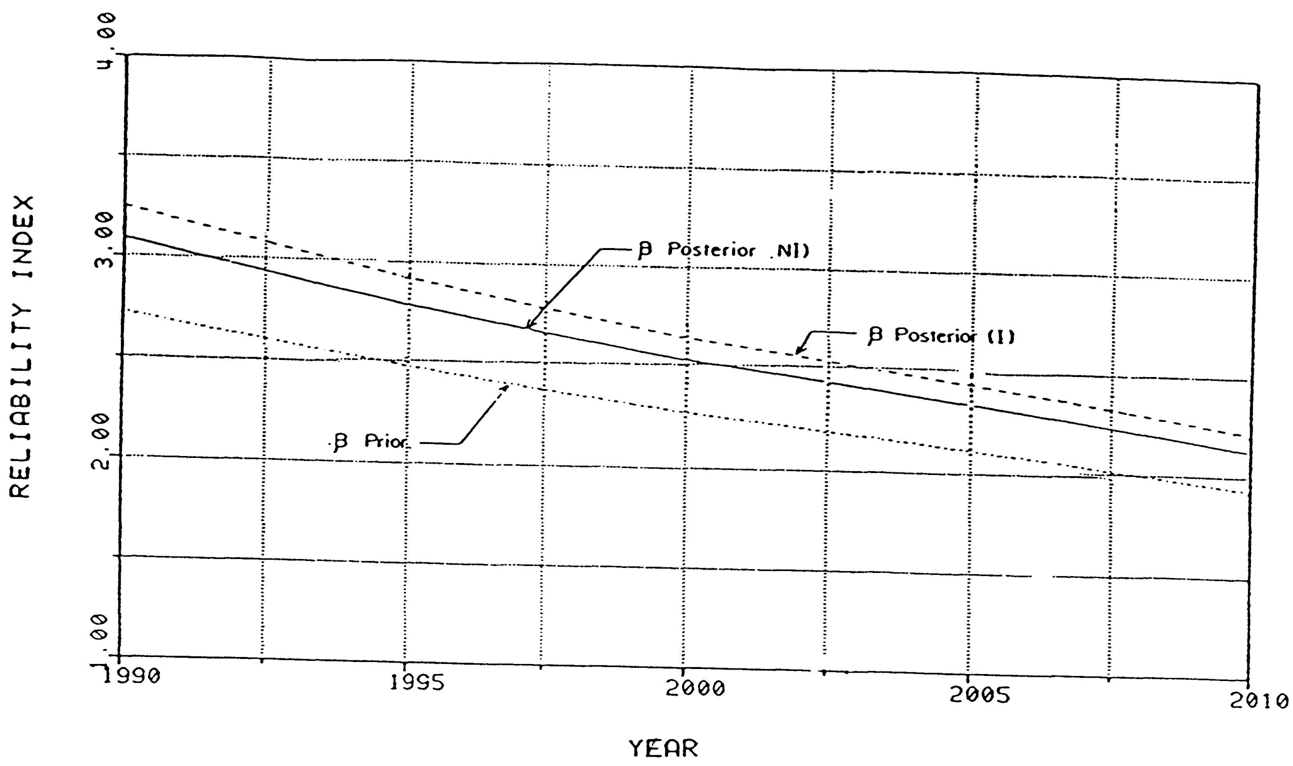

Fig 1 Reliability index vs. time for inspected (I) and not inspected (NI) joints.

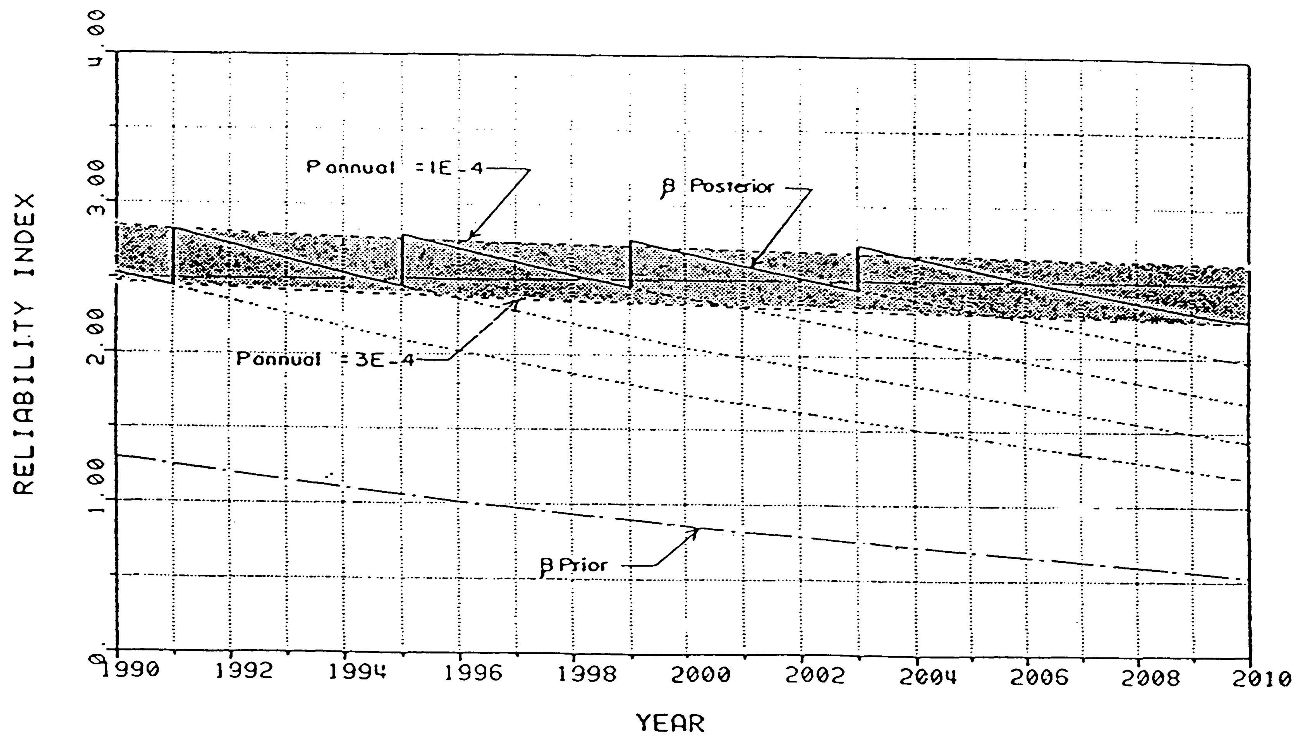

Fig 2 Reliability index vs. time and recommended inspection program.

- revised earthquake catalogues;
- specific attenuation relationship for the platform site [14];
- reliability based definition of the return periods at which SLE and RIE should be associated to be in accordance with current safety philosophy in the offshore industry [15]; SLE and RIE have been associated to 200 and 2000 years return periods respectively.

Although the new return periods for the representative PGA's are more conservative than those assumed in design, the application of the new attenuation law and the more accurate characterization of seismicity allowed to obtain lower values for the peak ground acceleration. In particular, the SLE was associated to 0.09 g, while the RIE to 0.18 g, introducing a 10% - 15% reduction with respect to design values.

The new results expressed in terms of PGA versus return period are also included in Figure 3 demonstrating the lower values obtained through re-analysis. The method in Ref.[16] has been then used and the results have demonstrated that earthquake is not endangering platform safety, if compared to the original design assumptions.

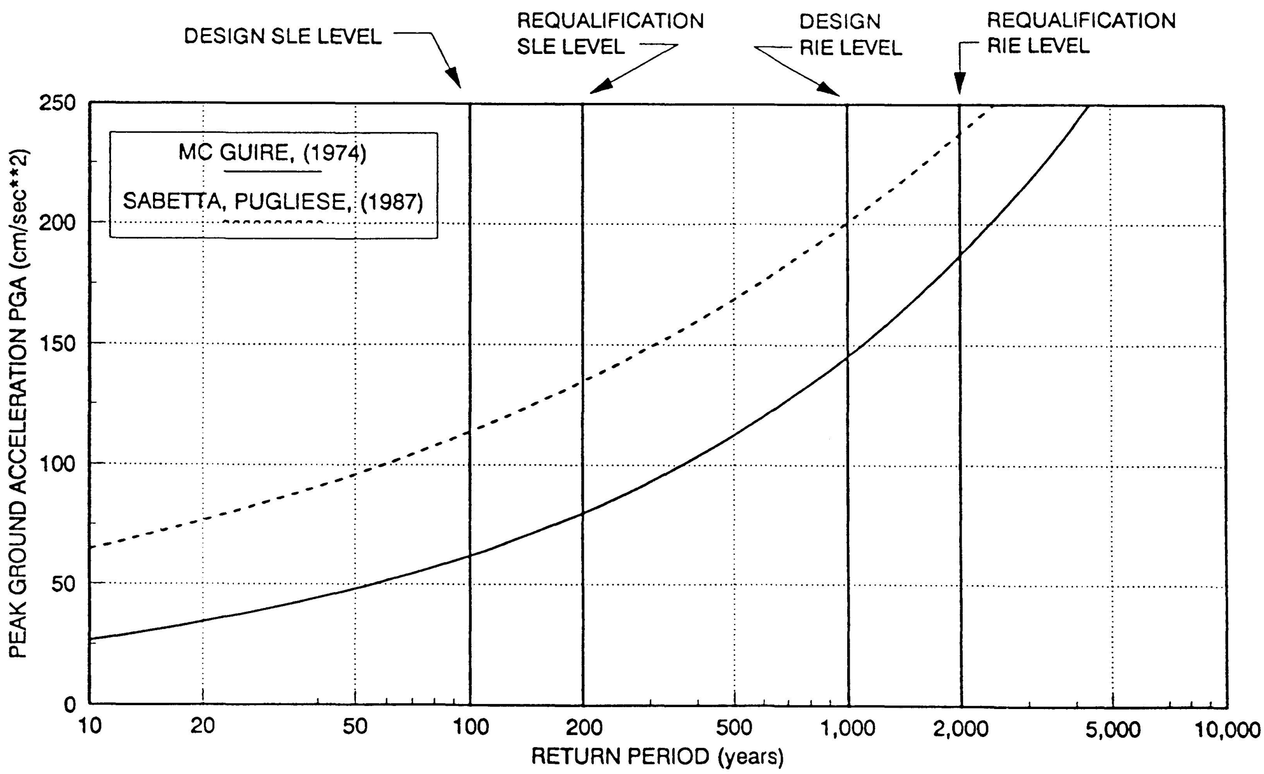

Fig. 3 Peak Ground Accelerations obtained adopting design and re-qualification attenuation laws

5. REFERENCES

1. HASOFER, A.M., LIND, N.C., An exact and invariant first-order reliability format, J. Eng. Mech. Div. ASCE, 1974, 111-121
2. HOHENBICHLER, M., RACKWITZ, R., Non-normal dependent vectors in structural reliability, J. Eng. Mech. Div. ASCE, 1981, 1127-1138
3. MADSEN, H.O., KRENK, S., LIND, N.C., Methods of structural safety, Prentice-Hall, Englewood Cliffs, New Jersey, 1986
4. CEB-FIP, Model code, Paris, London, Berlin, 1978
5. DET NORSKE VERITAS (DnV), Rules for the design, construction and inspection of offshore structures, Høvik, Norway, 1981
6. DIAMANTIDIS, D., Reliability aspects for design and re-design of offshore structures, Proc. 5th OMAE-ASME Conf., Tokyo, Japan, 1986, 29-36
7. RACKWITZ, R., Implementation of probabilistic safety concepts in design and organizational codes, Proc. 3rd Int. Conf. Struct. Safety and Reliability, Trondheim, Norway, Elsevier, Amsterdam, 1981, 593-614
8. VANZINI, R., ROSSETTO, P., CONZ, L., FERRO, G., RIGHETTI, G., Re qualification of offshore platforms on the basis of inspection results and probabilistic analysis, Off. Techn. Conf. (OTC), Houston, 1989
9. DIAMANTIDIS, D., RIGHETTI, G., FERRO, G., ZUCCARELLI, F., Reliability based re-qualification criteria for existing jacket platforms, Off. Mech. and Arctic Eng. (OMAE), Stavanger, Norway, 1991
10. PARIS, P., ERDOGAN, F., A critical analysis of crack propagation laws, Journal of Basic Engineering, Trans. ASME, vol. 85, 1963, 528-534
11. MADSEN, H.O., Probabilistic and deterministic models for predicting damage accumulation due to time varying loading, DIALOG 5-82, Danish Engineering Academy, Lyngby, Denmark
12. McGUIRE, R. K., Seismic structural response risk analysis incorporating peak response regressions on earthquake magnitude and distance, MIT Dept. of Civil Engineering, Research Report R74-51, 1974
13. American Petroleum Institute (API), Recommended practice for planning, designing and constructing fixed offshore platforms, API RP2A, 19th Ed., Dallas, 1989
14. SABETTA, F., PUGLIESE, A., Attenuation of peak horizontal acceleration and velocity from Italian strong-motion records, Bulletin of the Seismological Society of America, vol. 77, pp. 1491-1513, 1987
15. MOSES, F., Development of preliminary load and resistance design document for fixed offshore platforms, Final Report, API-PRAC Project No. 85-22, American Petroleum Institute, Dallas
16. BEA, R.G., Reliability criteria for new and existing platforms, Offshore Technology Conference, Texas, 1990

Traffic Load Estimation by Long-Term Strain Measurements

Estimation des charges due au trafic au moyen de mesures de contraintes à long terme

Abschätzung von Verkehrslasten mittels Langzeit-Dehnungsmessungen

Holger WAUBKE
Civil Eng.
Techn. Univ. of Munich
Munich, Germany

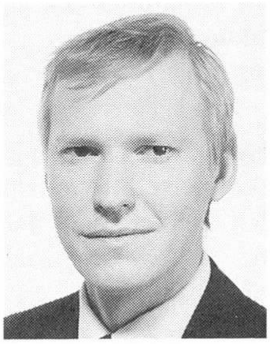

Holger Waubke, born 1964, received his engineering degree at the Technical University of Munich and was employed at the Technical University of Munich in 1990. He has been involved in theory and measurements of wave propagation and developing computer programmes.

Werner BAUMGÄRTNER
Dr. Eng.
Techn. Univ. of Munich
Munich, Germany

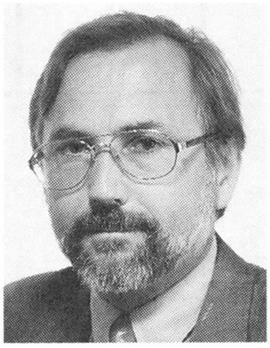

Werner Baumgärtner, born 1944, received his engineering degree at the Technical University of Munich and then worked in construction offices involved in bridges and buildings. Since 1972 he has been employed by the Technical University of Munich and works in the field of structural mechanics, especially dynamics.

SUMMARY

Because the installation of the equipment for in situ measurement becomes more expensive than the equipment itself, it is reasonable to use the installation not simply for short-term measurements. Using the installation for long-term measurements will result in useful information about stress history, which can be used for traffic load estimation and service life estimation. As an example first results of the long-term measurement at a motorway bridge are presented.

RÉSUMÉ

L'installation d'instruments de mesure est devenu plus chère que leurs frais d'acquisition. Il est donc raisonnable de les utiliser non seulement pour des mesures à court terme, mais aussi à long terme. Ces dernières conduisent à des informations très utiles sur l'histoire des contraintes permettant l'estimation des charges et de la durée possible d'utilisation de la structure. Des mesures effectuées pour un pont autotoutier sont données à titre d'exemple.

ZUSAMMENFASSUNG

Da die Installation von Messgeräten am Bauwerk inzwischen teurer geworden ist als deren Anschaffungskosten, ist es sinnvoll die Installationen nicht ausschliesslich für Kurzzeitsmessungen einzusetzen. Langzeitsmessungen liefern nützliche Informationen zur Spannungsgeschichte, die für Belastungs- und zur Lebensdauerabschätzung verwendet werden können. Als Beispiel werden die Messungen an einer Autobahnbrücke vorgestellt.

1. Introduction

In autumn 1991 the bridge Fischerdorf in Germany was opened. The Bridge crosses the danube near Deggendorf and is connecting the motorway A12 Munich-Deggendorf to three roads on the other side of the danube. To get a control of the theoretical calculations of the complex construction as shown in figures 1 and 2 measurements with static loads were projected. To get more information about the structural behaviour it was decided to use the installations for additional dynamic long term measurements.

2. Bridge Structure

The bridge has two main girders which cross-section is shown in figure 2. Transverse beams connect both main beams to rods which are connected to one middle arch. The cross-section of the main beams are a steel construction with a concrete deckslab. The construction bears the loads in a combination of torsion and bending of the main girders and the arch.

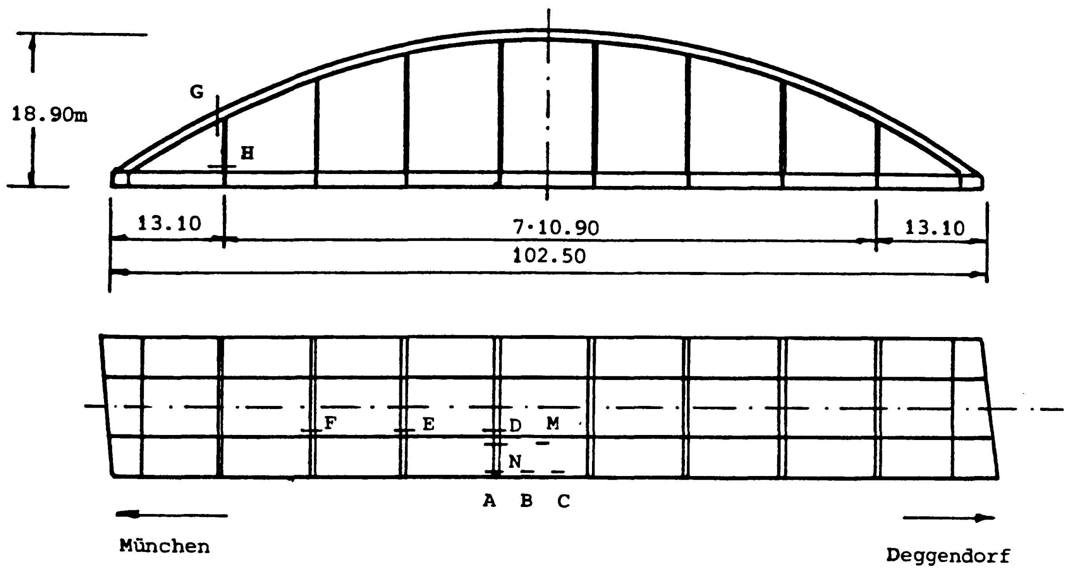

fig. 1 Bridge Fischerdorf

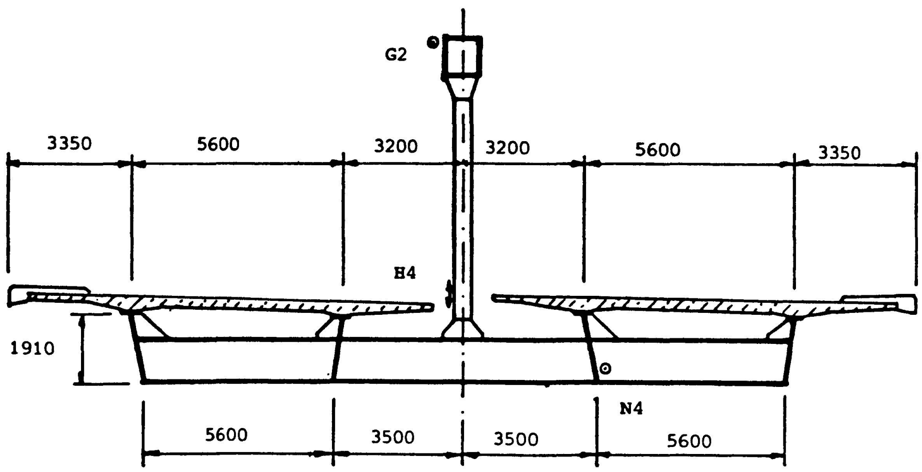

fig. 2 Bridge Fischerdorf cross-section

3. Measurements

3.1. Measurement Equipment

Fourty points were selected at which the strains were measured. Four of them were at the arch (point G1-G4) near the first rod. Another group of four points were installed at the first rod. (Points H1-H4). The transverse beams have three groups of strain gages (D1-D4, E1-E4, F1-F4). The other measurement points (A1-A4, B1-B4, C1-C4, M1-M4, N1-N4) were at different locations of one of the main griders, at the webs near the deckslab and the bottomslab.

At each measurement point one active strain gage and one for compensation were connected to one Whetstone´s half bridge to compensate temperature effects. The gages for compensation were fixed to little steel plates which were seperated from the steel construction with a special paste, with the consequnece that the plate has the same temperature as the main construction without having its stresses. To get longer stability of the strain gages some of them are capsuled. The long time measurement will also improve the stability of this different type of strain gages. Eight of the fourty measurement points can be measured at the same time. An amplifier HBM-MGA is used as a signal conditioner. The calculation of collectives or spectra are done by different personal computers with build in analog-digital-boards of type Data Translation 2801A and Analogic MS-DAS 16.

3.2. Stress Collectives

Two personal computers were used to evaluate the stress collectives permanently.The program was developed at the Lehrstuhl für Baumechanik [1]. The hystereses counting method (rainflow method) is used to classify the stresses into a matrix with 64 rows and columns. The calculation is done without interrupting the measurement. Also hypothesis for life time estimations are included, in this way nonlinear hypothesis can be calculated incrementally. A calculation of nonlinear hypothesis afterwards is impossible, because of the unknown time history of the stress-cycles. Additional information about life time estimation is given in [2]. At the moment the results of the collectives at different points covering one week measurements can be presented. The tree lines in figure3 show the collective after 2 hours, 20 hours and 160 hours.

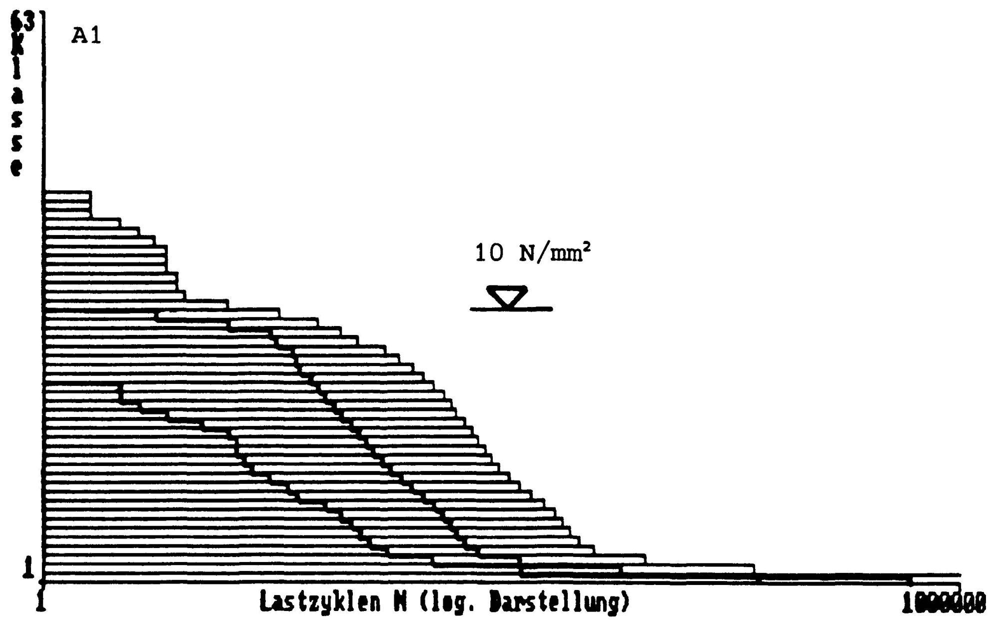

fig. 3 Stresscollectives of measurement point A1 after 2 hours, 20 hours, 160 hours

The collectives after 160 hours at points G2 and H4 of the construction is shown in figure 4

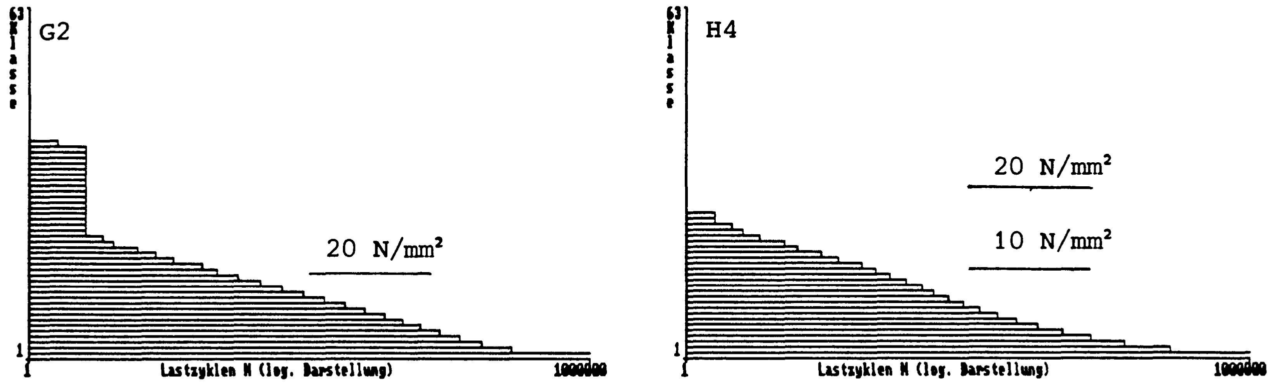

fig. 4 Stress collectives of measurement locations G2 and H4 after 160 hours

The stress cycles at the highest levels are not the result of the traffic loads but due to the temperature gradient between day and night. Therefore about one cycle per day can be calculated from the collectives. Strain-cycles due to high level stresses are measured at the arch. The point A1 near the road way shows much more stress-cycles at low level stresses than the rod and the arch, for which the local stresses are not important.

3.3. Time Series

After the short time measurements with static loads were done in autumn 1991, some short time measurements with dynamic loads followed. Figures 5 and 6 show the dynamic response of the first rod (location H1) to a transporter with a weigt of 91 tones. Figure 5 belongs to a speed of 30 km/h. The influence of crossing wooden plank placed on the driving lane in the middle of the bridge can be recogniced in figure 6. It shows the possible influence of dynamic effects on fatique life.

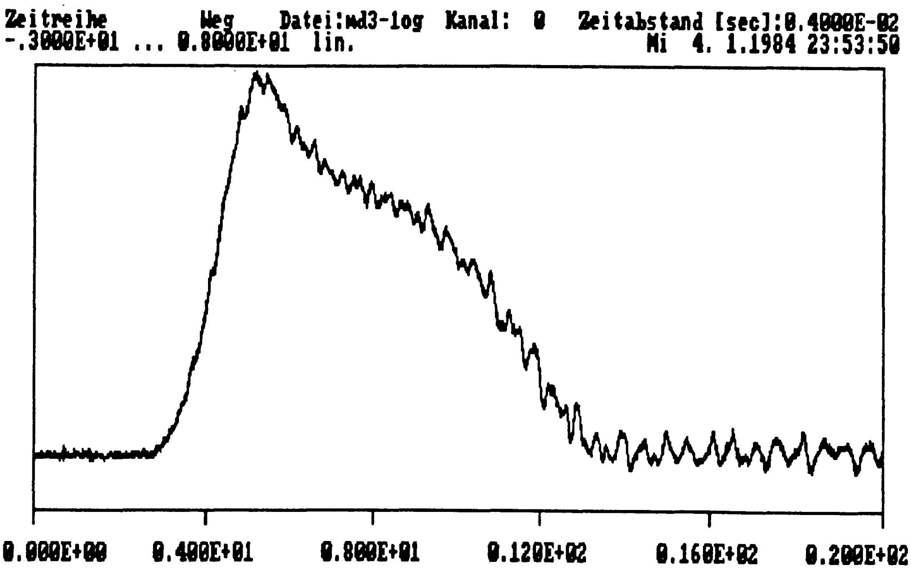

fig. 5 Short time measurements at point H1 of a transporter without a plank.

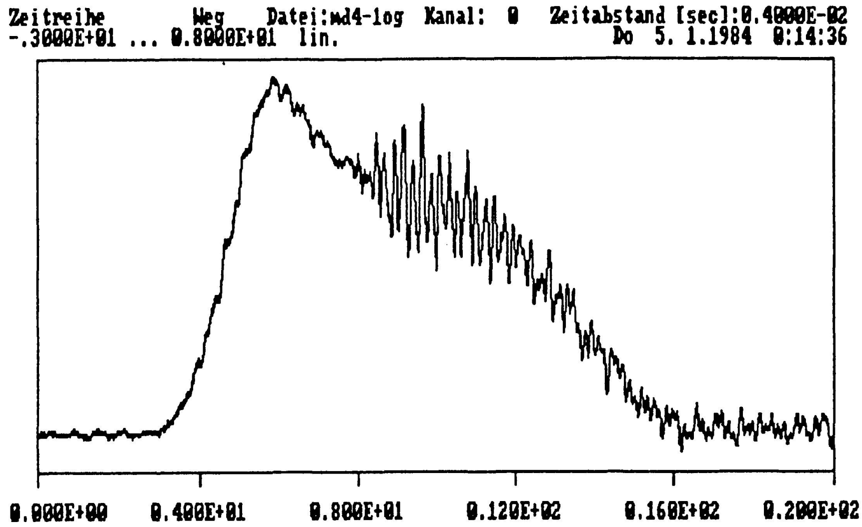

fig. 6 Short time measurements at point H1 of a transporter with a plank.

Some time series were recorded for about twenty minutes. Two clips of one of the records (figure 7) are displayed in figure 8 to show the different response of point N4 due to crossing vehicel In the first clip a static response of the bridge is visible while in the second clip a dynamic reaction of the bridge is shown. The influence on fatique life of the second vehicle is much greater than that of the first one. Therefore strain measurements as described in chapter 3.2 are necessary to calculate a more realistic life time estimation.

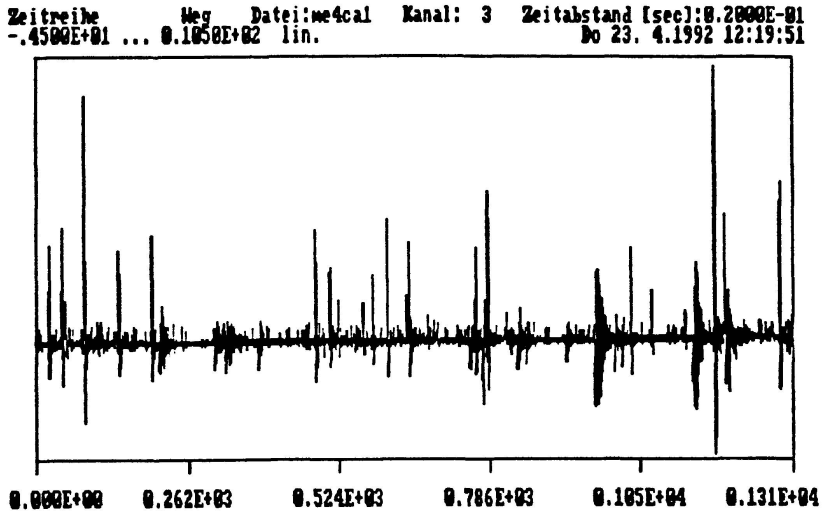

fig. 7 Time record at point N4

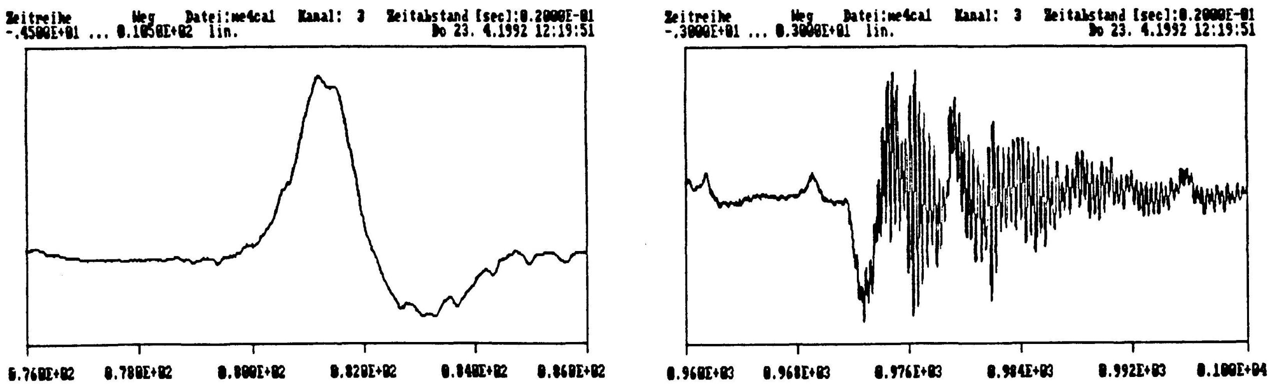

fig. 8 Two clips of the time record with showing different reactions of the bridge

The measured static response of the bridge due to the crossing vehicel in the first clip can be compared to a calculated influence line of the moment, which is porportional to the measured strains, because the vehicel is driving with a constant velocity.

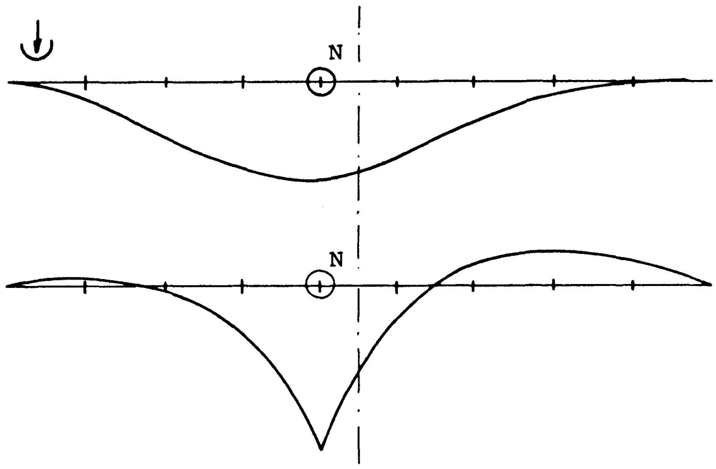

fig. 9 Static influence line of deflection and moment at point N4 calculated with finite elements method.

The frequency spectrum of the second figure has two significant frequencies which correspondends to two neighboured eigenfrequencies of the bridge.

3.4.Averaged Frequency Spectrum

Using a group of time series the spectrum can be averaged using the amplitudes of the spectra with no respect to the phases. Averaging of the complex amplitudes is impossible because a measurement without triggering results in random phases. Averaging amplitudes smooths the noise but does not eleminate the noise. The following figures show the frequency spectra with traffic load after about 1400 averages. The effect of smoothing the noise for random signals gives the possibility to determine the eigenfrequencies without using determined loads ore impacts. Averaging the traffic load spectrum has similar the effect as using a banded white noise excitation.

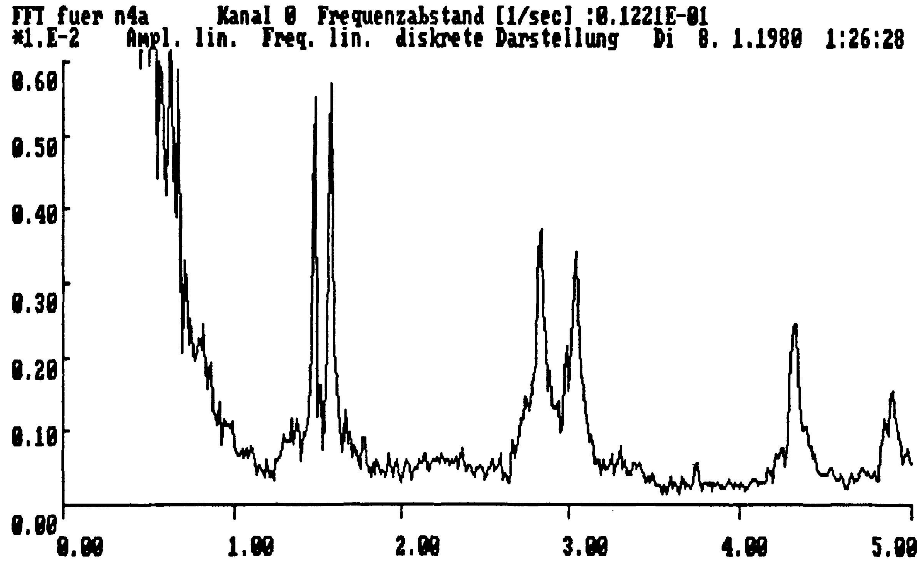

fig. 10 Averaged frequency spetrum for point N4

<u>3.5.Standard Deviation of banded Frequency Spectrum</u>

A possible way to control changements in traffic during time is to control the change in a banded frequency spectrum between averaged groups. Therefore in a first step the frequency spectra are averaged. In this case 10 spectra are chosen for one group. In a second step groups are averaged with a calculation of the standard deviation. In this example 140 averages of groups are done. The deviation is of the same order as the average. This is the result of the differences between day and night and at the weekend. To reduce this effect a special time control is introduced into the program, which measures the groups always at the same time and the same day. Long time observation with this time control might get information about long time changes in the traffic load.

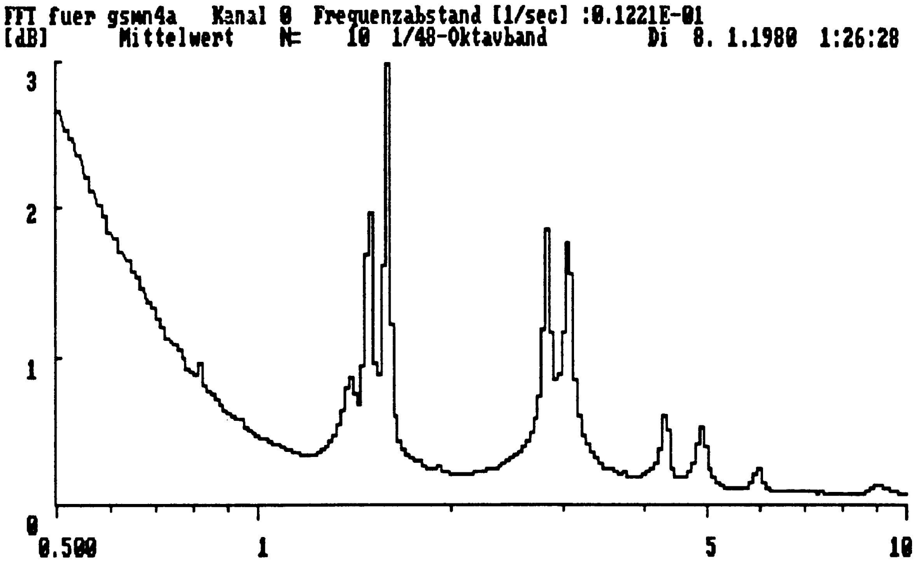

<u>fig. 11</u> Averaged banded frequency spektrum at point N4

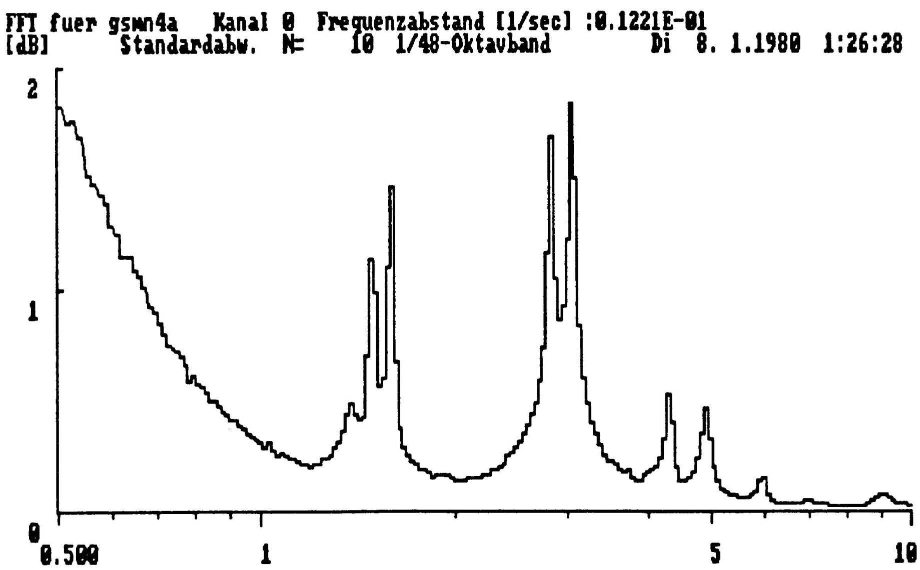

<u>fig. 12</u> Standard deviation of the frequency spectrum at point N4

4.Traffic Load Estimation

The direct calculation of the traffic loads based on the measured stresses is difficult. All driving lanes have different influence lines. Also the speed of the vehicels are variable, therefore only stochastic calculations are possible. Another problem is the dynamic response of the bridge to harmonic loads as shown in chapter 3.3. This effect is dicussed in [3] there the response of a beam to a moving harmonic load is displayed.

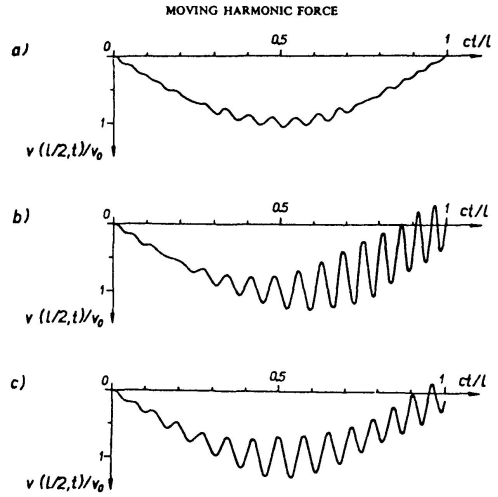

fig. 13 Deflection of a massless beam to a moving harmonic load with different speeds [3]

Changements in the traffic load will produce changing stresses at the measured points. Using long time measurements it is possible to control changing in traffic loads easily by controlling the development of numbers of stresscycles and their distribution. As an example an increase of heavy vehicles will result in an increase of the high level stress cycles. As a second possibilty a measurement of the resonant frequencies can control the development of vehicels with bad dampers, which are predistined to get in resonance with the bridge structure. This vehicels can reduce the fatique life of a bridge rapidly.

5.Conclusions

The results of the long term measurements can be used for life time estimation of the bridge. Using transfer function a life time estimation of arbitrary points of the bridge can be calculated.

An exact estimation of the traffic load is difficult because of the dynamic response of the bridge, but the measurements can control the development and the composition of the traffic loads. The only way to calculate the traffic load is to use statistical functions.

Because of the difficulties to develop a realistic load model it is better to measure the stresses of bridges at dufferent points. The results of this points can be used to calculate different points with respect to the dynamic eigenfunctions, the distribution in the frequency spectrum and the stress collectives.

REFERENCES

1. WAUBKE, H.: Kontinuierliche Erfassung von Schwingungsbeanspruchungen mit paraleller Ermüdungsbewertung unter Berücksichtigung von nichtlinearen Schadensakkumulations-hypothesen, Diplomarbeit Nr, 29, Lehrstuhl für Baumechanik der TU München, 1988
2. BAUMGÄRTNER, W., WAUBKE, H.: Service life estimation of bridges. To be presented at: 2nd Int. Conf. on Bridge Management, University of Surrey, UK,1993
3. FRÝBA, L: Vibration of solids and structures under moving loads, Noordhof International Publishing, Groningen, 1972

Monitoring of Trial Loiadings of Bridges using Optical Fiber Sensors
Surveillance des charges d'épreuve des ponts à l'aide de fibres optiques
Probelastungen von Brückenbauwerken überwacht mit optischen Sensoren

Reinhard WOLFF
Dr. Eng.
SICOM GmbH
Cologne, Germany

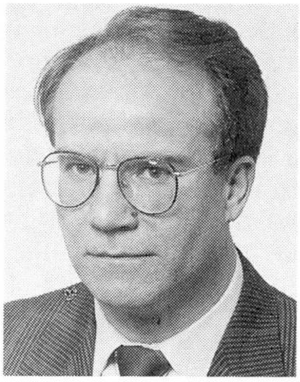

Reinhard Wolff, born 1945. Doctorate at Darmstadt Techn. Univ. Several years in the Central Dep. of Engineering and Design at Strabag Bau-AG's headquarters. Wide experience in the field of bridge construction, construction of tunnels, administration and industrial buildings as well as in environment engineering. Since 1991 managing director of SICOM- Gesellschaft für Sensor- und Vorspanntechnik GmbH (Sensor and Prestressing Techniques Ltd.).

Hans-Joachim MIESSELER
Civil Eng.
SICOM GmbH
Cologne, Germany

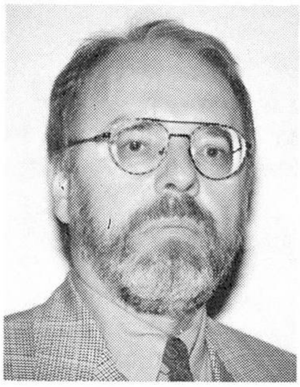

Hans-Joachim Miesseler, born 1944, studied constructional engineering in Wuppertal. From 1967 in the design office of Strabag head office in Cologne. From 1987-1990 manager of the department research and development in the central engineering and product management division. Since 1991 Technical Manager of SICOM.

SUMMARY

Monitoring of structures - especially of bridges - is getting more and more important. The reasons for this are the increase of heavy goods traffic, of air pollution and in precipitations, de-icing salts and the fact that prices for traditional maintenance and repairs are going up. In order to guarantee the durability of concrete structures over a long period of time it is necessary to monitor these structures on a permanent basis. In prestressed structures cracks in the concrete and the change in the stress-strain behaviour of the tendons must be observed.

RÉSUMÉ

La surveillance des constructions - surtout des ponts - devient de plus en plus importante. Cela est dû surtout à l'augmentation du trafic des poids lourds, à la pollution atmosphérique et au fait que les coûts de maintenance ou de réparation conventionelles augmentent en permanence. Afin de garantir la durabilité des constructions en béton pendant une longue période, il est nécessaire de surveiller en permanence. Dans le cas des bâtiment précontraints, il faut surveiller les fissures dans la précontrainte ainsi que l'allongement des éléments de précontrainte.

ZUSAMMENFASSUNG

Die Überwachung von Bauwerken - insbesondere von Brückenbauwerken - gewinnt eine immer grössere Bedeutung. Dies ist vor allem auf die Zunahme des Schwerlastverkehrs, Luftverschmutzung, Schmutzpartikel in Niederschlägen und auf Streusalze zurückzuführen sowie auf die Tatsache, dass die Kosten für die konventionellen Instandhaltungs- und Reparaturmassnahmen stetig steigen. Um die Dauerhaftigkeit von Betonbauwerken über einen langen Zeitraum hinweg gewährleisten zu können, ist es erforderlich, die Bauwerke permanent zu überwachen. In vorgespannten Bauwerken müssen Risse im Beton und Veränderungen im Dehnungsverhalten der Spannglieder ständig kontrolliert werden.

1. INTRODUCTION

For the monitoring of buildings with optical fiber sensors in principle two different types of application can be distinguished. On the one hand the monitoring of concrete structures, e.g. monitoring of crack formation and their further development and on the other hand monitoring of prestressing tendons comprising fiber composite materials. For the monitoring of crack formations in concrete structures the optical fiber sensors especially designed for this case of application are directly embedded in new buildings at critical positions of the load bearing structure known from statics. Their function is to provide information about eventually required maintenance works at a very early stage so that the costs for repair works can be reduced at a minimum. In already existant buildings - especially already damaged buildings - these optical fiber sensors are installed at a later date in the structural elements which shall be monitored in order to monitor cracks and their further development or the repair works which already have been realized with regard to the load bearing capacity of the structural element. In case of fiber composite prestressing tendons the optical fiber sensors are directly embedded in the fiber composite bar in order to indicate its intactness.

2. SENSOR TECHNOLOGY

In order to monitor buildings in a useful way it is necessary to develop appropriate sensors which are able to guarantee reliable measured values during a long period of time. Nowadays the intelligent processing of the high quantity of measured values is no problem due to the available and efficient personal computers.

The sensor technology is - regarding to the monitoring of buildings - only in the beginning of its development. The application of strain gauges on the prestressing steel or the measurement of the prestressing forces with the aid of load cells is not possible in case of prestressing with post-bond. Moreover it is not a durable solution in case of prestressing without bond.

Only the application of fiber composite materials facilitates a permanent control of the prestressing element over its entire length due to the integration of copper wire sensors or optical fiber sensors. Even the monitoring of each individual bar is possible. The sensors are already integrated into the tendon during its fabrication. The sensors indicate the integrity of the tendon or they locate the damage.

Besides the monitoring of the prestressing elements the observation of the stress/strain behaviour of the concrete in the zone subject to tensile forces is very important. Therefor the tensile zone above the piers and the spans are monitored permanently with integrated optical fiber sensors with a measurement exactitude of $\pm$ 0,2 mm.

2.1 The crack detection sensor

In the case of this type of sensor several optical fiber sensors or one optical fiber sensor are stranded with each other with one or several steel wires. If this sensor - which is connected normally to the structural element which shall be monitored in a distance of 1 m through a bearing material - is exposed to tensile load, the sensor effect is created by a loss of light intensity as a result of micro-bending. This light attenuation allows an integral measurement of the changes of the length of the sensor with a long term accuracy of $\pm$ 0,2 mm. The localization of these extensions changes (e.g. cracks) is carried out with an Optical Time Domaine Reflector (OTDR) by reflection measurements and a local dissolution of $\pm$ 0,5 m.

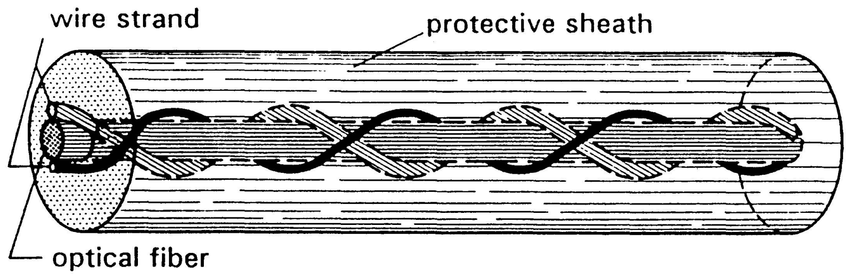

Figure 1:

2.2 The crack width sensor

The crack width sensor is a loop bended optical fiber sensor which is fixed at two bars. These bars are directly connected to the structure on the right and on the left of the joints or cracks which shall be monitored. The sensor monitors and measures permanently changes in the joints or crack width with a measuring sensitivity of 0,02 mm and a measurement range of 0,1 -10 mm.

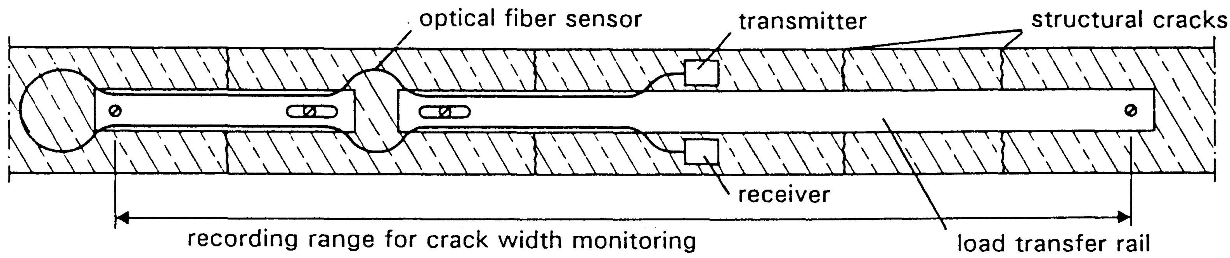

Figure 2:

2.3 The reflector sensor

A light signal is passed through the optical fiber sensor. The reflectors (Fig. 3) reflect part of the light while non-reflected light travels to the next reflector. In this way up to 30 measuring points can be monitored with a single sensor. Velocity measurements provide data on the deformations. An other design is the parallel arrangement of several optical fiber sensors (Fig. 4). In this case a light signal is passed one after the other through each optical fiber sensor with the aid of a multiplexer. With velocity measurements the length of the respective optical fiber sensor is measured and then compared with the sensor length of the parallel arrangement.

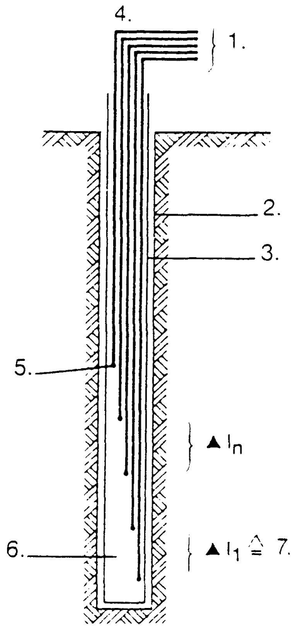

Figure 3:

1. Analysis electronic
2. Bore hole
3. Glass fibre composite pipe
4. n optical fibre sensors
5. Reflective end of sensor
6. Synthetic resin
7. Basic length as required
8. Semi-permeable reflector

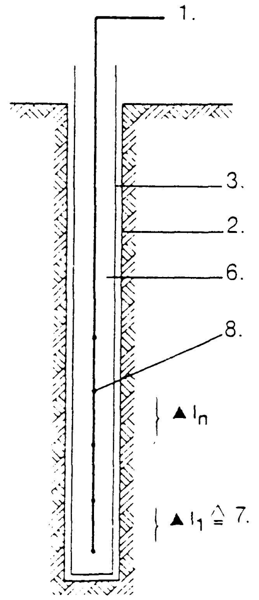

Figure 4:

3. TRIAL LOADINGS

3.1 Marienfelde Bridge, Berlin

The design of the Berlin-Marienfelde pedestrian bridge, a two span TT beam bridge, is an example of the first fully monitored bridge structure. In addition to glass fiber prestressing tendons (partial prestressing as external prestressing) with integrated sensors, a whole series of optical fiber sensors have been embedded directly inside the concrete or been retro-applied. During a trial loading carried out in November 1989 using 250 concrete slabs (weight per slab 1 t), this was able to be monitored with the aid of sensors. By using particularly highly sensitive sensors, evidence was even able to be recorded on the dynamic bahaviour of this bridge.

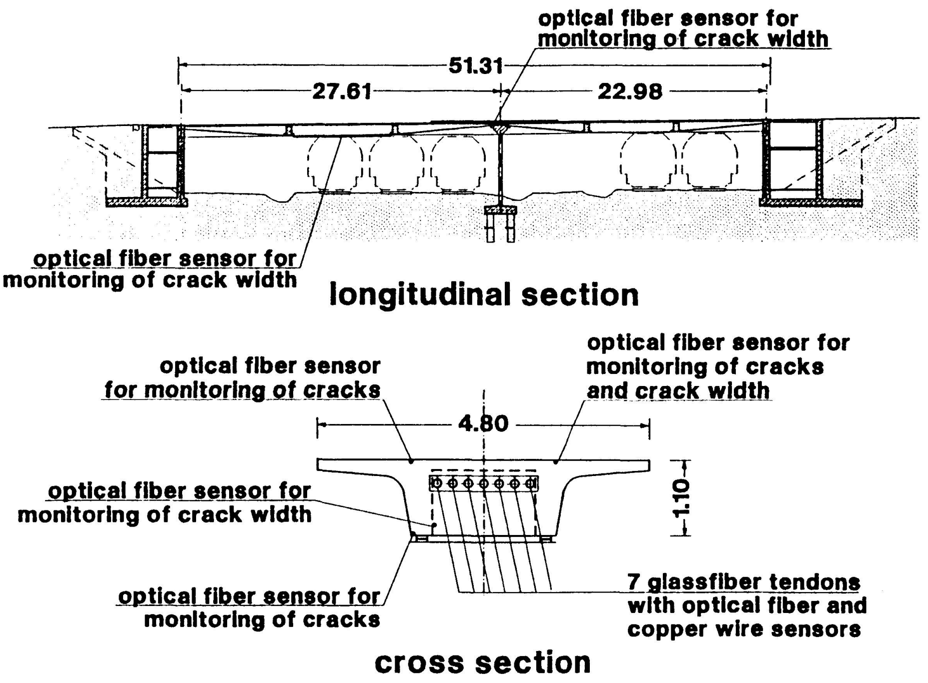

Figure 5: Measurement layout

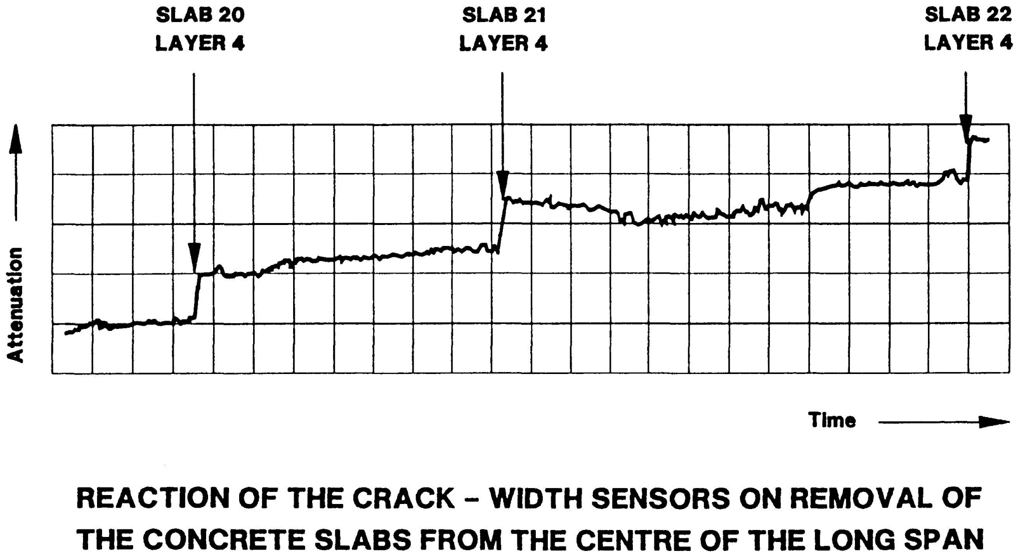

Figure 6: Monitoring of the test load by means of the optical fiber sensors embedded in the concrete

3.2 Schiessbergstrasse Bridge, Leverkusen

This three span, solid concrete slab bridge (bridge classification 60/30), is designed with limited prestressing comprising 27 glass fiber prestressing tendons (working load 600 kN) and post-bonding. Three glass fiber bars per tendon are provided with sensors and there are to be four additional optical fiber sensors integrated directly into the concrete on the upper and four on the lower side of the slab. The trial loading of the Schiessbergstrasse Bridge which has been realized on 31st of March 1992 showed in an impressive way the efficiency of the optical fiber sensors embedded in the concrete construction. By means of the loading of the bridge with a truck of a total load of 27,5 t it was possible to measure additional extensions of the bridge in the μ-range.

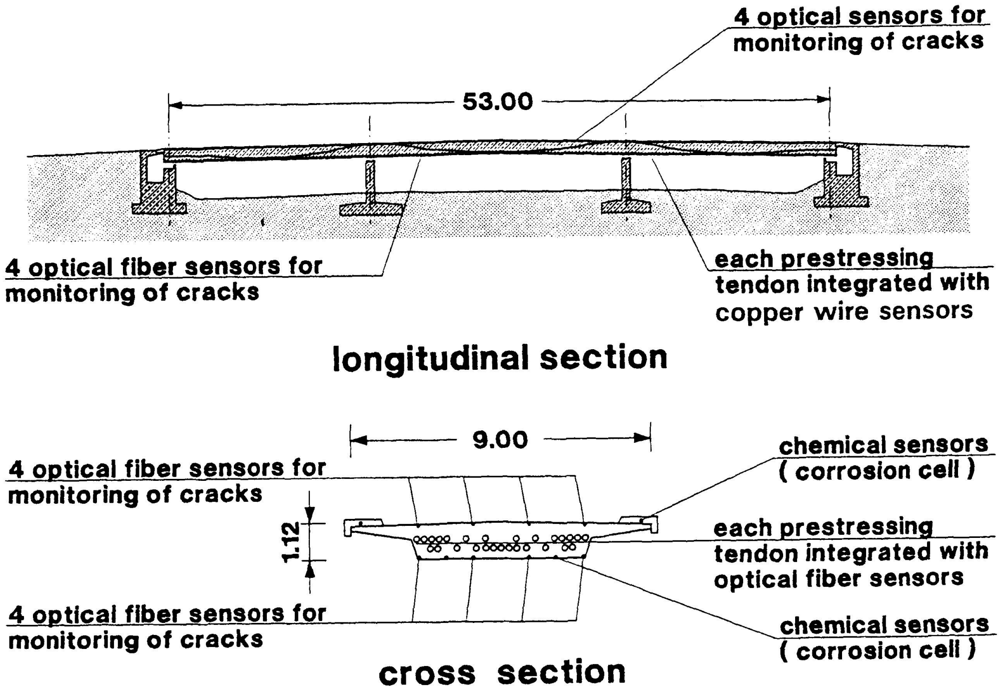

Figure 7: Sensor layout

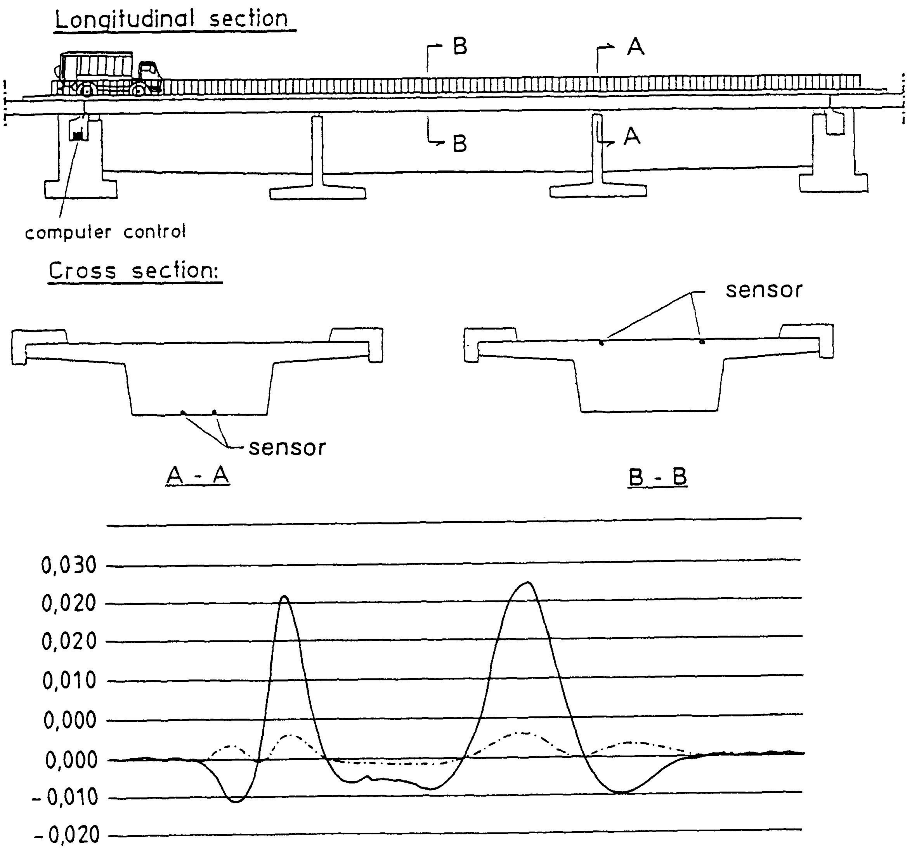

Figure 8: Trial loading

3.3 Nötsch Bridge, Kärnten, Austria

The Nötsch Bridge is the first bridge in Austria with glass fiber composite prestressing tendons, and is designed with limited prestressing comprising 41 glass fiber prestressing tendons (working load 600 kN) and post-bonding. Similar to the Bridge Schiessbergstrasse the suitability of the sensors has been proved by a trial loading. Two trucks with a total load of 2 x 22 t did produce additional extensions in the middle field of approx. 50 μm.

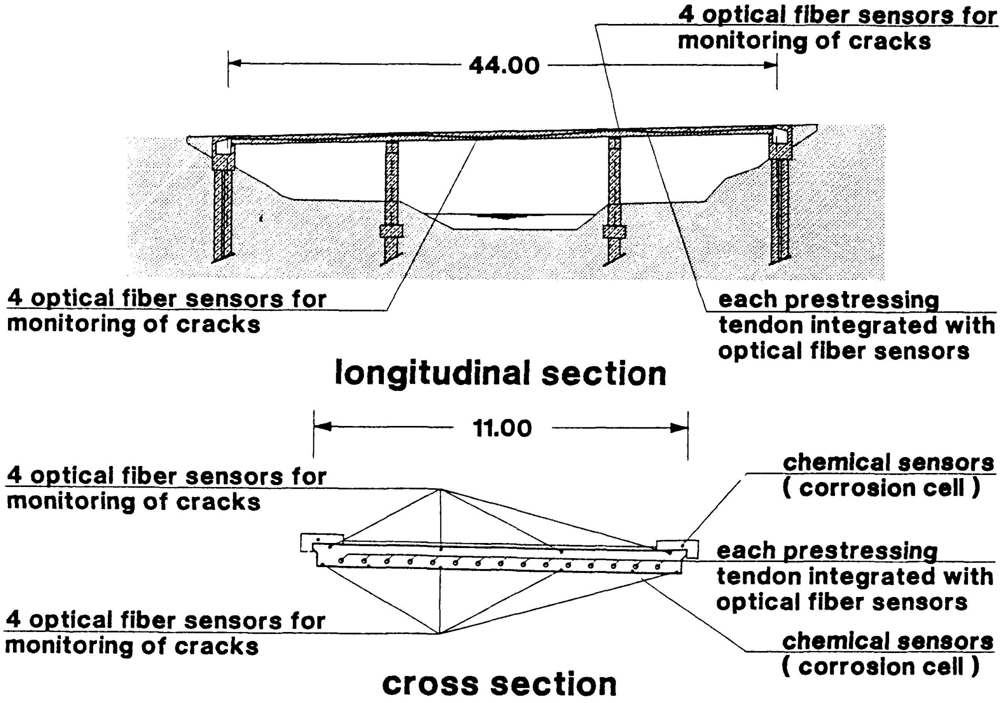

Figure 9: Sensor layout

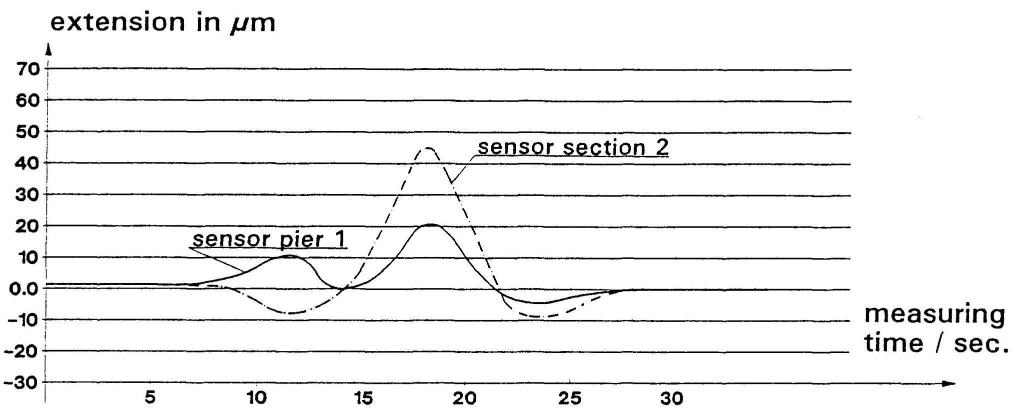

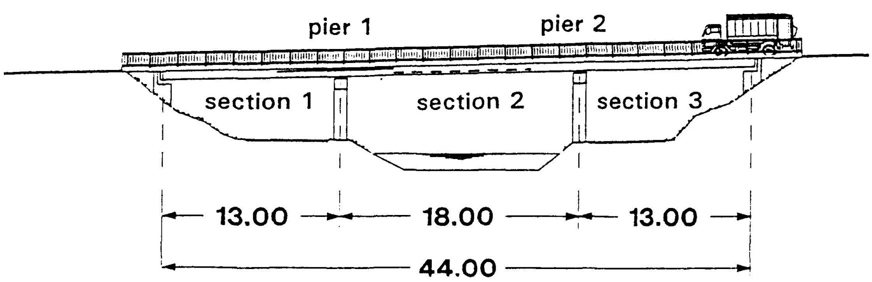

Figure 10: Trial loading

4. CONCLUSIONS

The current constantly increasing requirements and demands on heavy building structures make the question of the utilised materials' durability and the useful life of such structures in general to be of ever greater and wider interest. Compared with essentially new construction, investment for the preservation of building structures claims a not inconsiderable proportion of the funds available.
The possibility of integrating sensors, on the one hand directly into the bar materials during production, and on the other the embedding of such sensors in the concrete, opens completely new horizons for the permanent monitoring of building structures.

5. REFERENCES

1. Miesseler, H.-J.; Lessing, R.: Experiences in monitoring of load bearing structures with optical fiber sensors. IABSE-Congress, Lisbon 1989.

2. Miesseler, H.-J.; Preis, L.: High performace glass fiber composite bars as reinforcement in concrete and foundation structures. Bauen mit Kunststoffen, Issue 2/1988, Pages 4-14.

3. Miesseler, H.-J.; Wolff, R.: Experience with the monitoring of structures using optical fiber sensors. FIP XIth International Congress on Prestressed Concrete, Hamburg, 4-9 June 1990.

4. Wolff, R.; Miesseler, H.-J.: Application and experience with intelligent prestressing systems based on fiber composite materials. FIP XIth International Congress on Prestressed Concrete, Hamburg, 4-9 June 1990.

5. Wolff, R.; Miesseler, H.-J.: New Materials for Prestressing and Monitoring Heavy Structures. Concrete International, 9.1989, Vol. 11, No. 9.

Evaluation of the Capacity of an Existing Steel Truss Bridge
Évaluation de la capacité d'un pont existant à treillis métallique
Ermittlung der Traglast einer bestehenden Stahlfachwerkbrücke

Bruno MASSICOTTE
Assist. Prof. in Civil Eng.
École Polytechnique
Montréal, PQ, Canada

Constantin HALCHINI
Princ. Bridge Testing Eng.
Quebec Min. of Transport
Montréal, PQ, Canada

Jocelyn LABBÉ
Bridge Engineer
Quebec Min. of Transport
Montréal, PQ, Canada

Bruno Massicotte was born in 1959. He received his Ph.D. at the University of Alberta. He worked for two years for the Quebec Ministry of Transportation Bridge Department. In 1990 he joined the École Polytechnique where he does research in bridge engineering.

Constantin Halchini graduated in 1953 in Bucarest as bridge engineer. He worked for 26 years in Romania for the Railway Institute of Research as bridge testing engineer. He joined recently the Quebec Ministry of Transportation where he is the leader of the bridge testing programme.

Jocelyn Labbé was born in 1961. He received his B.Sc. from Laval University in 1984. He worked for several consulting companies before he joined the Quebec Ministry of Transportation in 1989 as bridge engineer.

SUMMARY
The paper presents the evaluation of the load capacity of a top deck steel truss bridge. Conventional analyses, load testing and extensive finite element analyses were used to evaluate the actual capacity. It is shown that conventional analyses are overly conservative compared to the actual bridge behaviour. A load testing programme, coupled with finite element analyses, led to important savings.

RÉSUMÉ
Cet article décrit l'évaluation d'un pont à trellis métallique avec dalle supérieure. Des analyses conventionelles, des essais de chargement et des analyses par éléments finis ont été utilisés afin d'évaluer la capacité réelle. On démontre que les analyses conventionelles sont trop conservatrices. Les essais de chargement couplés avec des analyses par éléments finis ont permis des économies appréciables.

ZUSAMMENFASSUNG
Der Beitrag berichtet von der Ermittlung der Traglast einer Stahlfachwerkbrücke mit oben liegender Fahrbahn. Dabei wurden herkömmliche Berechnungen, Belastungsversuche und umfangreiche Finite-Elemente-Berechnungen eingesetzt. Wie sich zeigt, sind die herkömmlichen Berechnungsverfahren zu konservativ im Vergleich zum tatsächlichen Verhalten der Brücken. Die Kombination von Probebelastungen und Finite-Elemente-Berechnungen ermöglichten bedeutende Einsparungen.

1. INTRODUCTION

Evaluation of existing bridges is a growing concern for bridge engineers. Several options are possible to evaluate the carrying capacity of an existing bridge: conventional or sophisticated analyses and bridge testing.

One can use conventional analyses coupled with design codes modified specifically for bridge evaluation. Frequently this lead to unrealistic evaluations of bridge carrying capacity. However conventional methods have several advantages. They are simple to use and many bridges can be analyzed rapidly. They are thus essential to classify bridges in categories to determine the priority of action and the type of intervention.

The degree of complexity of analyses can vary from simple static or empirical distribution factors to complex finite element. In an other perspective, load test can be performed. The tests can be set up to measure load effects at service load level in various instrumented members, they can be proof tests in which the load is added to the neighborhood of the ultimate capacity or at onset of nonlinear behavior, or they can be performed up to failure.

The combination of a properly carried load test and refined analyses approach an ideal situation. This type of action was undertaken for the Massawippi River bridge.

This paper presents the evaluation of the load carrying capacity of a deck slab steel truss bridge carried using a conventional approach, a load testing program and sophisticated analyses. The aim of this paper is to illustrate the steps involved in the strength evaluation procedure of an existing bridge. The emphasis is directed toward rational strength evaluation involving, when possible, refined analyses coupled with load testing.

2. BRIDGE DESCRIPTION

The Massawippi River bridge, located on Highway 108, south of Sherbrooke Québec, was built in 1937 and is owned by the Ministère des Transports du Québec (MTQ). This 183 m long bridge has eight simply supported spans: six with four reinforced concrete beams, and two with two 32.3 m steel trusses at a skew angle of about 53 degrees (Fig. 1). The top deck above the trusses is made of a 8.7 m wide and 220 mm thick reinforced concrete slab with a 125 mm asphalt cover. The deck also includes stringers and floor beams as shown in Fig. 2. Although the concrete slab was completely replaced some years ago, it was not mechanically connected to the steel beams so no composite action can theoretically be developed. Despite an important number of years in service, the bridge steel and concrete spans are still in good condition and only a limited number of elements require replacement or strengthening. Until recently, the bridge sustained an intense daily traffic of cars and trucks of any configuration and weight since the bridge had no posted weight limits. In an effort to identify all deficient bridges, the Bridge Department at the MTQ evaluates all substandard bridges, starting with those potentially critical located on highways. Considering its age and its location, the bridge evaluation became recently a priority. A conventional strength evaluation was then performed.

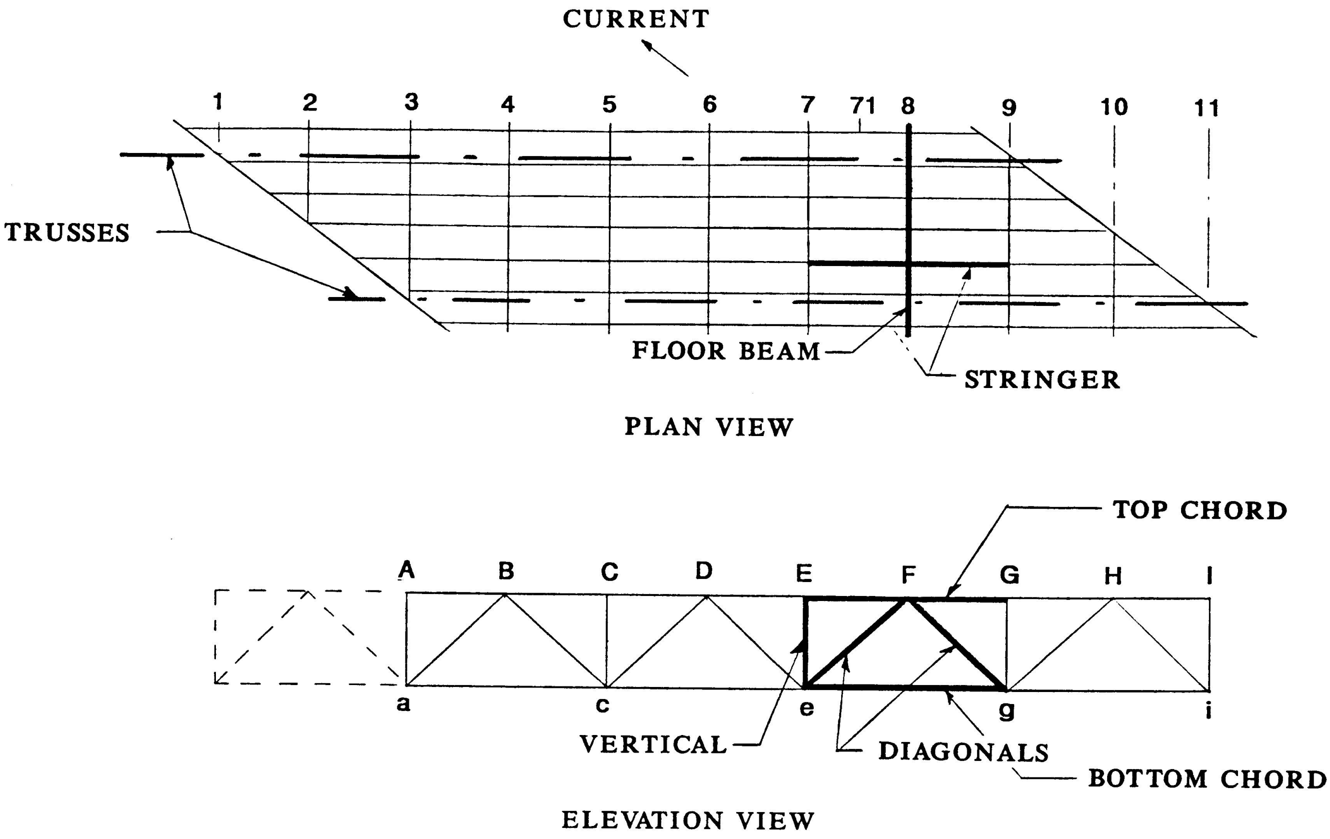

Fig. 1 Geometry of the bridge

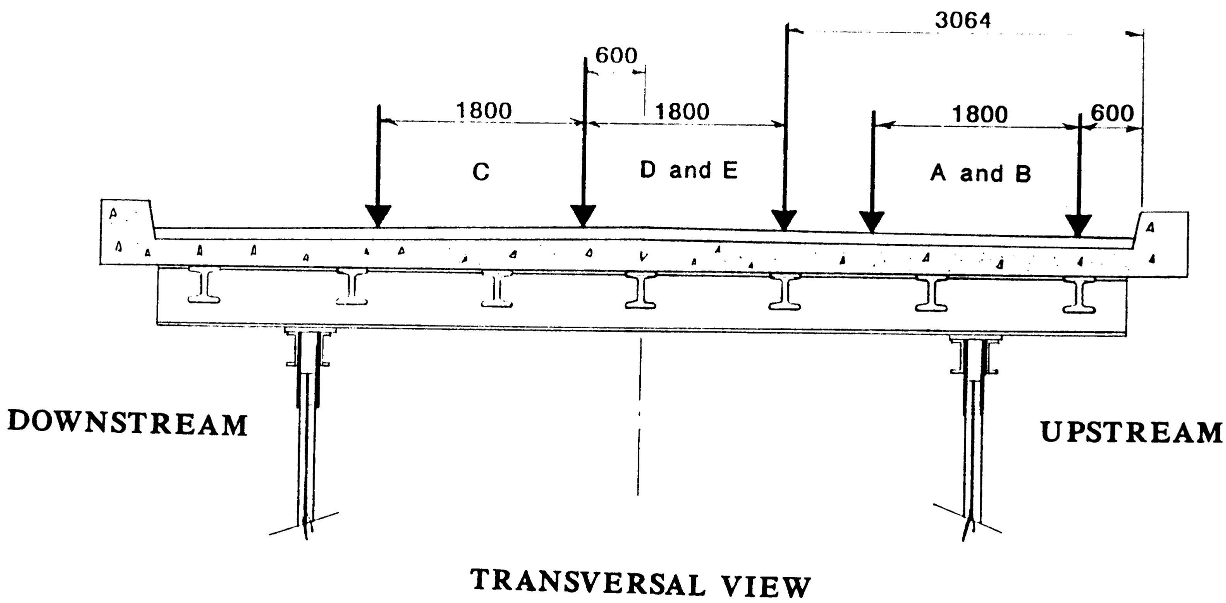

Fig. 2 Deck system

3. CONVENTIONAL STRENGTH EVALUATION

The MTQ Bridge Department evaluated the load carrying capacity of the Massawippi River bridge according to the latest provisions of the Canadian Bridge Code S6-M88 [1]. The assumptions used for the analysis were the same as in the original design. The dead and live load distribution between trusses were obtained following a conventional approach since the bridge structural system is satically determinate. The two trusses were assumed to behave independently, ignoring the transverse bracing in the analysis. Moreover, since no indication was available, no contribution of the deck, from either floor beams, stringers or the concrete slab could be included for the evaluation of the trusses. Also, the supports were assumed free to move horizontally at one end of the trusses.

The live load shearing between both trusses was considered following a conventional approach, with floor beams being simply supported on the top chords of the two trusses. The distribution factor, for the calculation of the most critical live load effects on a given truss according to clause 12 of S6-M88[1],is equal to 1.16 times the loading model. The bridge calculated first natural frequency of approximately 3.8 hertz produces a corresponding dynamic load allowance factor of 40%. The live load rating factors obtained from the evaluation are listed in Table 1 for the steel trusses and the concrete beams. The steel spans exhibited the lowest LLRF giving posting limits of 25, 31 and 36 tonnes for two-axle, semi-trailer and train-trailer trucks respectively.

Table 1: Live load rating factors (LLRF)

Members	2 axles-truck	Semi-trailler	Train-trailler
Tension chord	0.87	0.61	0.54
Compression chord	0.89	0.64	0.54
Tension diagonal:	1.03	0.72	0.64
Compression diag.	0.88	0.85	0.85
Posting (tonnes)	25	31	36

Considering the amount of vehicles traveling on the bridge daily, its location and its economical importance, it was decided to increase the bridge carrying capacity to legal load limits. However, due to the high cost of strengthening the steel trusses, it was decided to postpone the intervention to give engineers the time to explore other alternatives.

4. LOAD TESTING PROGRAM

In 1990, the MTQ acquired a mobile laboratory dedicated to bridge testing. This mobile unit has two data acquisition systems for static and dynamic load tests. The Massawippi River bridge test was the first duty for the mobile laboratory team and its new acquisition.

The instrumentation of the bridge lasted 15 days during which 49 strain gages were installed in a section of the upstream truss. Members instrumented within the truss were: 1 bottom chord, 2 top chords, 1 vertical member and 2 diagonals (Fig. 1). One member of a vertical bracing between the two trusses, 1 floor beam and 2 stringers were also instrumented. Finally, 1 strain gage was installed on the concrete slab soffit, parallel to a strain gage on a stringer, to give some indication on the composite action between the concrete slab and the steel beam.

The test itself took placed on September 26, 1990, and lasted 3 hours, during which the bridge was closed intermittently. The loading vehicle was a 43 tonne 5 axle semi-trailer truck, loaded with gravel, carefully weighted and measured. Five load paths along the bridge, named A to E (Fig. 2) and identified with marking lines on the road, were used to measure load effects on truss members.

For all members the axial force and bending moments were calculated from the strain measurements. For most of the truss members, the axial load was predominant. However even small bending moments measured justified the utilisation of 4 strain gages per members. Without then the measurements could have lead to unrealistic results with significant errors. The floor beams and stringers exhibited a certain degree of composite action with the concrete slab.

A comparison of load effects predicted by the conventional analysis and the corresponding measured values, clearly indicated a significant discrepancy between the behavior observed in the test and the one assumed in the analysis. The diminution of live load effects measured in the test, compared to the values obtained using the same assumptions as in the evaluation, were up to 67% for the tension and compression chords whereas it was 39% for the diagonals. This indicates that the bridge capacity obtained initially could be modified using different assumptions for the behavior.

Although field measurements represent the actual bridge behavior, test results were available only for 6 of the truss 25 main members. This amount of information is not sufficient to indicate clearly the reasons for such discrepancy and safely allow for any significant increase in the bridge load carrying capacity. It was therefore appropriate to proceed with sophisticated analyses using the finite element approach to study more deeply the bridge behavior.

5. FINITE ELEMENT ANALYSIS

Linear finite element analyses were carried out to model correctly the bridge. A 3-dimensional model was created in which steel trusses, floor beams, stringers, all bracing and the concrete slab were carefully discretized. To model adequately the bridge behavior, two factors were used for calibration: the longitudinal restraint of the truss supports and the participation of the deck system, including floor beams, stringers and the concrete slab, in the carrying mechanism.

The first parameter only accounts for the horizontal restraining action of free supports at one end of the trusses. Although they should theoretically allow free longitudinal movements of the bridge, the truss supports were rusted and suspected to be frozen. Analyses involved only two cases for the movement: free or fixed. To model the effects of the second parameter, two independent meshes were used to discretize the bridge. A first mesh describes the two trusses and the bracing system joining them (horizontal and vertical), and a second mesh for the deck system: the concrete slab, the floor beams and the stringers (Fig. 1). Vertical connection members between the two meshes were used to simulate various degrees of participation of the deck system in the load carrying mechanism.

Calibration of the two parameters was achieved with only one loading case. From the load effects in the bottom chord, it became rapidly obvious that the mobile supports were actually frozen horizontally. The second step in the calibration process involved only the stiffness of the connection member which was then modified in a trial and error process until satisfactory agreement between test results and analysis were obtained for this load case. The model was then considered adhequate to represent satisfactorily the bridge behavior and all load cases of paths A, B and C were analyzed. Some of the results are presented in Figs. 3 and 4 for the load path B, together with results of the conventional analysis used initially for the bridge evaluation and test measurements.

A close examination of the results indicates a significant reduction in load effects in top and bottom chords due to some composite action between the the trusses and the deck system. This interaction, although partial, increases the effective inertia of the two trusses which reduces the live load effects on horizontal chords. The skewness of the bridge deck induces an important load transfer between the two trusses through the vertical bracing. Frozen supports have also some influence on the load carrying mechanism making the bridge working like an arch.

These effects, important for the truss top and bottom chords, are however less significant for web members. For the diagonals and the vertical members, a less pronounced live load reduction is observed since vertical shear forces are mainly carried by the trusses. The modification in the load carrying mechanism can be observed by comparing reactions from dead load effects at truss supports. In Table 2 reactions calculated using the various approaches are presented. These results indicate that the dead load distribution is notably affected by the skew angle and the transversal bracing. However, for most of the truss members, the results indicate that the composite action has a more important effect than the frozen supports.

Table 2: Dead load reactions at supports

Support	Conventional 2D		Conventional 3D		Finite element	
	Free	Fixed	Free	Fixed	Free	Fixed
Other-most	661.5	661.5	507.4	579.9	436.1	523.1
Inner-most	697.0	697.0	853.3	827.0	922.4	863.8

6. EVALUATION OF THE NEW LOAD CARRYING CAPACITY

The confidence gained in the comparison of the finite element model with test results, allows one to proceed further and use the finite element model to calculate the live load effects in the truss members for posting. However, the evaluation of the actual carrying capacity using the finite element model must consider assumptions on the conservative side which can differ from those used for the comparison with test data. The contribution of the deck and the skewness of the bridge have a clear effect on the bridge behavior and thus on load effects supported by the bridge main members. These beneficial aspects of the bridge behavior are assumed to remain the same at service load level. However, the role played by frozen supports in the apparent gain in carrying capacity must be reconsidered.

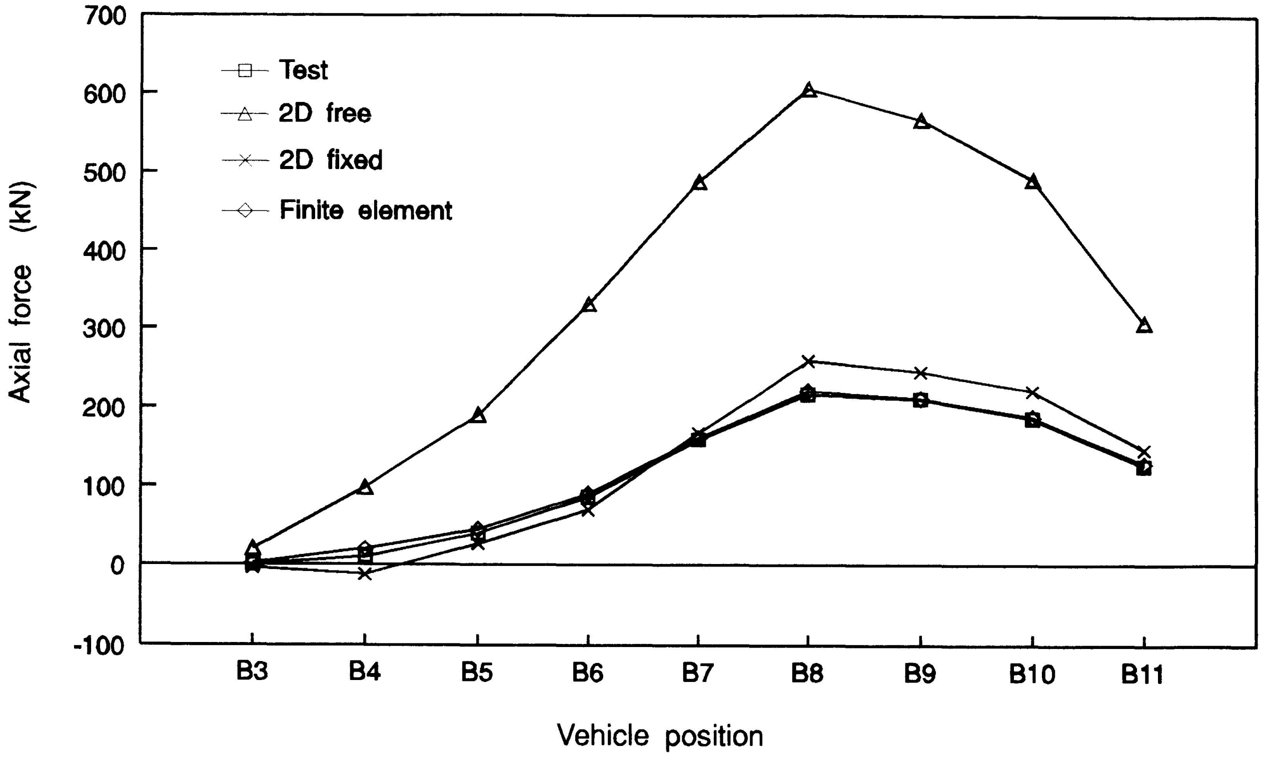

Fig. 3 Axial forces in the bottom chord

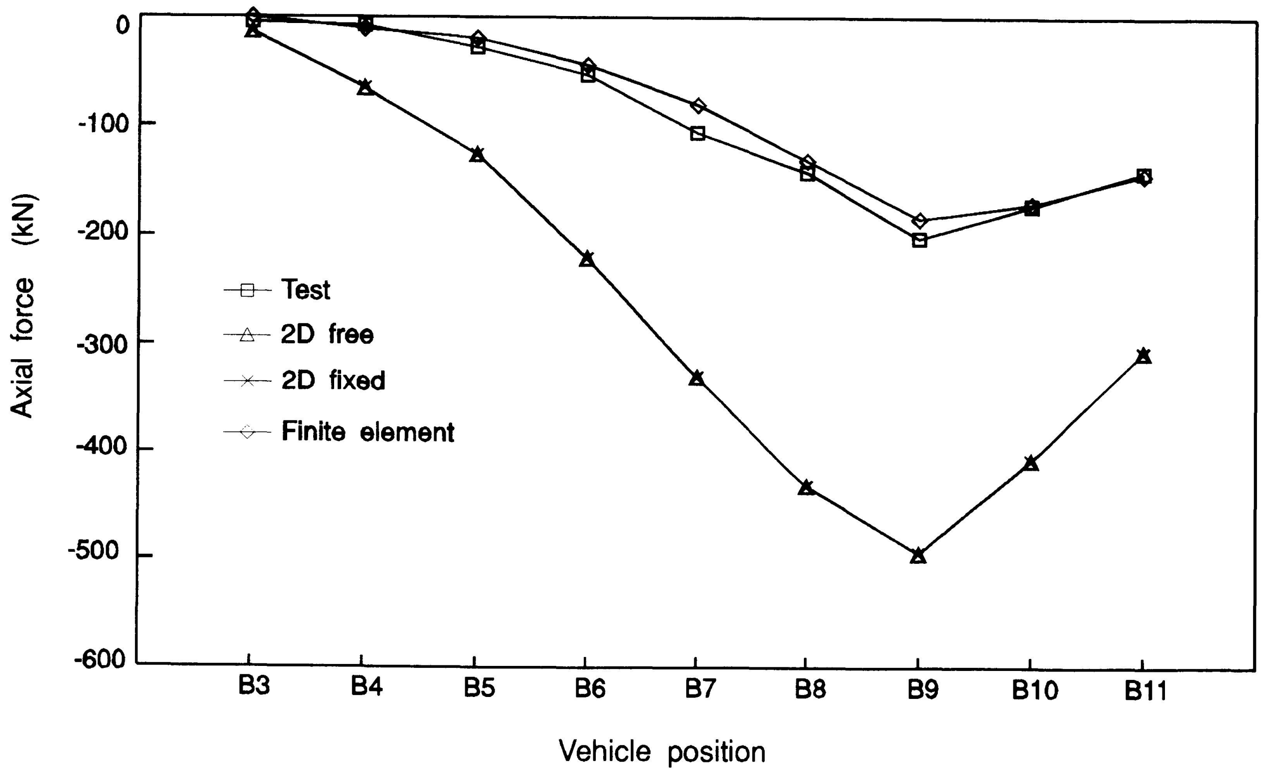

Fig. 4 Axial forces in the top chord

This assumption, although based on careful measurements and sensitive analyses, confront engineers with a dilemma: should the analysis to determine the actual carrying capacity be done with frozen supports or not? On the other hand, is it reasonable to repair the frozen supports to allow free longitudinal movements since the bridge apparently behaves correctly in its current situation? The answer are not simple and this matter requires special attention to be assess correctly.

For weight limit posting, both free and frozen support conditions at one end of the bridge were considered. Since it is difficult to determine accurately the bridge history, the dead load effects retained were those obtained from the conventional analysis or calculated using the finite element model with free or fixed supports, whichever produces the worst effects. For live load effects, the values obtained with the finite element model with free supports at one end were used.

An interesting fact observed in the analysis is that the most critical member governing posting is the vertical strut a-A (Fig. 2) located at the inner-most corner which carries higher compression forces due to load transfer between the two trusses through the vertical bracing. The weakness of this member was not identify in the conventional analysis. This mean that classical analysis although usually on the safe side, may sometimes be unconservative.

7. STRENGTHENING

Although posting limits did not apparently increase very much after all these efforts, the top and bottom chords, the weakest members previously, were not critical any more and only web members remain critical. Thus only the strengthening of a few members is now required, bringing down the costs by more than $200 000. This economy almost justifies by itself the acquisition of the mobile laboratory. The strengthening of the bridge was done in the summer of 1992.

8. CONCLUSION

The need for strengthening a bridge and the cost involved justified the utilization of a field testing campaign combined with refined analyses to increase the understanding of the load carrying mechanism of the bridge. This effort resulted in a slight increase in the actual safe carrying capacity of the bridge and in a significant reduction of members requiring strengthening, leading to important savings. The success of the project is an excellent example of the benefit obtained when advantages of two complementary approaches are efficiently combined.

REFERENCES

1. CANADIAN STANDARD ASSOCIATION, 1988. "Design of highway bridges". CAN/CSA-S6-M88. Rexdale, Ontario.

ACKNOWLEDGMENTS

The authors would like to thanks the *Ministère des Transports du Québec* Officials who believed in their dreams of performing bridge testing. Without their strong supports such work could not have been possible.